ROLE OF DNA DAMAGE AND CELLULAR SENESCENCE IN OSTEOARTHRITIS PATHOPHYSIOLOGY

Michaela Copp

A dissertation submitted to the faculty at the University of North Carolina at Chapel Hill in partial fulfillment of the requirements for the degree of Doctor of Philosophy in the Department of Biomedical Engineering in the School of Medicine.

Chapel Hill
2023

Approved By:

William Polacheck

Brian Diekman

Jeremy Purvis

Koji Sode

Richard Loeser

ABSTRACT

Michaela Copp: Role of DNA damage and Cellular Senescence in Osteoarthritis Pathophysiology
(Under the direction of Brian Diekman)

Osteoarthritis (OA) is a common degenerative joint disease characterized by progressive degradation of the articular cartilage that protects the ends of bones. Aging has been identified as the most dominant risk factor for the development of OA, and a better understanding of age-related dysfunction in joint tissues may contribute to more effective therapeutic interventions. Chapter 1 introduces two components of aging – cellular senescence and DNA damage – as well as their interaction and potential role in OA. Senescence is a state of stable cell-cycle arrest that cells enter in response to stress. Senescent chondrocytes have been found to accumulate within the joint throughout aging and contribute to cartilage dysfunction by secreting inflammatory and matrix-degrading molecules. In Chapter 2, we demonstrate that treatment of cadaveric cartilage tissue with the combination of damage (through 10 Gy irradiation) and cell-expansion stimuli (through growth factor treatment) induces a substantial percentage of chondrocytes to become senescent (~10%). In Chapter 3, we use the single-cell gel electrophoresis “comet” assay to show that older and OA chondrocytes have significantly higher levels of DNA damage compared to chondrocytes derived from young donors. In Chapter 4, we demonstrate that chondrocyte’s capacity to repair DNA damage declines with age, but can be improved by activating SIRT6, an enzyme involved in DNA repair. In Chapter 5, we show a moderate decrease in senescence induction when reducing DNA damage in cartilage explants from cadaveric and murine sources by SIRT6 activation. In a pilot *in vivo* study, we show that repeated intra-articular injections of MDL-800 (a SIRT6 activator) reduces DNA damage but may not be sufficient to mitigate senescence as measured by a $p16^{tdTom}$ senescence reporter allele. Chapter 6 summarizes how this dissertation contributes to the fields of aging biology and OA and identifies further areas of research. Collectively, this work provides novel insights connecting senescence, DNA damage, and OA. By uncovering the underlying mechanisms

behind senescence and DNA damage within the joint, this research establishes a foundation for the development of next generation OA therapeutics.

ACKNOWLEDGEMENTS

Completing a PhD is no small feat, and I have (oh so) many people to thank for helping me reach this point. First, I want to thank my research advisor, Brian Diekman. Under his enthusiastic guidance, I have been able to explore my interests in the field of aging research and grown as a scientist. I am incredibly grateful that he was flexible and supportive of my numerous extra-curriculars. I also want to thank all the members of the Diekman Lab, notably Matt Rich and Garrett Sessions. I owe a lot of my research skills to your guidance, and working with you two was always entertaining and exciting. Additionally, I would like to thank my committee: Richard Loeser, Jeremy Purvis, Koji Sode, and especially Bill Polacheck for serving as my committee chair.

The Department of Biomedical Engineering at UNC Chapel Hill has given me the opportunity to meet remarkable scientists and build valuable friendships. Vilma Berg is the backbone of the BME department, and without her I would have been lost on several occasions. To all my friends, I am so thankful for your endless emotional support and the fun memories we made (and will continue to make).

Anyone who has worked in a lab will recognize the outlandish costs of scientific research. A large portion of my doctoral work over the past three years was funded by a National Institute of Health (NIH) – F31 Predoctoral Fellowship. This funding enabled me to make great strides in my research on DNA damage and repair.

Finally, I would like to extend the ultimate thanks to my wonderful family and amazing partner, Ricky. The Sunday evening dinners with my parents, weekly vent-sessions with my sister, and constant support from Ricky have made the PhD experience one that I will look back on fondly. Your continuous love and encouragement mean the world to me.

TABLE OF CONTENTS

LIST OF FIGURES

LIST OF ABBREVIATIONS

ACL	Anterior Cruciate Ligament
BER	Base Excision Repair
bFGF	Basic Fibroblastic Growth Factor
BMP	Bone Morphogenetic Proteins
BrdU	5-bromo-2'-deoxyuridne
CCN1	Cellular Communication Network Factor 1
CDKI	Cyclin Dependent Kinase Inhibitor
CI	Confidence Interval
DDR	DNA Damage Response
DMM	Destabilization of the Medial Meniscus
DNA	Deoxyribonucleic Acid
DSB	Double Stranded Break
EdU	5-ethynyl-2'-deoxyridine
ELISA	Enzyme Linked Immunosorbent Assay
FFA	Free Fatty Acids
GC	Gas Chromatography
H&E	Hematoxylin & Eosin
HGPS	Hutchinson-Gilford Progeria Syndrome
HPLC	High Performance Liquid Chromatography
HR	Homologous Recombination
IA	Intra-Articular
IF	Immofluorescence
IGF1	Insulin Growth Factor 1
IHC	Immunohistochemical Assay
IL-1β	Interleukin 1β
IR	Irradiation
MFI	Mean Fluorescence Intensity

MMP	Matrix Metalloproteinases
MMR	Mismatch Repair
MMS	Methyl Methanesulfonate
MS	Mass Spectrometry
mTOR	Mammalian Target of Rapamycin
NAD	Nicotinamide Adenine Dinucleotide
NER	Nucleotide Excision Repair
NHEJ	Nonhomologous End Joining
NSAIDS	Non-Steroidal Anti-Inflammatory Drugs
OA	Osteoarthritis
OIS	Oncogene Induced Senescence
PARP1	Poly (ADP-Ribose) Polymerase 1
PCR	Polymerase Chain Reaction
PTOA	Post Traumatic Osteoarthritis
qPCR	Quantitative Polymerase Chain Reaction
RB	Retinoblastoma
ROS	Reactive Oxygen Species
SAHF	Senescence-Associated Heterochromatin Foci
SASP	Senescence Associated Secretory Phenotype
SAβGal	Senescence-Associated β-Galactosidase
SEM	Standard Error of the Mean
SIRT6	Sirtuin 6
SSB	Single Stranded Break
TGF-β1	Transforming Growth Factor Beta 1
UV	Ultraviolent
WS	Werner Syndrome
X-gal	5-bromo-4-chloro-3-indolyl-β-D-galactoside
XRCC1	X-Ray Repair Cross Complementing 1

CHAPTER 1: INTRODUCTION

1.1 INTRODUCTION TO OSTEOARTHRITIS PATHOGENESIS

1.1.1 Epidemiology of Osteoarthritis

Osteoarthritis (OA) is a chronic degenerative joint disease defined by gradual loss of articular cartilage. Among the numerous types of arthritis, OA is the most prevalent, impacting upwards of 32.5 million adults in the United States[1,2]. The impact of OA extends beyond joint pain, affecting sleep quality, work behavior, and overall mood[3]. Unfortunately, there are no FDA-approved disease modifying drugs for osteoarthritis[4]. The current treatment paradigm for OA includes conservative pain management (i.e., NSAIDs), followed by targeted pharmacological treatment (i.e., COX2 inhibitors), intra-articular injections of hyaluronic acid or steroids, and ultimately total joint replacement surgery for advanced cases[4,5]. Considering the low efficacy of nonsurgical OA treatments, over half of patients undergo total joint arthroplasty[6], representing a substantial medical cost. The average direct cost of OA in the United States averages to $11,500 per person annually, with total incremental costs – the sum of direct and indirect costs associated with OA – adding up to $136.8 billion[1,6]. There is a pressing need to identify therapies that are better adept at preventing osteoarthritis and factor in the multi-faceted etiology of the disease[7]. This will become increasingly more urgent as the prevalence of OA is expected to increase along with the rapidly aging population and rising obesity rates[8].

1.1.2 Pathophysiology of Osteoarthritis

The major tissues involved in OA include the cartilage, synovium, and bone. Cartilage is a firm, visco-elastic tissue composed of chondrocytes, which produce a matrix of collagen, proteoglycans, and non-collagenous proteins. In healthy conditions, cartilage surrounds bones and provides a barrier between bone ends for smooth movement. A boundary layer of lubrication on the cartilage surface is supplied by lubricin and hyaluronic acid secreted by chondrocytes and synovial cells[9]. Chondrocytes are the only cellular component of cartilage and make up 1-2% of the total cartilage volume[10]. In a healthy environment, mature chondrocytes are quiescent and rarely initiate turnover of the collagen matrix[11]. As

adult articular chondrocytes are physically confined within the pericellular matrix, they maintain a relatively low rate of metabolism, which functions to preserve an equilibrium between catabolic and anabolic processes[10].

Osteoarthritis initiates the breakdown of articular cartilage, leading the underlying bone to become exposed. This impacts the entire joint space with pathological changes occurring in all relevant tissues: degradation of the articular cartilage, osteophyte formation, synovial inflammation, subchondral bone thickening, and deterioration of ligaments and the menisci[11]. As cartilage degrades, the underlying bone begins to remodel and form bony outgrowths (i.e., osteophytes) while the synovium - the tissue that produces the joint lubricating synovial fluid - becomes inflamed. The chondrocytes begin to produce inflammatory molecules - cytokines and chemokines - and proteolytic enzymes that contribute to cartilage breakdown. Further, the chondrocytes become 'activated', triggering cell proliferation, the formation of cell clusters, and an escalated production of both matrix proteins and matrix-degrading enzymes[12].

Another feature of osteoarthritis is a disrupted cartilage homeostasis that skews the balance between anabolic and catabolic processes towards catabolism. Chondrocytes begin to secrete catabolic factors such as matrix metalloproteinases (MMPs), interleukin-1β (IL-1β), free radicals, and growth factors[4,9]. Conversely, anabolic factors such as insulin growth factor 1 (IGF1) and bone morphogenetic proteins (BMPs) are produced to repair cartilage damage and stimulate cartilage regeneration[4]. A schematic overview of the changes that occur with osteoarthritis is presented in **Figure 1.1**. While the pathophysiology of OA has become more complete, the cause(s) of the homeostatic imbalance are unclear.

Understanding the biological changes leading to OA has been hindered considering its prior association as a "wear and tear" disease. While joint injury can lead to post traumatic OA, this is only a single factor that can advance OA development. OA etiology is multi-factorial, with older age, obesity, joint damage, muscle weakness, genetics, and biological sex all playing a role in the development of OA[13]. The strongest risk factor for OA is advanced age[14]. While OA and aging are independent processes, there are several aging hallmarks –altered intercellular communication, deregulated nutrient sensing, epigenetic alterations, etc.[15] – that could contribute to OA pathogenesis. The following sections

of this introduction will touch on two of these hallmarks of aging – cellular senescence and DNA damage – and how they are implicated in osteoarthritis.

1.2 INTRODUCTION TO CELLULAR SENESCENCE

Cellular senescence is a state of stable cell cycle arrest that cells enter upon being stressed[16]. While beneficially inhibiting the replication of damaged cells, senescence has been implicated in the decline of tissue function[17], inflammation[18], tumorigenesis[19], and age-related diseases[20]. These findings have driven researchers in the aging field to further characterize the senescent phenotype and investigate the pharmacological removal of senescent cells as a therapeutic option.

1.2.1 The Senescence Phenotype

The concept of a senescent phenotype was first introduced by Leonard Hayflick and Paul Moorhead upon their discovery that normal human fibroblasts have a finite replicative potential[21]. Hayflick and Moorhead termed this state of halted proliferation 'cellular senescence' and suggested that it could be a driver of aging[21]. This limited capacity to replicate is a unique characteristic to normal cells, as compared to cancer cells, which can proliferate indefinitely[22]. Since this discovery, numerous studies have shown that the senescence phenotype can be induced in a variety of cellular contexts and in response to multiple stimuli. Further, senescent cells have been identified in various physiological processes and pathological disorders. The following sections will discuss (1) the known biomarkers and mechanisms of senescence, (2) the role senescent cells play in aging-related disorders, and (3) methods to detect and target senescent cells.

1.2.2 Physiological Roles of Senescence

There are a vast array of environmental contexts and cellular stimuli that have been shown to trigger the senescent phenotype. A common theory is that the purpose of senescence is to remove damaged cells and promote tissue remodeling[22,23]. In the Nature review, "Cellular senescence: from physiology to pathology", Espín and Serrano propose that senescence supports tissue renewal in a three step sequence: (1) initiation of a stable cell cycle arrest (i.e., senescence), (2) secretion of inflammatory molecules (SASP) that recruit an immune system response, and (3) enrollment of progenitor cells to regenerate the tissue[22]. This process – senescence, clearance, regeneration – has proven beneficial

during embryonic development and wound healing but becomes harmful in advanced age when the system becomes disrupted and senescent cells accumulate.

1.2.2.1 Beneficial Roles of Senescence

In a transient setting, senescence is engaged in a variety of important physiological processes. During normal embryonic development, senescence helps destroy temporary embryonic structures and ensure proper cell type numbers[24]. Further, senescent cells contribute to wound healing by promoting tissue regeneration[25] and stimulating insulin secretion by pancreatic beta cells[26]. In the tumor microenvironment, senescence acts as a protective response by halting the replication of dysfunctional or preneoplastic cells and preventing malignancies[27]. When cancer-stressed cells are induced to senescence, an immune system response is triggered aiding in tumor elimination[28,29].

1.2.2.2 Senescence and Aging

Unfortunately for aged and/or damaged tissues, the effect of senescent cells becomes harmful. In these contexts, inadequate macrophage recruitment leads to the accumulation of senescent cells[30]. These cells have been shown to increase with age in humans[31], monkeys[32], and mice[33], and in a variety of tissues. Notably, senescent chondrocytes have been shown to accumulate in aged and arthritic cartilage[34]. As the cartilage is avascular and inhibits immune cell access[35], senescent cell clearance by macrophages is not viable for this tissue. The conversion of normal articular chondrocytes to senescence is likely due to accumulated damage (discussed further in **Chapter 3**). This increase in senescence is dangerous in part due to the secretion of inflammatory molecules in the SASP. Indeed, senescent cells have been noted in numerous age-related disorders such as atherosclerosis[36], diabetes[37], lung disease[17], and osteoarthritis[34]. Notably, prior work in the Diekman Lab has demonstrated that $p16^{INK4a}$ expression in chondrocytes is affiliated with aging and dysfunction[38]. Senescence additionally impacts stem and progenitor cells which negatively influences the regenerative potential of tissues[39]. The combination of elevated SASP, limited regeneration, and ineffective clearance provide an explanation for the accumulation of senescent cells with age and how these cells contribute to age-related pathologies.

Altogether, cellular senescence is considered an example of evolutionary antagonistic pleiotropy, with both beneficial and detrimental roles in physiological processes[40]. The balance between positive and negative effects is largely dependent on context and whether the immune system can remove the

senescent cells. The temporary induction of senescence seen in development is beneficial since it leads to the elimination of damaged cells. However, when aged tissues and disease lead to persistent and accumulating senescence, the effect becomes harmful.

1.2.2.3 Senescence Induction Methods

Cells enter the senescent phenotype in response to damage from a wide range of intrinsic and extrinsic stimuli. Telomere shortening, oncogenic activation, epigenetic changes, chromatin disorganization, mitochondrial dysfunction, irradiation, injury, chemotherapeutic agents, nutrient deprivation (and more) have all been shown to induce cells to senesce[40]. These various stress activators give rise to distinct types of senescence that are broadly categorized into replicative cellular senescence, oncogene-induced senescence, and stress-induced cellular senescence[41].

The senescence that arises due to serial proliferation of cells is replicative cellular senescence, and is the type that Hayflick and Moorhead identified in 1961[21]. This form of senescence is dependent on the critical shortening of telomeres, the protective structure at the end of chromosomes, after excessive proliferation without endogenous telomerase activity[42]. Oncogene-induced senescence (OIS) results when oncogenes – mutant versions of normal genes – are activated or tumor suppressor genes are inactivated. Although the pathways involved in OIS are not fully understood, the proliferative arrest is dependent on the activation of both the RB and p53 pathways[43]. Finally, senescence can appear in normal cells following exposure to stress from a physical or chemical agent. Stress-induced senescence can arise from irradiation, oxidative stress and/or hyperoxia, chemotherapeutic drugs, cytokines and adipokines, and copper[41]. Regardless of the method of induction, these inducers all unite to activate the CDK inhibitors p16, p15, p21 and p27[16].

The development of models of senescence are critical for the mechanistic study of senescence induction and the identification of senotherapeutics (see section *1.2.5 Senotherapeutics*). Towards this end, it is vital to create physiologically relevant senescence induction models. For example, although chondrocytes replicate in monolayer culture, they are hypo-replicative in the extracellular matrix of the cartilage[44]. Thus, replicative senescence is unlikely to be the driving factor for accumulating senescent chondrocytes in the joint space. The development of a physiologically relevant cartilage explant model of senescence is the topic of focus in **Chapter 2** of this thesis.

1.2.3 Biomarkers of Senescent Cells

Due in part to the varied physiological and environmental conditions that give rise to senescence, the senescent phenotype is highly heterogenous, and no single marker has been identified to date that selectively and universally detects senescent cells. These cells are distinguishable from other non-proliferating cells (i.e., terminally differentiated cells and quiescent cells) by the presence of DNA damage markers, upregulation of cell cycle arrest proteins, altered metabolic rates, morphological changes *in vitro*, increased lysosomal activity, chromatin remodeling, and the secretion of a complex mix of proinflammatory and tissue-remodeling factors coined the senescence-associated secretory phenotype (SASP)[15,45,46]. While these markers are affiliated with senescence, none of them are common among all senescent cell types and have been found in other physiological processes. Thus, several of the described measures must be used in conjunction to confirm a cell as being senescent.

The inability to proliferate in conditions that would typically promote cell division is a notable feature of senescent cells[40]. Compared to quiescence which halts the cell cycle in the G0 phase, senescence tends to occur in the G1 phase[47]. Further, quiescent cells are able to re-enter the cell cycle upon treatment with mitogenic signals (i.e., growth factors) or favorable growth conditions, while senescent cells cannot[48,49]. Two approaches are commonly used to validate cell cycle arrest: (1) direct measurement of proliferative markers and DNA synthesis rate, and (2) quantification of the expression levels of cyclin dependent kinase inhibitors (CDKIs) p16 and p21[45]. When cells are senescent, they will be absent of proliferative markers, such as the Ki67 protein, and will not incorporate BrdU (5-bromo-2'-deoxyuridine) or EdU (5-ethynyl-2'-deoxyridine) in DNA synthesis assays[50]. Similarly, senescent cells upregulate apoptosis resistance proteins, notably the BCL proteins, Bcl-2 and Bcl-xL[51].

Cell cycle arrest in senescence is regulated by the activation of the $p16^{INK4A}$/pRB and/or p53/p21CIP1 tumor suppressor pathways[52]. Both p53 and pRB are key transcriptional regulators, with p21WAF1/CIP1 acting downstream of p53 and $p16^{INK4A}$ acting upstream of pRB. These drivers of senescence are encoded in the CDKN2A (p16), CDKN2B (p15), and CDKN1A (p21) loci. The transcriptional activation of p16 in particular has been used to mark senescent cells *in vivo*[53]. Research has shown that persistent over-expression of p53, pRB, p16, or p21 can induce senescence in human diploid fibroblasts[54]. Despite the conventional thought that cell cycle arrest is irreversible in senescence,

studies have proven that senescent cells are capable of re-entering the cell cycle in particular situations, such as in the tumor microenvironment or when reprogrammed into induced pluripotent stem cells[40].

A commonly used method for senescence detection is the senescence-associated β-galactosidase (SAβGal) assay. Senescent cells have increased β-galactosidase activity which can be detected at pH 6.0[31]. This differs from other cells where β-galactosidase activity is acidic and detectable only at pH 4.0. The elevated lysosomal activity in senescent cells is considered to be a function of the higher levels of autophagy and enlarged lysosomal compartment of senescent cells[55,56]. The traditional approach for measuring SAβGal is by cytochemical or histochemical methods which require fixed cells or tissue to be incubated with the chromogenic substrate, 5-bromo-4-chloro-3-indolyl-β-D-galactoside (X-gal). When β-galactosidase cleaves X-gal, the substrate produces an insoluble blue compound that is distinguishable by eye[57]. Further iterations of the SaβGal assay using similar principles to the colorimetric assay have been developed for flow cytometry and are described in more detail in **Chapter 2**[58].

When cells are introduced to damage – either intrinsically (e.g., oxidative damage) or extrinsically (e.g., chemotherapy drugs) – they activate a DNA damage response (DDR)[45]. Unresolved or persistent damage, particularly that caused by double stranded breaks (DSBs), can trigger cells to exit the cell cycle and become senescent[49]. At sites of DSBs, the DDR recruits and binds the ATM kinase, driving the phosphorylation of histone H2AX[59]. The presence of γH2AX, measured by immunofluorescence, is an indicator of lasting DNA damage, and is one method of detecting senescent cells. Conversely, staining for phosphorylated p53 can be used as this is a key regulator in the DDR[22]. Although the DDR is involved in the senescence induction process, it is not selective for senescence as cells initiate repair when reacting to transient damage[49]. More information on DNA damage and repair are provided in the following section.

Senescence is associated with wide-spread changes to the chromatin. A common indicator of senescent cells is the deficit of Lamin-B1, a scaffolding protein of the nuclear envelope[60]. One consequence of the loss of Lamin-B1 is the formation of cytoplasmic chromatin fragments (CCFs), which are fortified with epigenetic features affiliated with DNA damage. These CCFs can stimulate a proinflammatory response via activation of the cGAS/STING pathway when secreted into the extracellular environment via exosomes[61]. Another consequence of the degradation of Lamin-B1 is the formation of senescence-associated heterochromatin foci (SAHFs). SAHFs contain qualities of heterochromatin, such

as H3K9me3 and HP1g, which may be visualized by DAPI staining[45,48]. However, these foci are not universally shared among all senescence programs and are not present in mouse cells[62].

Lastly, senescent cells *in vitro* can be detected based on their morphology. Cells that have undergone senescence in monolayer appear to be flattened and exhibit an enlarged fried-egg appearance. Further, these cells often display multi-nucleation and enlarged vacuoles which are observable by traditional bright-field microscopy. Changes in the cell size and shape can also be measured by immunofluorescence of cytoplasmic proteins vimentin or actin[45,62]. A summary overview of the senescence biomarkers presented in this section are illustrated in **Figure 1.2**. In the perspective piece published by Cell, Gorgoulis et al. describe a three-step process for detecting senescence cells: (1) screening for senescence via SA-β-gal and/or lipofuscin staining, (2) verification with additional markers frequently upregulated in senescence – $p16^{INK4A}$ and $p21^{WAF1/Cip1}$ – or downregulated (proliferation and Lamin B1), and (3) lastly staining for specific markers of senescence (SASP, DNA damage, mTOR)[48].

1.2.4 The Senescence Associated Secretory Phenotype (SASP)

Although senescent cells do not actively proliferate, they remain metabolically active and upregulate a set of genes that encode a suite of secreted proteins. These secreted factors include a mix of inflammatory chemokines, cytokines, growth factors, and extracellular matrix proteases. Collectively, these molecules make up the senescence associated secretory phenotype (SASP). Through the SASP, senescent cells can communicate with neighboring cells and reinforce the stress response in an autocrine and paracrine approach[49].

The composition of the SASP is highly heterogenous and varies based on the type of cell undergoing senescence and the environmental context[49]. Common SASP markers that are measured include the following: cytokines (IL-1a, IL-6, and IL-8), chemokines (CCL2), metalloproteinases (MMP-1 and MMP-3), and growth factors (TGFβ, IFG1, bFGF)[45,62,63]. Of note, several central SASP factors – IL-1, IL-6, and MMP-3 – coincide with mediators of OA inflammation[34]. The SASP is largely regulated by the proinflammatory transcription factor, NF-kB[64], but has also been found to be controlled by the cGAS/STING pathway[65], mammalian target of rapamycin (mTOR)[66], and p38MAPK signaling pathways[67].

Depending on the biological context, the SASP has been found to be both beneficial and damaging. In positive contexts, the SASP can activate an immune response that will remove senescent

cells[39], facilitate developmental senescence[24], and support wound healing[25]. Conversely, SASP factors have been shown to promote chronic inflammation, termed inflammaging[68], and initiate tumorigenesis by stimulating angiogenesis and metastasis[63]. The low-level chronic inflammation produced by the SASP has been strongly connected with aging and age-related diseases.

Numerous studies have concluded that the SASP plays an important role in the activity of senescent cells[40,63]; however, the SASP is too heterogenous and general to solely be used as a biomarker for senescence. An emerging theme in senescence research is the characterization of senescent cells by different senescence induction methods and cell types[69]. Quantifying the SASP composition of these different programs would be one approach towards defining these individual senescent phenotypes.

1.2.5 Senotherapeutics

Due to the growing body of evidence implicating senescence in the pathogenesis of age-associated disorders, approaches have been made to selectively target and inhibit senescent cells to mitigate their pro-aging effects, a field termed senotherapeutics[70]. Transgenic mouse models – INK-ATTAC[71] and p16-3MR[72] – have enabled researchers to investigate the physiological effects of clearing senescent cells in a variety of disease states[40]. Two classes of senotherapeutics have been pursued: (1) senolytics, which selectively kill senescent cells, and (2) senomorphics, which suppress the pathological SASP without causing cell death[70]. Many of these tactics to target senescent cells are based on the biomarkers identified in the prior section (*1.2.3 Biomarkers of Senescence*).

The majority of senolytics that have been identified work by targeting the important proteins in anti-apoptotic mechanisms, particularly the p53, p21 and Bcl-2 family proteins[70,73]. Upregulation of these pro-survival family of proteins help senescent cells resist apoptosis. Small molecules that inhibit the anti-apoptotic proteins, such as ABT-263 (navitoclax)[73], therefore induce cell death in senescent cells. Conversely, senomorphics suppress the SASP expression of senescent cells by targeting the NF-κB, mTOR, IL-1a, p38 MAPK and other signaling pathways[20,70]. Commonly used senomorphics include rapamycin, metformin, resveratrol, and aspirin.

The promise of senotherapies for treating age-related diseases has been strengthened by the ability of senolytics to mitigate chronic diseases in mouse models and simultaneously increase mouse

lifespan and healthspan, the time that an organism lives without age-associated chronic diseases[71,74,75]. A drawback of senotherapies is the heterogenous nature of senescent cells. The majority of validated senolytics are limited in efficacy to specific types or sub-populations of senescent cells. Continued research on the pathways that initiate and propagate senescence in different tissues will provide valuable insight for potential biomarkers to target senescent cells.

1.2.5.1 Senolytics and Osteoarthritis

Our lab has previously reported on the use of a $p16^{tdTom}$ reporter allele – a knocked-in tdTomato fluorescent protein regulated by the endogenous $p16^{INK4a}$ promoter – to quantify the induction and removal of senescent chondrocytes in a physiologically relevant cartilage explant model using ABT-263 (alternatively known as navitoclax)[76]. This *in vitro* system of senescence induction in murine hip cartilage enables the mechanistic study of alternative approaches to remove or prevent senescent cell accumulation, as described in **Chapter 5**. Efforts to target senescent chondrocytes in the joint as a therapy were spearheaded by Jeon et al, who found that removal of senescent cells by intraarticular injection of a proprietary senolytic molecule (UBX0101) resulted in improved joint function and minimized injury-induced OA after transection of the anterior cruciate ligament (ACL)[75]. Additional work from this study investigated the effect of selective removal of age-accumulated senescent cells on OA development. Using the INK-ATTAC transgenic mouse model[71] and AP20187, a molecule that induces apoptosis in $p16^{INK4a}$ positive cells, the removal of senescent cells significantly reduced age-related cartilage degeneration compared to vehicle treatment controls[75]. Lastly, the use of senolytics in murine models of OA have been shown to promote a pro-chondrogenic environment[73].

1.2.6 Limitations & Future Directions

A better understanding of the aging process at the cell and tissue level has the potential to transform the treatment of chronic diseases and promote healthy aging. Cellular senescence has been identified as a key phenotype that drives age-related dysfunction via the inflammatory SASP. Mounting evidence has shown that the accumulation of senescent cells in the joint during both aging and in response to injury contribute to the development of OA[34]. However, there is a critical knowledge gap in understanding *how* aging drives joint dysfunction, and the *mechanisms behind* senescence induction within the joint space. With clinical trials that target senescent cells in the joint underway (NCT04210986)

or completed with no significant results (NCT03513016), it is important to ascertain the physiological contexts that trigger senescence induction and identify the types of senotherapeutics most effective at targeting senescence chondrocytes. The next chapter of this thesis, **Chapter 2: The Combination of Mitogenic Stimulation and DNA Damage Induces Chondrocyte Senescence**, provides some insight into these knowledge gaps.

1.3 INTRODUCTION TO DNA DAMAGE & REPAIR

Deoxyribonucleic acid (DNA) is composed of four chemical building blocks called nucleotides – adenine (A), thymine (T), guanine (G), and cytosine (C) – that encode an organism's genetic information. The nuclear genome is critical for cellular and tissue health, yet DNA is only present in two distinct copies and the maintenance of its integrity is dependent on continuous repair[77]. Under physiological conditions – aqueous, oxygen-rich, pH 7.4 – DNA is chemically unstable and prone to harm from endogenous and exogenous sources of damage[78]. This genomic instability means the genome is susceptible to mutations – irreversible and transmittable changes to the DNA sequence – such as base substitutions, deletions or insertions, chromosomal variations or retro-transposition[77]. While at times evolutionarily beneficial, mutations predominantly create an adverse effect on an organism by causing cancer or genetic diseases. The following sections will detail how DNA damage arises, the various types of DNA damage, and the numerous mechanisms that organisms have developed to repair DNA. A broad overview of this content is illustrated in **Figure 1.3**.

1.3.1 Sources of DNA Damage

DNA lesions can originate from exogenous and endogenous sources. Exogenous DNA damage arises from environmental (i.e., ultraviolet and ionizing radiation from the sun), toxins (i.e., alkylating agents and aromatic amines), and chemical agents (i.e., chemotherapeutics)[79,80]. Conversely, endogenous DNA damage comes from DNA replication errors and intra-cellular oxidative stress. The three most pressing hazards for DNA integrity arise from: (1) spontaneous hydrolysis of nucleotide residues, (2) generation of reactive oxygen species (ROS) from metabolic processes, and (3) exposure to UV light and ionizing radiation[81]. While environmental agents can be potent, they can be largely avoided.

On the other hand, ROS and nitrogen species are produced during essential organism functions, such as respiration, and are thus a constant threat to the nuclear genome[82].

1.3.2 Types of DNA Damage

DNA damage can materialize in a variety of forms: abasic sites, inter- and intra-strand crosslinks, chemical modifications, breaks, and gaps in the DNA[77]. These are broadly categorized into base damage, single stranded breaks (SSB), and double stranded breaks (DSB). Damage to the DNA that impacts a single nucleotide base is the most diverse of the types of DNA damage. Oxidative stress is the main source of base damage, creating abasic sites and causing deamination[81,83]. Abasic sites are constantly created when the glycosidic bond between the DNA base and sugar phosphate group is hydrolytically cleaved[80]. These sites are generally unstable and quick to convert into SSBs. Other types of base damage produced by reactive oxygen species and radiation include O^6-methylguanine, thymine glycols, base adducts, or reduced/oxidized/fragmented bases[84].

Single stranded breaks occur when there is a lesion in the DNA sugar phosphate backbone localized to one of the two strands of the DNA double helix. SSBs are frequently created in the repair process of damaged bases. This type of damage can make use of the complementary strand of DNA as a template for repair and is typically fixed through base excision repair (BER) or nucleotide excision repair (NER). BER is used to correct damage done to a single base produced by oxidation, deamination, alkylation, or hydrolysis. Conversely, NER is deployed when repairing bulky, helix-altering lesions, like pyrimidine dimers[83].

Double stranded breaks are the most dangerous type of lesion considering its propensity to cause changes within the DNA sequence and mutations if repaired incorrectly. DSBs can be produced after exposure to radiation and particular toxins, as well as through improper DNA replication and repair[79]. Base damage and SSBs that persist for a prolonged period increase the risk of facing a replication fork which further elevates the likelihood of replication errors and DSB formation[83]. Altogether, an estimated 10^5 DNA lesions occur daily in an active mammalian cell, with spontaneous hydrolysis alone producing approximately 10^4 abasic sites[85].

1.3.3 DNA Damage Repair

Exogenous and endogenous agents are continuously inducing lesions and breaks to the nuclear DNA. Fortunately, the cell has evolved robust mechanisms to sense DNA damage, halt genome replication, and ultimately repair the vast number of genomic insults occurring daily. When a cell is damaged, a complex system called the DNA damage response (DDR) is initiated. The DDR encompasses multiple DNA damage sensors, DNA repair pathways, and cell-cycle checkpoints aimed at ensuring the genome maintains its integrity[82]. There are five major DNA repair pathways – mismatch repair (MMR), base excision repair (BER), nucleotide excision repair (NER), homologous recombination (HR), and nonhomologous end joint (NHEJ)[80]. The activation of these pathways is dependent on the type of damage and stage of cell-cycle[86].

Mismatch repair is typically initiated to repair replication errors and as such is active in the S phase of the cell cycle[87]. Conversely, BER is the pathway of choice to correct small chemical alterations that do not significantly distort the DNA double-helix[82]. In BER, the oxidative lesions or single strand breaks are removed from the sugar-phosphate backbone by lesion-specific DNA glycosylases, an AP endonuclease incises the damaged strand, and the single nucleotide gap is refilled by means of DNA synthesis[81]. When the damage induces bulky lesions that disturb the helix structure, NER is activated. The lesions that are substrates for BER and NER are located on one of the strands of the double helix and removed in a “cut-and-patch mechanism”. For both pathways, the complementary strand acts as a template for the repair of the damaged strand[88]. Single stranded breaks are transiently detected by the enzyme poly(ADP-ribose) polymerase 1 (PARP1), which rapidly undergoes a cycle of ribosylation and dissociates from the DNA. The chains of PARP are thought to act as a platform to recruit the appropriate repair factors[80]. SSBs may be repaired by either the NER or BER pathways.

Occasionally, a damaging agent will impact both strands of the double helix and form a DSB. Chromatin remodeling at the site of the DSB starts a series of events including ATM activation, phosphorylation of H2AX, chromatin PARylation, recruitment of 53BP1 and BRCA1[80,89]. There are two major pathways cells use to resolve DSBs – nonhomologous end joining (NHEJ) and homologous recombination (HR). NHEJ operates in a “cut-and-paste” manner, ligating the two ends of the DSB. While efficient, repair of DSBs through NHEJ may introduce additions or deletions of nucleotides at the

generated junction. NHEJ mainly occurs before replication in the G1 phase of the cell cycle. The other method of fixing DSBs is HR, which uses a homologous sister chromatid to align the broken ends and accurately insert the missing genetic information. As HR requires an identical sister chromatid, it operates exclusively within the S- and G2-phases[90]. Altogether, cells have evolved a suite of repair pathways and cell cycle checkpoints to sense and repair DNA damage and maintain the integrity of the genome.

Compared to actively proliferating cell types, differentiated chondrocytes are uniquely susceptible to DNA damage as they rarely pass through DNA damage checkpoints and are limited to the repair mechanisms available in the G1 phase of the cell cycle[91–93]. The DNA damage checkpoints (or cell cycle checkpoints) are biochemical pathways that halt or stop cell cycle progress when damage is detected[84]. When activated, these checkpoints can arrest the cell temporarily or permanently (i.e., senescence), stimulate specific DNA repair pathways, and influence the conversion of unfixed DNA lesions into chromatid breaks[83]. Unfortunately, mature chondrocytes generally cannot benefit from these checkpoints as they are hypo-replicative and not actively progressing through the cell cycle. In another post-mitotic cell type – neurons – researchers have proposed that the most notable damage arises during cellular metabolism and the generation of oxidative DNA damage[94]. The tendency for chondrocytes to accumulate DNA damage is explored in more detail in **Chapter 4**.

1.3.4 Measuring DNA Damage & Repair

Measuring DNA damage in cells is a challenge as the level of damage to be assessed is relatively low with respect to the rest of the genome. Additionally, it is methodologically difficult to accurately measure the many different chemical alterations that impact DNA. Despite these limitations, researchers have developed a suite of direct and indirect techniques to detect DNA damage, as well as methods to assess the repair response[95].

DNA lesions and breaks fragment the DNA, causing a reduction in the molecular weight of the DNA strand that can be detected through agarose gel electrophoresis or polymerase chain reaction (PCR). A commonly used approach for assessing single or double strand breaks is the comet assay, or single-cell gel electrophoresis[96]. This assay uses fluorescence and an applied electrophoretic field to separate undamaged DNA (a spherical nuclear mass referred to as a comet head) from damaged DNA (the comet tail), which migrates through the agarose at a faster rate[97]. This method can detect single and

double strand breaks, as well as alkali-labile sites, and is discussed in greater detail in **Chapter 3**. The information provided from this technique has been expanded in modified comet assays by adding lesion-specific repair enzymes (e.g., OGG1) or bacterial glycosylases (e.g., Fpg) to the experimental pipeline[98,99]. These enzymes convert their specified lesion into single strand breaks, enabling the recognition of various oxidized and alkylated bases, dimers, mis-incorporated uracil and BER sites. Alternatively, PCR and quantitative PCR (qPCR) have been used to detect damage and certain genes. Sites of damage disrupt DNA replication and PCR amplification, resulting in a decreased amount of PCR product and lower number of DNA templates[100].

Direct measurements of DNA lesions can be performed by high performance liquid chromatography (HPLC) or gas chromatography (GC), combined with mass spectrometry (MS). These methods extract and digest the DNA into monomeric units, separate the hydrolyzed products via chromatography, and use MS to detect and quantify specific lesions. HPLC-MS is the method of choice for measuring modified DNA bases, such as alkylated BER products[101]. GC-MS can detect a variety of DNA damage products, such as heterocyclic bases, as well as measure the kinetics of DNA repair enzymes[102,103]. Although these assays are accurate, high equipment costs and specialized technical knowledge limit how widespread these approaches are used.

Chemiluminescent strategies such as enzyme linked immunosorbent assay (ELISA), immunohistochemical assay (IHC), or immunofluorescence (IF) have been used to measure specific enzymes and antigens. These involve the use of antibodies raised against DNA lesions, while others use antibodies raised against enzymes or protein modifications involved in the DDR. The gold standard for DSB detection is H2AX, which is phosphorylated by the ATM protein at sites of DSBs. This phosphorylation event occurs within 1 to 3 minutes of DNA damage[104]. Immunofluorescence is the primary method for detecting γH2AX and the resulting “foci” may be counted to determine the number of DSBs. Alternative DNA repair proteins that have been used as biomarkers for DNA damage include the Ku protein – a heterodimer involved in NHEJ of DSBs[105] – and the X-ray repair cross complementing 1 (XRCC1) protein, which interacts with several repair enzymes involved in SSB repair[106].

1.3.5 The Contribution of DNA Damage to Aging, Senescence, and OA

It is well established that DNA damage promotes the development of cancer[81]; however, DNA damage has also been affiliated with apoptosis, cellular senescence, and aging itself[77]. Aging has been defined as the "accumulation of unrepaired damage to cellular and organismal components over time."[107] In support of this, mounting evidence suggests that DNA damage is a contributing factor to senescence and other aspects of aging[77,78]. When DNA damage remains unrepaired, signaling cascades for apoptosis or senescence are triggered to avoid the replication of a faulty genome. Although a protection from cancer, these defense mechanisms accelerate the aging process[78].

A large body of evidence has demonstrated that all pathways involved in DNA repair – MMR, base excision repair, SSB and DSB repair – become deficient with age, contributing to both cancer and aging-related disorders (reviewed in [108] and [109]). Multiple studies have proven that older organisms have higher loads of DNA damage[108,110,111]. The accumulation of lesions and breaks to the DNA with aging has been affiliated with gradual functional decline in cells and tissues. This is further evidenced by the fact that premature aging disorders, such as Hutchinson-Gilford progeria syndrome (HGPS) and Werner syndrome (WS), have faulty DNA repair mechanisms and accumulate large levels of DNA damage[112–114].

DNA damage is a common source used in the induction of cellular senescence. The initiation of DDR pathways – p53-p21 and/or $p16^{INK4a}$-pRB – activate the cyclin-dependent kinase inhibitors p16, p21 and p27 that lead to withdrawal from the cell-cycle and sustained cell-cycle arrest. Aged organisms show significant increases in γH2AX foci[115] and DNA oxidation[116], providing further evidence that DNA damage and its associated repair mechanisms are a contributing factor to cellular senescence. Additionally, the NF-κB transcription factor, which is heavily involved in the SASP, is highly activated in aging[117]. This is relevant as studies have shown a link to DNA repair deficiency and aging through the SASP[109]. The rising levels of inflammation from the SASP has been termed inflammaging and underlies the development of age-related disorders[68].

In the context of cartilage, OA chondrocytes have been found to have significantly increased amounts of DNA damage compared to normal chondrocytes[118,119]. Rose et al. showed that DNA damage in articular chondrocytes induces both a senescent phenotype and dis-coordinated gene expression, consistent with OA chondrocytes[118]. Altogether, a vicious cycle emerges with inefficient DNA repair

promoting the accumulation of DNA damage, which produces an inflammatory environment via the SASP, leading to further DNA damage and inhibition of DNA repair.

1.3.6 Limitations & Future Directions

A significant portion of the research conducted on DNA damage and repair to date has centered around approaches to inhibit the DDR for the treatment of cancer (e.g., PARP inhibitors in BRCA-deficient ovarian and breast tumors)[83,120]. While these findings are crucial for the development of cancer therapeutics, they are not as applicable for age-related diseases that arise from the accumulation of DNA damage. Investigators have begun to explore interventions that improve DNA repair and reduce DNA damage as a therapeutic approach for treating age-associated pathologies[83]. Considering DNA repair encompasses the coordinated action of many proteins, this is more involved than simply overexpressing one protein, which may not result in improved DNA repair[78]. Thus, approaches to activate DNA repair pathways must consider the multifactorial nature of the DDR.

An additional limitation to this body of work is that the study of DNA damage repair, and its decline with age, has predominantly been limited to fibroblasts and lymphocytes. The work presented in this dissertation addresses this limitation by investigating the accumulation of DNA damage (**Chapter 3**) and decline in repair efficiency (**Chapter 4**) with aging in primary articular chondrocytes.

1.4 INTRODUCTION TO SIRTUIN 6

Sirtuins 1-7 (SIRT1-7) are the mammalian orthologs of yeast silent information regulator 2 (Sir2), a widely recognized longevity gene[121]. These nicotinamide adenine dinucleotide (NAD) – dependent histone and non-histone protein deacetylases modulate many processes including transcriptional regulation, metabolism, development, chromatin dynamics, and the focus of this thesis, DNA repair[107]. Depending on their function, the sirtuins evolved to localize in differing cellular regions: SIRT1 and SIRT2 in the nucleus and cytoplasm, SIRT3-5 in the mitochondria, and SIRT6 and SIRT7 exclusively in the nucleus[122]. Although SIRT1 has been the most extensively studied sirtuin thus far, a growing body of research has indicated that SIRT6 is an important mediator of DNA repair. The following section will discuss the mechanisms of SIRT6-faciliated DNA repair, and the detrimental effects that arise when SIRT6 activity is disrupted.

1.4.1 SIRT6 as a DNA Repair Agent

SIRT6 is a key regulator of gene expression, DNA repair, metabolism, and lifespan, as evidenced by SIRT6 knockout mouse models[123]. Research has elucidated that SIRT6 has three enzymatic functions: (1) deacetylase, (2) mono-ADP-ribosyl-transferase, and (3) defatty-acylase activities[122]. Among these, SIRT6's function as a histone deacetylase is its most robust enzymatic activity.

In normal physiology, the nuclear DNA is packaged with histones in a structure called the chromatin. The compact chromatin inhibits transcription and recombination but limits the accessibility of DNA repair factors when damage arises[82,107]. SIRT6 facilitates DNA repair by rapidly localizing to sites of DNA damage and initiating chromatin remodeling, which enables the recruitment and function of DNA repair proteins[124–126]. SIRT6 is involved in HR, NHEJ, and BER by targeting PARP1[124], DNA-PKcs (DNA-dependent protein kinase, catalytic subunit)[127], and SNF2H[125].

In the occurrence of base damage and SSB, SIRT6 regulates BER by modulating BER factors and/or adjusting the density of the chromatin to enable accessibility to the DNA damage site[128]. Conversely, SIRT6 facilitates the repair of DSB by detecting the lesion site, deacetylating H3K9 and H3K56, modulating chromatin accessibility through interactions with SNF2H and CHD4, and associating with PARP1 and stimulating PARP1 polymerase activity[124,127,129,130]. This sequence of events stimulates the repair of DNA damage through HR or NHEJ. An overview of the manners in which SIRT6 acts as a DNA repair agent are illustrated in **Figure 1.4**.

1.4.2 SIRT6 in Aging and Senescence

Previous work has demonstrated that SIRT6 is heavily involved in several processes that become dysfunctional with advanced age[131,132]. Work conducted in mouse models have revealed that SIRT6 knockdown leads to premature aging phenotypes[131], while SIRT6 overexpression produces an increase in male mice lifespan[133]. Altogether, this research suggests a critical role of SIRT6 in both aging and age-related diseases. In support of this, Xu et al. identified a strong negative correlation between age and the expression levels of SIRT6[128].

A number of disorders have been associated with deficient SIRT6 activity, including diabetes, obesity, cancer, and cardiovascular diseases[122,129]. Additionally, depletion of SIRT6 coincides with an accumulation of senescent cells[134]. This is unsurprising as SIRT6 activity blocks senescence by

maintaining telomere chromatin structure, preserving genome stability following DNA damage, and inhibiting the transcription of proteins relevant in senescence[129]. Further, the deacetylase activity of SIRT6 at H3K9ac limits the transcription of NF-κB, a prominent player in the age-dependent induction of cellular senescence[135].

The relationship between diminishing SIRT6 activity and aging pathologies has supported the development of therapeutics that activate this repair agent. As SIRT6 influences critical DNA repair functions, like NHEJ and BER, SIRT6 re-activation is a promising approach to mitigate advanced age phenotypes.

1.4.3 SIRT6 Modulation

With mounting evidence showing the promise of SIRT6 activation on DNA repair and genome maintenance, a growing area of research involves the identification and development of small molecule modulators for SIRT6. Consistent with the other mammalian sirtuins, SIRT6 has a core catalytic domain spanning 250 amino acids[136]. SIRT6 consists of three structural regions: a large Rossmann fold, a small zinc-binding region, and a hydrophobic channel spanning the two domains[137]. The Rossmann fold, which is responsible for NAD^+ binding, is composed of 6 β-sheets situated between 2 α-helices on one side and 4 α-helices on the other. The hydrophobic channel accommodates long-chain acyl SIRT6 substrates, while the zing-binding motif is solely structural and does not participate in any catalytic activity[136,138].

Despite SIRT6 deacetylase activity being 100 – 1000 times lower than other active sirtuins, the most prominent enzymatic activity for SIRT6 is deacetylation, with H3K9 being SIRT6's main substrate[137]. Early studies demonstrated that free fatty acids (FFAs), such as myristic acid, increased this deacetylation efficiency up to 35-fold[139], paving the way for further investigation of SIRT6 activators. To overcome issues such as metabolic instability, low water solubility, and poor permeability, researchers began to investigate synthetic activators[138]. One such activator includes, MDL-800, which was identified by computationally predicting an allosteric site on SIRT6 and virtually screening compounds, followed by *in vitro* evaluation of the top calculated binders[140]. MDL-800 treatment was shown to increase SIRT6 deacetylase activity by 22-fold with an EC_{50} value of 10.3 μM, while not displaying any effect on the enzymatic activities of SIRT1/3/4 and HDAC1.

Due to the dichotomous nature of SIRT6 in cancer and inflammation[141], inhibition of SIRT6 in certain contexts may be desirable. Inhibitors of SIRT6 can be generally broken into 4 categories: product inhibitors (i.e., nicotinamide), thioacyl-lysine warheads, isoform-specific small molecule inhibitors of deacetylation, and competitive inhibitors of long-chain deacylation (i.e., myristic acid)[136,142]. One sirtuin inhibitor, EX-527, acts as an isoform-specific small molecule inhibitor by stabilizing the closed enzyme conformation and preventing product release[143]. The development or identification of SIRT6 inhibitors remains a key area of research as many of the discovered inhibitors lack either efficacy or specificity towards SIRT6. The experiments in **Chapter 4** and **Chapter 5** will make use of MDL-800 to activate SIRT6, and EX-527 to inhibit SIRT6.

1.4.4 SIRT6 and Joint Tissue Homeostasis

Studies using Sirt6 conditional knockout mice, as well as loss- and gain-of-function models, have confirmed that SIRT6 plays a critical role in cartilage homeostasis, chondrocyte senescence, and osteoarthritis[144,145]. SIRT6 provides a protective measure for articular chondrocytes by maintaining redox homeostasis[146], and intra-articular injection of a lentivirus encoding Sirt6 has been shown to minimize cartilage degradation in a surgery-induced post traumatic OA (PTOA) mouse model[147]. Conversely, Sirt6 haploinsufficiency – when one gene copy is inactivated and the other copy cannot produce enough gene product to maintain proper function – instigates joint inflammation, osteophyte development, and chondrocyte hypertrophy in a diet-induced obesity model of OA[148].

Collins et al. showed that SIRT6 activity was significantly reduced in chondrocytes isolated from older and osteoarthritic donors[146]. Overexpressing Sirt6 in murine chondrocytes reduced the expression of SA-β-Gal and genes dependent on NF-κB, and improved the Safranin-O staining and OARSI scores of knee joint cartilage[147]. This suggests that Sirt6 activation may mitigate OA development by preventing the accumulation of senescent chondrocytes. Consistent with these findings, Nagai et al. showed that deleting Sirt6 increased DNA damage and induced senescence in chondrocytes[134]. Lastly, work done by Ji et al. revealed that intra-articular injections of adenovirus-Sirt6 significantly reduced DMM-induced OA[144].

1.4.5 Limitations & Future Directions

Although the functional and mechanistic role of SIRT6 in the context of osteoarthritis and cartilage homeostasis has begun to be explored, it remains largely undefined. Further, the work done thus far has been conducted in injury- or diet- induced models of OA, rather than the more prevalent age-induced OA. The recent study by Ji et al.[144] successfully showed that Sirt6 deficiency accelerated chondrocyte senescence and OA progression, while Sirt6 activation mitigated OA development after surgical injury. This introduces an interesting hypothesis that enhanced DNA damage repair capacity through SIRT6 activation could prevent senescence and OA. The translational work presented in **Chapter 5** was driven by this hypothesis and explores the effect of continuous Sirt6 activation on senescence induction and osteoarthritis.

1.5 CONCLUSION

As discussed in the prior sections, research has begun to elucidate the connection between DNA damage, senescence, and osteoarthritis progression. However, there is limited biological understanding of (1) how senescence is stimulated within the joint space, (2) whether DNA damage accumulates in chondrocytes, (3) how DNA repair is impacted with age in chondrocytes, and (4) the effect of continuous activation of the DNA repair protein, SIRT6, on senescence induction and osteoarthritis development. The following chapters provided in this dissertation will address these knowledge gaps.

1.6 FIGURES

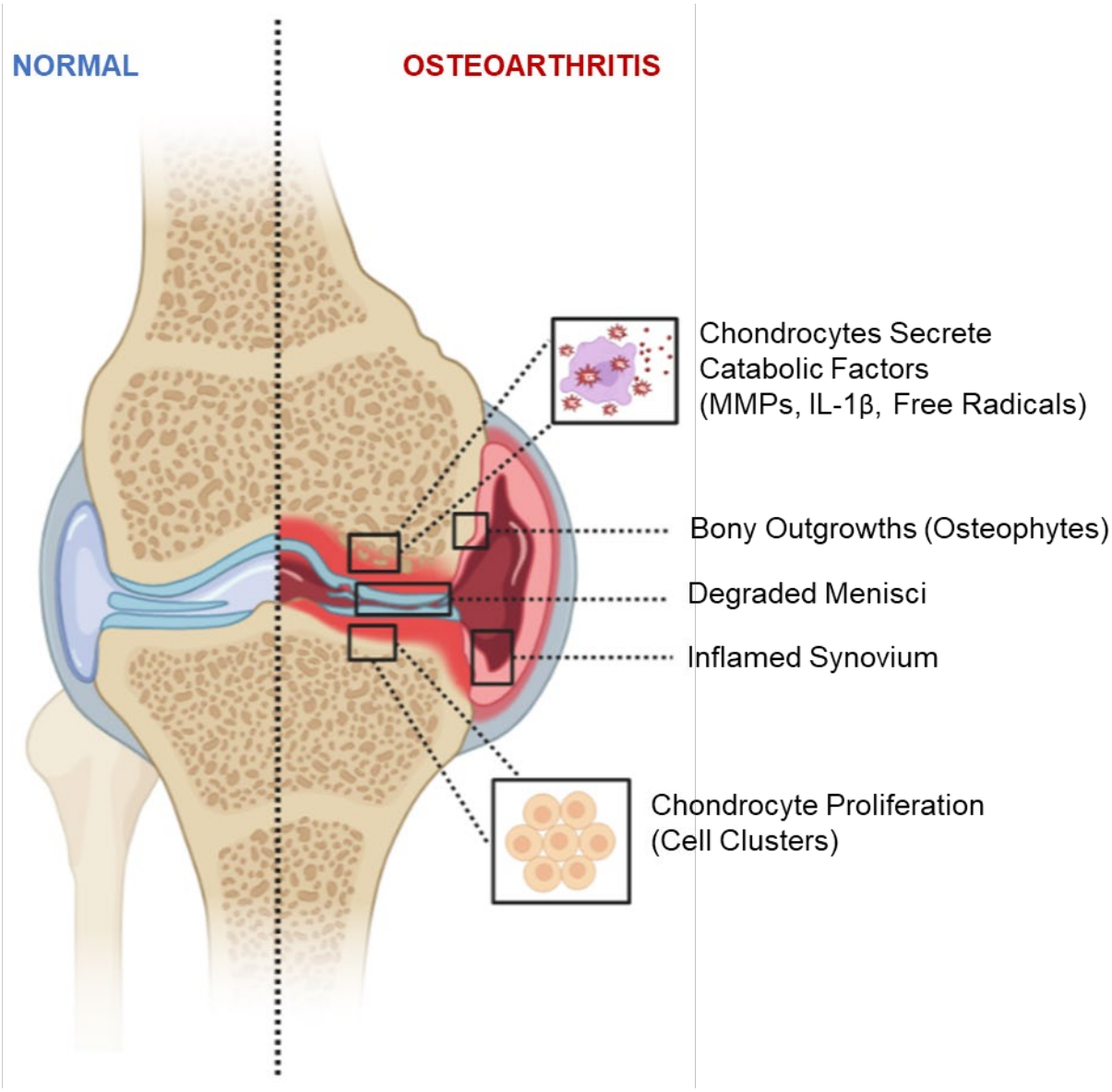

Figure 1.1: Overview of the changes that develop with OA progression: Osteoarthritis initiates the breakdown of articular cartilage, leading to synovial inflammation, osteophyte formation, subchondral bone thickening, and degradation of the menisci and surrounding ligaments. Additionally, chondrocytes begin to produce inflammatory molecules and enter a hypertrophic state.

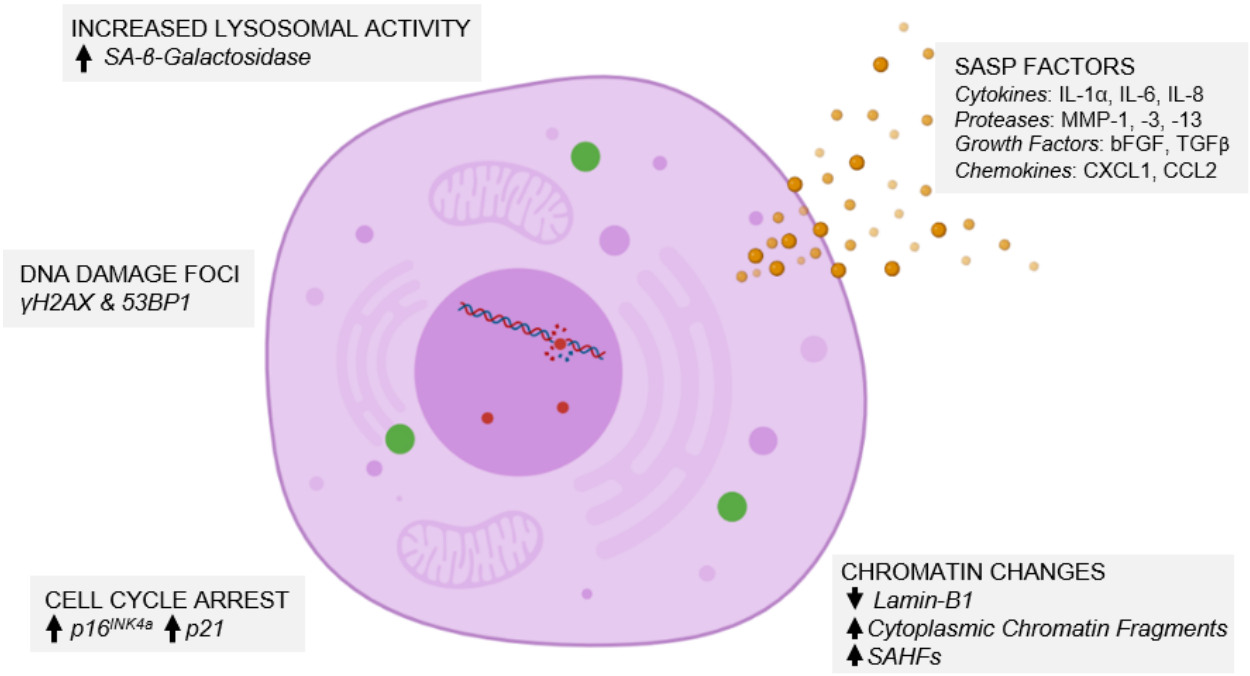

Figure 1.2: Biomarkers of Cellular Senescence. Senescent cells exhibit stable cell cycle arrest, demonstrated by increased expression of cell-cycle arrest proteins, p16 and p21. Persistent DNA damage is a common marker of senescence, identified by the presence of γH2AX and 53BP1 foci. A suite of inflammatory molecules called senescent associated secretory phenotype (SASP) are secreted by senescent cells. Other biomarkers of senescence include elevated lysosomal activity, alterations to the chromatin and increased NF-κB signaling.

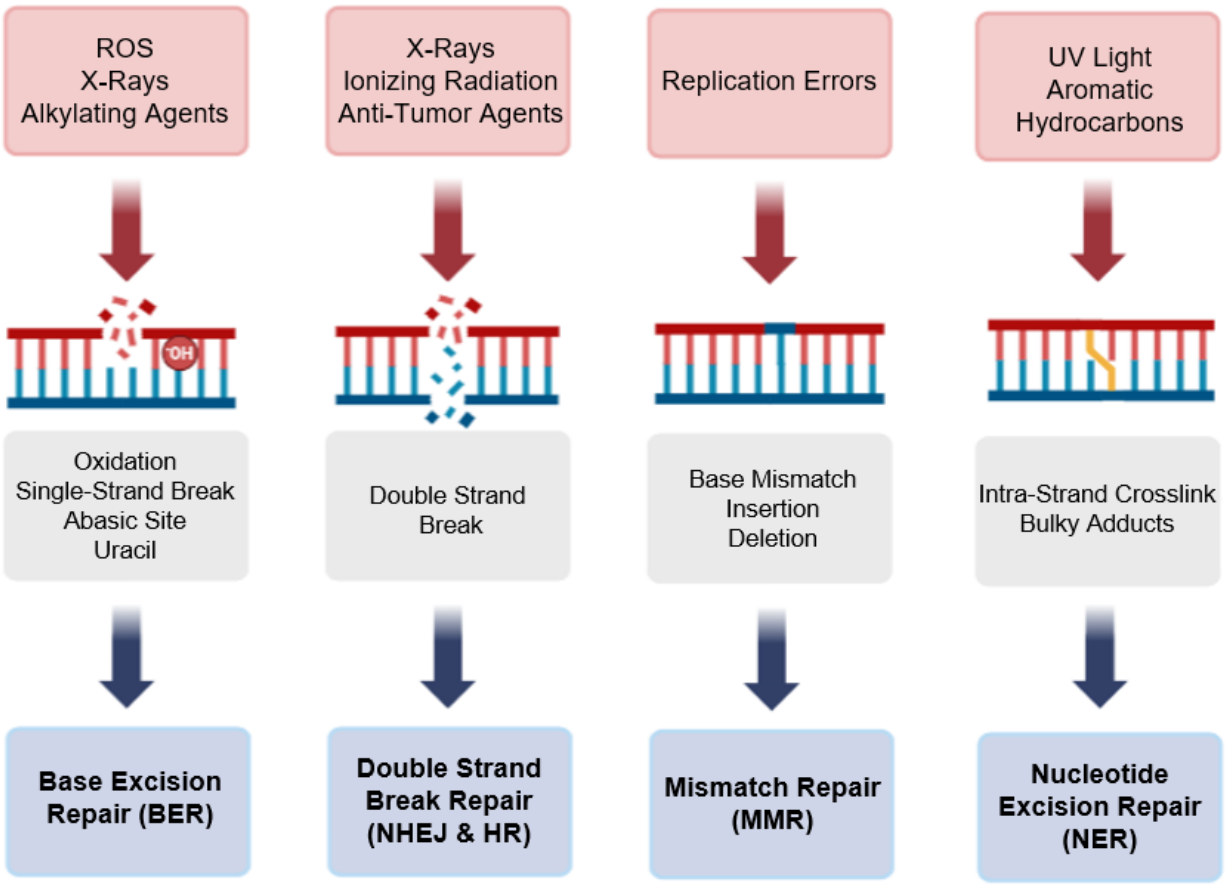

Figure 1.3: A general overview of the various damaging agents, types of DNA damage, and the repair pathways cells use to mend those lesions. The four major repair pathways include base excision repair, mismatch repair, nucleotide excision repair, and double strand break repair.

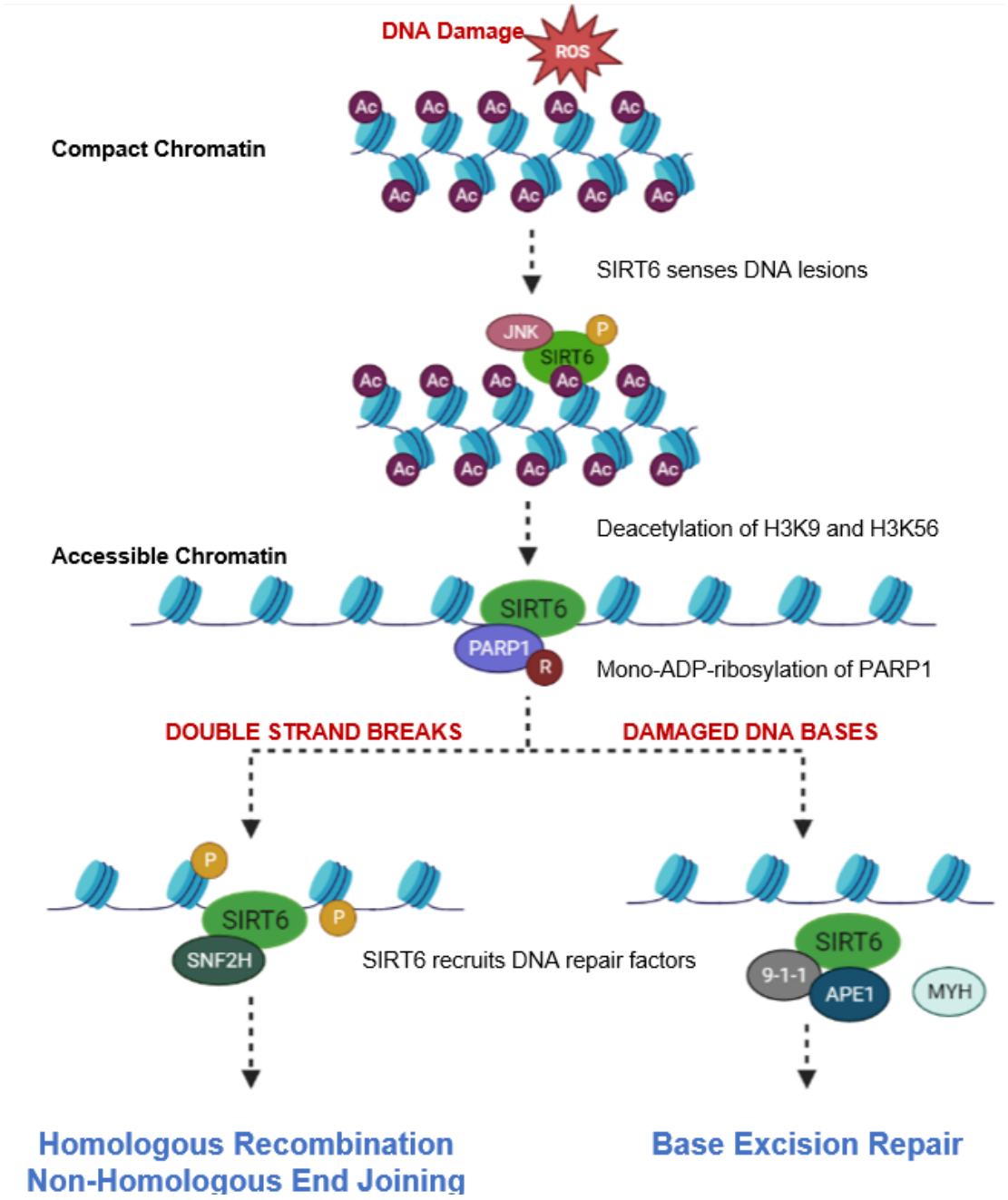

Figure 1.4: SIRT6 as a DNA Repair Agent. SIRT6 facilitates DNA repair by opening the compact chromatin of DNA and making it accessible for downstream repair factors. JNK-dependent phosphorylation of SIRT6 assists in SIRT6's recruitment to sites of DNA damage. DNA repair is initiated by SIRT6 deacetylation of H3K9 and H3K56, followed by PARP1 ADP-ribosylation. Depending on the type of DNA damage, SIRT6 will recruit the appropriate repair factors for NHEJ/HR (double strand breaks) or BER (base damage). Figure created in Biorender.com.

REFERENCES

1. Hochberg M, Cisternas M. Osteoarthritis. BMUS: The Burden of Musculoskeletal Diseases in the United States. Accessed February 14, 2023. https://www.boneandjointburden.org/fourth-edition/iiib10/osteoarthritis

2. Cisternas MG, Murphy L, Sacks JJ, Solomon DH, Pasta DJ, Helmick CG. Alternative Methods for Defining Osteoarthritis and the Impact on Estimating Prevalence in a US Population-Based Survey. *Arthritis Care Res (Hoboken)*. 2016;68(5):574-580. doi:10.1002/acr.22721

3. Leardini G, Salaffi F, Caporali R, et al. Direct and indirect costs of osteoarthritis of the knee. *Clin Exp Rheumatol*. 2004;22(6):699-706.

4. Wieland HA, Michaelis M, Kirschbaum BJ, Rudolphi KA. Osteoarthritis — an untreatable disease? *Nat Rev Drug Discov*. 2005;4(4):331-344. doi:10.1038/nrd1693

5. Jevsevar DS. Treatment of Osteoarthritis of the Knee: Evidence-Based Guideline, 2nd Edition. *JAAOS - Journal of the American Academy of Orthopaedic Surgeons*. 2013;21(9):571. doi:10.5435/JAAOS-21-09-571

6. Losina E, Paltiel AD, Weinstein AM, et al. Lifetime Medical Costs of Knee Osteoarthritis Management in the United States: Impact of Extending Indications for Total Knee Arthroplasty. *Arthritis Care & Research*. 2015;67(2):203-215. doi:10.1002/acr.22412

7. Grässel S, Muschter D. Recent advances in the treatment of osteoarthritis. *F1000Res*. 2020;9:F1000 Faculty Rev-325. doi:10.12688/f1000research.22115.1

8. Barbour KE, Helmick CG, Boring M, Brady TJ. Vital Signs: Prevalence of Doctor-Diagnosed Arthritis and Arthritis-Attributable Activity Limitation - United States, 2013-2015. *MMWR Morb Mortal Wkly Rep*. 2017;66(9):246-253. doi:10.15585/mmwr.mm6609e1

9. Loeser RF, Goldring SR, Scanzello CR, Goldring MB. Osteoarthritis: a disease of the joint as an organ. *Arthritis Rheum*. 2012;64(6):1697-1707. doi:10.1002/art.34453

10. Ammendola S, Scotto d'Abusco A. Chapter 7 - Oxidative stress, senescence and Mediterranean diet effects on osteoarthritis. In: Preedy VR, Patel VB, eds. *Aging (Second Edition)*. Academic Press; 2020:73-81. doi:10.1016/B978-0-12-818698-5.00007-9

11. Goldring MB. Chondrogenesis, chondrocyte differentiation, and articular cartilage metabolism in health and osteoarthritis. *Ther Adv Musculoskelet Dis*. 2012;4(4):269-285. doi:10.1177/1759720X12448454

12. Goldring MB, Marcu KB. Cartilage homeostasis in health and rheumatic diseases. *Arthritis Res Ther*. 2009;11(3):224. doi:10.1186/ar2592

13. Zhang Y, Jordan JM. Epidemiology of Osteoarthritis. *Clin Geriatr Med*. 2010;26(3):355-369. doi:10.1016/j.cger.2010.03.001

14. Johnson VL, Hunter DJ. The epidemiology of osteoarthritis. *Best Pract Res Clin Rheumatol*. 2014;28(1):5-15. doi:10.1016/j.berh.2014.01.004

15. López-Otín C, Blasco MA, Partridge L, Serrano M, Kroemer G. The hallmarks of aging. *Cell*. 2013;153(6):1194-1217. doi:10.1016/j.cell.2013.05.039

16. Kuilman T, Michaloglou C, Mooi WJ, Peeper DS. The essence of senescence. *Genes Dev*. 2010;24(22):2463-2479. doi:10.1101/gad.1971610

17. van Deursen JM. The role of senescent cells in ageing. *Nature*. 2014;509(7501):439-446. doi:10.1038/nature13193

18. Ren JL, Pan JS, Lu YP, Sun P, Han J. Inflammatory signaling and cellular senescence. *Cellular Signalling*. 2009;21(3):378-383. doi:10.1016/j.cellsig.2008.10.011

19. Prieur A, Peeper DS. Cellular senescence in vivo: a barrier to tumorigenesis. *Current Opinion in Cell Biology*. 2008;20(2):150-155. doi:10.1016/j.ceb.2008.01.007

20. Zhang L, Pitcher LE, Yousefzadeh MJ, Niedernhofer LJ, Robbins PD, Zhu Y. Cellular senescence: a key therapeutic target in aging and diseases. *J Clin Invest*. 2022;132(15):e158450. doi:10.1172/JCI158450

21. Hayflick L, Moorhead PS. The serial cultivation of human diploid cell strains. *Experimental Cell Research*. 1961;25(3):585-621. doi:10.1016/0014-4827(61)90192-6

22. Muñoz-Espín D, Serrano M. Cellular senescence: from physiology to pathology. *Nat Rev Mol Cell Biol*. 2014;15(7):482-496. doi:10.1038/nrm3823

23. Feng T, Meng J, Kou S, et al. CCN1-Induced Cellular Senescence Promotes Heart Regeneration. *Circulation*. 2019;139(21):2495-2498. doi:10.1161/CIRCULATIONAHA.119.039530

24. Muñoz-Espín D, Cañamero M, Maraver A, et al. Programmed cell senescence during mammalian embryonic development. *Cell*. 2013;155(5):1104-1118. doi:10.1016/j.cell.2013.10.019

25. Demaria M, Ohtani N, Youssef SA, et al. An Essential Role for Senescent Cells in Optimal Wound Healing through Secretion of PDGF-AA. *Dev Cell*. 2014;31(6):722-733. doi:10.1016/j.devcel.2014.11.012

26. Helman A, Klochendler A, Azazmeh N, et al. p16(Ink4a)-induced senescence of pancreatic beta cells enhances insulin secretion. *Nat Med*. 2016;22(4):412-420. doi:10.1038/nm.4054

27. Collado M, Blasco MA, Serrano M. Cellular Senescence in Cancer and Aging. *Cell*. 2007;130(2):223-233. doi:10.1016/j.cell.2007.07.003

28. Senescent Cells in Cancer Therapy: Friends or Foes? - ScienceDirect. Accessed February 18, 2023. https://www-sciencedirect-com.libproxy.lib.unc.edu/science/article/pii/S240580332030159X?via%3Dihub

29. Sturmlechner I, Zhang C, Sine CC, et al. p21 produces a bioactive secretome that places stressed cells under immunosurveillance. *Science*. 2021;374(6567):eabb3420. doi:10.1126/science.abb3420

30. Ovadya Y, Landsberger T, Leins H, et al. Impaired immune surveillance accelerates accumulation of senescent cells and aging. *Nat Commun*. 2018;9(1):1-15. doi:10.1038/s41467-018-07825-3

31. Dimri GP, Lee X, Basile G, et al. A biomarker that identifies senescent human cells in culture and in aging skin in vivo. *Proc Natl Acad Sci U S A*. 1995;92(20):9363-9367.

32. Herbig U, Ferreira M, Condel L, Carey D, Sedivy JM. Cellular senescence in aging primates. *Science*. 2006;311(5765):1257. doi:10.1126/science.1122446

33. Yousefzadeh MJ, Zhao J, Bukata C, et al. Tissue specificity of senescent cell accumulation during physiologic and accelerated aging of mice. *Aging Cell*. Published online January 25, 2020:e13094. doi:10.1111/acel.13094

34. Jeon OH, David N, Campisi J, Elisseeff JH. Senescent cells and osteoarthritis: a painful connection. *J Clin Invest*. 2018;128(4):1229-1237. doi:10.1172/JCI95147

35. Smith B, Sigal IR, Grande DA. Immunology and cartilage regeneration. *Immunol Res*. 2015;63(1):181-186. doi:10.1007/s12026-015-8720-7

36. Wu CM, Zheng L, Wang Q, Hu YW. The emerging role of cell senescence in atherosclerosis. *Clin Chem Lab Med*. 2020;59(1):27-38. doi:10.1515/cclm-2020-0601

37. Palmer AK, Gustafson B, Kirkland JL, Smith U. Cellular senescence: at the nexus between ageing and diabetes. *Diabetologia*. 2019;62(10):1835-1841. doi:10.1007/s00125-019-4934-x

38. Diekman BO, Sessions GA, Collins JA, et al. Expression of p16INK 4a is a biomarker of chondrocyte aging but does not cause osteoarthritis. *Aging Cell*. 2018;17(4). doi:10.1111/acel.12771

39. Krizhanovsky V, Xue W, Zender L, Yon M, Hernando E, Lowe SW. Implications of Cellular Senescence in Tissue Damage Response, Tumor Suppression, and Stem Cell Biology. *Cold Spring Harb Symp Quant Biol*. 2008;73:513-522. doi:10.1101/sqb.2008.73.048

40. Kumari R, Jat P. Mechanisms of Cellular Senescence: Cell Cycle Arrest and Senescence Associated Secretory Phenotype. *Frontiers in Cell and Developmental Biology*. 2021;9. Accessed February 8, 2023. https://www.frontiersin.org/articles/10.3389/fcell.2021.645593

41. Debacq-Chainiaux F, Ben Ameur R, Bauwens E, Dumortier E, Toutfaire M, Toussaint O. Stress-Induced (Premature) Senescence. In: Rattan SIS, Hayflick L, eds. *Cellular Ageing and Replicative Senescence*. Healthy Ageing and Longevity. Springer International Publishing; 2016:243-262. doi:10.1007/978-3-319-26239-0_13

42. Harley CB, Futcher AB, Greider CW. Telomeres shorten during ageing of human fibroblasts. *Nature*. 1990;345(6274):458-460. doi:10.1038/345458a0

43. Chandeck C, Mooi WJ. Oncogene-induced cellular senescence. *Adv Anat Pathol*. 2010;17(1):42-48. doi:10.1097/PAP.0b013e3181c66f4e

44. Aigner T, Hemmel M, Neureiter D, et al. Apoptotic cell death is not a widespread phenomenon in normal aging and osteoarthritis human articular knee cartilage: a study of proliferation, programmed cell death (apoptosis), and viability of chondrocytes in normal and osteoarthritic human knee cartilage. *Arthritis Rheum*. 2001;44(6):1304-1312. doi:10.1002/1529-0131(200106)44:6<1304::AID-ART222>3.0.CO;2-T

45. Hernandez-Segura A, Nehme J, Demaria M. Hallmarks of Cellular Senescence. *Trends in Cell Biology*. 2018;28(6):436-453. doi:10.1016/j.tcb.2018.02.001

46. He S, Sharpless NE. Senescence in Health and Disease. *Cell*. 2017;169(6):1000-1011. doi:10.1016/j.cell.2017.05.015

47. Di Leonardo A, Linke SP, Clarkin K, Wahl GM. DNA damage triggers a prolonged p53-dependent G1 arrest and long-term induction of Cip1 in normal human fibroblasts. *Genes Dev*. 1994;8(21):2540-2551. doi:10.1101/gad.8.21.2540

48. Gorgoulis V, Adams PD, Alimonti A, et al. Cellular Senescence: Defining a Path Forward. *Cell*. 2019;179(4):813-827. doi:10.1016/j.cell.2019.10.005

49. Herranz N, Gil J. Mechanisms and functions of cellular senescence. *J Clin Invest*. 2018;128(4):1238-1246. doi:10.1172/JCI95148

50. González-Gualda E, Baker AG, Fruk L, Muñoz-Espín D. A guide to assessing cellular senescence in vitro and in vivo. *The FEBS Journal*. 2021;288(1):56-80. doi:10.1111/febs.15570

51. Childs BG, Baker DJ, Kirkland JL, Campisi J, van Deursen JM. Senescence and apoptosis: dueling or complementary cell fates? *EMBO Rep*. 2014;15(11):1139-1153. doi:10.15252/embr.201439245

52. Rovillain E, Mansfield L, Caetano C, et al. Activation of nuclear factor-kappa B signalling promotes cellular senescence. *Oncogene*. 2011;30(20):2356-2366. doi:10.1038/onc.2010.611

53. Burd CE, Sorrentino JA, Clark KS, et al. Monitoring Tumorigenesis and Senescence In Vivo with a p16INK4a-Luciferase Model. *Cell*. 2013;152(1):340-351. doi:10.1016/j.cell.2012.12.010

54. McConnell BB, Starborg M, Brookes S, Peters G. Inhibitors of cyclin-dependent kinases induce features of replicative senescence in early passage human diploid fibroblasts. *Curr Biol*. 1998;8(6):351-354. doi:10.1016/s0960-9822(98)70137-x

55. Kurz DJ, Decary S, Hong Y, Erusalimsky JD. Senescence-associated (beta)-galactosidase reflects an increase in lysosomal mass during replicative ageing of human endothelial cells. *J Cell Sci*. 2000;113 (Pt 20):3613-3622. doi:10.1242/jcs.113.20.3613

56. Young ARJ, Narita M, Ferreira M, et al. Autophagy mediates the mitotic senescence transition. *Genes Dev*. 2009;23(7):798-803. doi:10.1101/gad.519709

57. Debacq-Chainiaux F, Erusalimsky JD, Campisi J, Toussaint O. Protocols to detect senescence-associated beta-galactosidase (SA-betagal) activity, a biomarker of senescent cells in culture and in vivo. *Nat Protoc*. 2009;4(12):1798-1806. doi:10.1038/nprot.2009.191

58. Copp ME, Flanders MC, Gagliardi R, et al. The combination of mitogenic stimulation and DNA damage induces chondrocyte senescence. *Osteoarthritis and Cartilage*. 2021;29(3):402-412. doi:10.1016/j.joca.2020.11.004

59. Shiloh Y. The ATM-mediated DNA-damage response: taking shape. *Trends Biochem Sci*. 2006;31(7):402-410. doi:10.1016/j.tibs.2006.05.004

60. Sadaie M, Salama R, Carroll T, et al. Redistribution of the Lamin B1 genomic binding profile affects rearrangement of heterochromatic domains and SAHF formation during senescence. *Genes Dev*. 2013;27(16):1800-1808. doi:10.1101/gad.217281.113

61. Ivanov A, Pawlikowski J, Manoharan I, et al. Lysosome-mediated processing of chromatin in senescence. *J Cell Biol*. 2013;202(1):129-143. doi:10.1083/jcb.201212110

62. Sharpless NE, Sherr CJ. Forging a signature of in vivo senescence. *Nature Reviews Cancer*. 2015;15(7):397-408. doi:10.1038/nrc3960

63. Coppé JP, Desprez PY, Krtolica A, Campisi J. The Senescence-Associated Secretory Phenotype: The Dark Side of Tumor Suppression. *Annu Rev Pathol*. 2010;5:99-118. doi:10.1146/annurev-pathol-121808-102144

64. Ohanna M, Giuliano S, Bonet C, et al. Senescent cells develop a PARP-1 and nuclear factor-{kappa}B-associated secretome (PNAS). *Genes Dev*. 2011;25(12):1245-1261. doi:10.1101/gad.625811

65. Yang H, Wang H, Ren J, Chen Q, Chen ZJ. cGAS is essential for cellular senescence. *Proc Natl Acad Sci U S A*. 2017;114(23):E4612-E4620. doi:10.1073/pnas.1705499114

66. Herranz N, Gallage S, Mellone M, et al. mTOR regulates MAPKAPK2 translation to control the senescence-associated secretory phenotype. *Nat Cell Biol*. 2015;17(9):1205-1217. doi:10.1038/ncb3225

67. Freund A, Patil CK, Campisi J. p38MAPK is a novel DNA damage response-independent regulator of the senescence-associated secretory phenotype. *EMBO J*. 2011;30(8):1536-1548. doi:10.1038/emboj.2011.69

68. Franceschi C, Campisi J. Chronic inflammation (inflammaging) and its potential contribution to age-associated diseases. *J Gerontol A Biol Sci Med Sci*. 2014;69 Suppl 1:S4-9. doi:10.1093/gerona/glu057

69. Hernandez-Segura A, de Jong TV, Melov S, Guryev V, Campisi J, Demaria M. Unmasking Transcriptional Heterogeneity in Senescent Cells. *Curr Biol*. 2017;27(17):2652-2660.e4. doi:10.1016/j.cub.2017.07.033

70. Zhang L, Pitcher LE, Prahalad V, Niedernhofer LJ, Robbins PD. Targeting cellular senescence with senotherapeutics: senolytics and senomorphics. *The FEBS Journal*. n/a(n/a). doi:10.1111/febs.16350

71. Baker DJ, Wijshake T, Tchkonia T, et al. Clearance of p16Ink4a-positive senescent cells delays ageing-associated disorders. *Nature*. 2011;479(7372):232-236. doi:10.1038/nature10600

72. Guzman SD, Judge J, Shigdar SM, et al. Removal of p16INK4 Expressing Cells in Late Life has Moderate Beneficial Effects on Skeletal Muscle Function in Male Mice. *Frontiers in Aging*. 2022;2. Accessed February 20, 2023. https://www.frontiersin.org/articles/10.3389/fragi.2021.821904

73. Yang H, Chen C, Chen H, et al. Navitoclax (ABT263) reduces inflammation and promotes chondrogenic phenotype by clearing senescent osteoarthritic chondrocytes in osteoarthritis. *Aging (Albany NY)*. 2020;12(13):12750-12770. doi:10.18632/aging.103177

74. Bussian TJ, Aziz A, Meyer CF, Swenson BL, van Deursen JM, Baker DJ. Clearance of senescent glial cells prevents tau-dependent pathology and cognitive decline. *Nature*. 2018;562(7728):578-582. doi:10.1038/s41586-018-0543-y

75. Jeon OH, Kim C, Laberge RM, et al. Local clearance of senescent cells attenuates the development of post-traumatic osteoarthritis and creates a pro-regenerative environment. *Nat Med*. 2017;23(6):775-781. doi:10.1038/nm.4324

76. Sessions GA, Copp ME, Liu JY, Sinkler MA, D'Costa S, Diekman BO. Controlled induction and targeted elimination of p16INK4a-expressing chondrocytes in cartilage explant culture. *FASEB J*. 2019;33(11):12364-12373. doi:10.1096/fj.201900815RR

77. Schumacher B, Pothof J, Vijg J, Hoeijmakers JHJ. The central role of DNA damage in the ageing process. *Nature*. 2021;592(7856):695-703. doi:10.1038/s41586-021-03307-7

78. Yousefzadeh M, Henpita C, Vyas R, Soto-Palma C, Robbins P, Niedernhofer L. DNA damage—how and why we age? Simon M, Tyler JK, eds. *eLife*. 2021;10:e62852. doi:10.7554/eLife.62852

79. Nikitaki Z, Hellweg CE, Georgakilas AG, Ravanat JL. Stress-induced DNA damage biomarkers: applications and limitations. *Frontiers in Chemistry*. 2015;3. Accessed February 22, 2023. https://www.frontiersin.org/articles/10.3389/fchem.2015.00035

80. Chatterjee N, Walker GC. Mechanisms of DNA damage, repair and mutagenesis. *Environ Mol Mutagen*. 2017;58(5):235-263. doi:10.1002/em.22087

81. Hoeijmakers JHJ. DNA damage, aging, and cancer. *N Engl J Med*. 2009;361(15):1475-1485. doi:10.1056/NEJMra0804615

82. Giglia-Mari G, Zotter A, Vermeulen W. DNA Damage Response. *Cold Spring Harb Perspect Biol*. 2011;3(1):a000745. doi:10.1101/cshperspect.a000745

83. Aziz K, Nowsheen S, Pantelias G, Iliakis G, Gorgoulis VG, Georgakilas AG. Targeting DNA damage and repair: Embracing the pharmacological era for successful cancer therapy. *Pharmacology & Therapeutics*. 2012;133(3):334-350. doi:10.1016/j.pharmthera.2011.11.010

84. Sancar A, Lindsey-Boltz LA, Ünsal-Kaçmaz K, Linn S. Molecular Mechanisms of Mammalian DNA Repair and the DNA Damage Checkpoints. *Annual Review of Biochemistry*. 2004;73(1):39-85. doi:10.1146/annurev.biochem.73.011303.073723

85. Lindahl T. Instability and decay of the primary structure of DNA. *Nature*. 1993;362(6422):709-715. doi:10.1038/362709a0

86. Branzei D, Foiani M. Regulation of DNA repair throughout the cell cycle. *Nat Rev Mol Cell Biol*. 2008;9(4):297-308. doi:10.1038/nrm2351

87. Aquilina G, Crescenzi M, Bignami M. Mismatch repair, G 2 /M cell cycle arrest and lethality after DNA damage. *Carcinogenesis*. 1999;20(12):2317-2326. doi:10.1093/carcin/20.12.2317

88. Izumi T, Mellon I. Chapter 17 - Base Excision Repair and Nucleotide Excision Repair. In: Kovalchuk I, Kovalchuk O, eds. *Genome Stability*. Academic Press; 2016:275-302. doi:10.1016/B978-0-12-803309-8.00017-3

89. Scully R, Panday A, Elango R, Willis NA. DNA double-strand break repair-pathway choice in somatic mammalian cells. *Nat Rev Mol Cell Biol*. 2019;20(11):698-714. doi:10.1038/s41580-019-0152-0

90. Mao Z, Bozzella M, Seluanov A, Gorbunova V. DNA repair by nonhomologous end joining and homologous recombination during cell cycle in human cells. *Cell Cycle*. 2008;7(18):2902-2906.

91. Reid DA, Reed PJ, Schlachetzki JCM, et al. Incorporation of a nucleoside analog maps genome repair sites in postmitotic human neurons. *Science*. 2021;372(6537):91-94. doi:10.1126/science.abb9032

92. Narciso L, Fortini P, Pajalunga D, et al. Terminally differentiated muscle cells are defective in base excision DNA repair and hypersensitive to oxygen injury. *Proc Natl Acad Sci U S A*. 2007;104(43):17010-17015. doi:10.1073/pnas.0701743104

93. Wu W, Hill SE, Nathan WJ, et al. Neuronal enhancers are hotspots for DNA single-strand break repair. *Nature*. 2021;593(7859):440-444. doi:10.1038/s41586-021-03468-5

94. Fishel ML, Vasko MR, Kelley MR. DNA repair in neurons: so if they don't divide what's to repair? *Mutat Res*. 2007;614(1-2):24-36. doi:10.1016/j.mrfmmm.2006.06.007

95. Figueroa-González G, Pérez-Plasencia C. Strategies for the evaluation of DNA damage and repair mechanisms in cancer. *Oncol Lett*. 2017;13(6):3982-3988. doi:10.3892/ol.2017.6002

96. Olive PL, Banáth JP. The comet assay: a method to measure DNA damage in individual cells. *Nat Protoc*. 2006;1(1):23-29. doi:10.1038/nprot.2006.5

97. Afanasieva K, Zazhytska M, Sivolob A. Kinetics of comet formation in single-cell gel electrophoresis: Loops and fragments. *ELECTROPHORESIS*. 2010;31(3):512-519. doi:10.1002/elps.200900421

98. Muruzabal D, Collins A, Azqueta A. The enzyme-modified comet assay: Past, present and future. *Food Chem Toxicol*. 2021;147:111865. doi:10.1016/j.fct.2020.111865

99. Smith CC, O'Donovan MR, Martin EA. hOGG1 recognizes oxidative damage using the comet assay with greater specificity than FPG or ENDOIII. *Mutagenesis*. 2006;21(3):185-190. doi:10.1093/mutage/gel019

100. Zhu S, Coffman JA. Simple and fast quantification of DNA damage by real-time PCR, and its application to nuclear and mitochondrial DNA from multiple tissues of aging zebrafish. *BMC Research Notes*. 2017;10. doi:10.1186/s13104-017-2593-x

101. Mullins EA, Rubinson EH, Pereira KN, Calcutt MW, Christov PP, Eichman BF. An HPLC-tandem mass spectrometry method for simultaneous detection of alkylated base excision repair products. *Methods*. 2013;64(1):59-66. doi:10.1016/j.ymeth.2013.07.020

102. Dizdaroglu M. Substrate specificities and excision kinetics of DNA glycosylases involved in base-excision repair of oxidative DNA damage. *Mutat Res*. 2003;531(1-2):109-126. doi:10.1016/j.mrfmmm.2003.07.003

103. Dizdaroglu M, Coskun E, Jaruga P. Measurement of oxidatively induced DNA damage and its repair, by mass spectrometric techniques. *Free Radic Res*. 2015;49(5):525-548. doi:10.3109/10715762.2015.1014814

104. Mah LJ, El-Osta A, Karagiannis TC. γH2AX: a sensitive molecular marker of DNA damage and repair. *Leukemia*. 2010;24(4):679-686. doi:10.1038/leu.2010.6

105. Fell VL, Schild-Poulter C. Ku Regulates Signaling to DNA Damage Response Pathways through the Ku70 von Willebrand A Domain. *Mol Cell Biol*. 2012;32(1):76-87. doi:10.1128/MCB.05661-11

106. London RE. The structural basis of XRCC1-mediated DNA repair. *DNA Repair (Amst)*. 2015;30:90-103. doi:10.1016/j.dnarep.2015.02.005

107. Lombard DB. Sirtuins at the Breaking Point: SIRT6 in DNA Repair. *Aging (Albany NY)*. 2009;1(1):12-16.

108. Gorbunova V, Seluanov A, Mao Z, Hine C. Changes in DNA repair during aging. *Nucleic Acids Research*. 2007;35(22):7466-7474. doi:10.1093/nar/gkm756

109. Chen Y, Geng A, Zhang W, et al. Fight to the bitter end: DNA repair and aging. *Ageing Res Rev*. 2020;64:101154. doi:10.1016/j.arr.2020.101154

110. Chevanne M, Caldini R, Tombaccini D, Mocali A, Gori G, Paoletti F. Comparative levels of DNA breaks and sensitivity to oxidative stress in aged and senescent human fibroblasts: a distinctive pattern for centenarians. *Biogerontology*. 2003;4(2):97-104. doi:10.1023/a:1023399820770

111. Singh NP, Danner DB, Tice RR, Brant L, Schneider EL. DNA damage and repair with age in individual human lymphocytes. *Mutat Res*. 1990;237(3-4):123-130. doi:10.1016/0921-8734(90)90018-m

112. Crabbe L, Jauch A, Naeger CM, Holtgreve-Grez H, Karlseder J. Telomere dysfunction as a cause of genomic instability in Werner syndrome. *Proceedings of the National Academy of Sciences*. 2007;104(7):2205-2210. doi:10.1073/pnas.0609410104

113. Gonzalo S, Kreienkamp R. DNA repair defects and genome instability in Hutchinson–Gilford Progeria Syndrome. *Current Opinion in Cell Biology*. 2015;34:75-83. doi:10.1016/j.ceb.2015.05.007

114. Caldecott KW. DNA single-strand break repair and human genetic disease. *Trends in Cell Biology*. 2022;32(9):733-745. doi:10.1016/j.tcb.2022.04.010

115. Sedelnikova OA, Horikawa I, Zimonjic DB, Popescu NC, Bonner WM, Barrett JC. Senescing human cells and ageing mice accumulate DNA lesions with unrepairable double-strand breaks. *Nat Cell Biol*. 2004;6(2):168-170. doi:10.1038/ncb1095

116. Hamilton ML, Van Remmen H, Drake JA, et al. Does oxidative damage to DNA increase with age? *Proc Natl Acad Sci U S A*. 2001;98(18):10469-10474. doi:10.1073/pnas.171202698

117. Adler AS, Sinha S, Kawahara TLA, Zhang JY, Segal E, Chang HY. Motif module map reveals enforcement of aging by continual NF-kappaB activity. *Genes Dev*. 2007;21(24):3244-3257. doi:10.1101/gad.1588507

118. Rose J, Söder S, Skhirtladze C, et al. DNA damage, discoordinated gene expression and cellular senescence in osteoarthritic chondrocytes. *Osteoarthr Cartil*. 2012;20(9):1020-1028. doi:10.1016/j.joca.2012.05.009

119. Davies CM, Guilak F, Weinberg JB, Fermor B. Reactive nitrogen and oxygen species in interleukin-1-mediated DNA damage associated with osteoarthritis. *Osteoarthritis Cartilage*. 2008;16(5):624-630. doi:10.1016/j.joca.2007.09.012

120. Farmer H, McCabe N, Lord CJ, et al. Targeting the DNA repair defect in BRCA mutant cells as a therapeutic strategy. *Nature*. 2005;434(7035):917-921. doi:10.1038/nature03445

121. Imai S ichiro, Armstrong CM, Kaeberlein M, Guarente L. Transcriptional silencing and longevity protein Sir2 is an NAD-dependent histone deacetylase. *Nature*. 2000;403(6771):795-800. doi:10.1038/35001622

122. Chang AR, Ferrer CM, Mostoslavsky R. SIRT6, a Mammalian Deacylase with Multitasking Abilities. *Physiol Rev*. 2020;100(1):145-169. doi:10.1152/physrev.00030.2018

123. Peshti V, Obolensky A, Nahum L, et al. Characterization of physiological defects in adult SIRT6-/- mice. *PLoS One*. 2017;12(4):e0176371. doi:10.1371/journal.pone.0176371

124. Mao Z, Hine C, Tian X, et al. SIRT6 promotes DNA repair under stress by activating PARP1. *Science*. 2011;332(6036):1443-1446. doi:10.1126/science.1202723

125. Toiber D, Erdel F, Bouazoune K, et al. SIRT6 recruits SNF2H to DNA break sites, preventing genomic instability through chromatin remodeling. *Mol Cell*. 2013;51(4):454-468. doi:10.1016/j.molcel.2013.06.018

126. Hou T, Cao Z, Zhang J, et al. SIRT6 coordinates with CHD4 to promote chromatin relaxation and DNA repair. *Nucleic Acids Research*. 2020;48(6):2982-3000. doi:10.1093/nar/gkaa006

127. Jia G, Su L, Singhal S, Liu X. Emerging roles of SIRT6 on telomere maintenance, DNA repair, metabolism and mammalian aging. *Mol Cell Biochem*. 2012;364(1-2):345-350. doi:10.1007/s11010-012-1236-8

128. Xu Z, Zhang L, Zhang W, et al. SIRT6 rescues the age related decline in base excision repair in a PARP1-dependent manner. *Cell Cycle*. 2015;14(2):269-276. doi:10.4161/15384101.2014.980641

129. Li X, Liu L, Li T, et al. SIRT6 in Senescence and Aging-Related Cardiovascular Diseases. *Frontiers in Cell and Developmental Biology*. 2021;9. Accessed January 4, 2023. https://www.frontiersin.org/articles/10.3389/fcell.2021.641315

130. Onn L, Portillo M, Ilic S, et al. SIRT6 is a DNA double-strand break sensor. *eLife*. 9:e51636. doi:10.7554/eLife.51636

131. Mostoslavsky R, Chua KF, Lombard DB, et al. Genomic instability and aging-like phenotype in the absence of mammalian SIRT6. *Cell*. 2006;124(2):315-329. doi:10.1016/j.cell.2005.11.044

132. Tasselli L, Zheng W, Chua KF. SIRT6: novel mechanisms and links to aging and disease. *Trends Endocrinol Metab*. 2017;28(3):168-185. doi:10.1016/j.tem.2016.10.002

133. Kanfi Y, Naiman S, Amir G, et al. The sirtuin SIRT6 regulates lifespan in male mice. *Nature*. 2012;483(7388):218-221. doi:10.1038/nature10815

134. Nagai K, Matsushita T, Matsuzaki T, et al. Depletion of SIRT6 causes cellular senescence, DNA damage, and telomere dysfunction in human chondrocytes. *Osteoarthritis and Cartilage*. 2015;23(8):1412-1420. doi:10.1016/j.joca.2015.03.024

135. Kawahara TLA, Michishita E, Adler AS, et al. SIRT6 links histone H3 lysine 9 deacetylation to NF-kappaB-dependent gene expression and organismal life span. *Cell*. 2009;136(1):62-74. doi:10.1016/j.cell.2008.10.052

136. Klein MA, Denu JM. Biological and catalytic functions of sirtuin 6 as targets for small-molecule modulators. *J Biol Chem*. 2020;295(32):11021-11041. doi:10.1074/jbc.REV120.011438

137. Pan PW, Feldman JL, Devries MK, Dong A, Edwards AM, Denu JM. Structure and Biochemical Functions of SIRT6. *J Biol Chem*. 2011;286(16):14575-14587. doi:10.1074/jbc.M111.218990

138. Fiorentino F, Mai A, Rotili D. Emerging Therapeutic Potential of SIRT6 Modulators. *J Med Chem*. 2021;64(14):9732-9758. doi:10.1021/acs.jmedchem.1c00601

139. Feldman JL, Baeza J, Denu JM. Activation of the protein deacetylase SIRT6 by long-chain fatty acids and widespread deacylation by mammalian sirtuins. *J Biol Chem*. 2013;288(43):31350-31356. doi:10.1074/jbc.C113.511261

140. Huang Z, Zhao J, Deng W, et al. Identification of a cellularly active SIRT6 allosteric activator. *Nat Chem Biol*. 2018;14(12):1118-1126. doi:10.1038/s41589-018-0150-0

141. Fiorentino F, Carafa V, Favale G, Altucci L, Mai A, Rotili D. The Two-Faced Role of SIRT6 in Cancer. *Cancers*. 2021;13(5):1156. doi:10.3390/cancers13051156

142. Parenti MD, Grozio A, Bauer I, et al. Discovery of novel and selective SIRT6 inhibitors. *J Med Chem*. 2014;57(11):4796-4804. doi:10.1021/jm500487d

143. Gertz M, Fischer F, Nguyen GTT, et al. Ex-527 inhibits Sirtuins by exploiting their unique NAD+-dependent deacetylation mechanism. *Proc Natl Acad Sci U S A*. 2013;110(30):E2772-E2781. doi:10.1073/pnas.1303628110

144. Ji M liang, Jiang H, Li Z, et al. Sirt6 attenuates chondrocyte senescence and osteoarthritis progression. *Nat Commun*. 2022;13(1):7658. doi:10.1038/s41467-022-35424-w

145. Dvir-Ginzberg M, Mobasheri A, Kumar A. The Role of Sirtuins in Cartilage Homeostasis and Osteoarthritis. *Curr Rheumatol Rep*. 2016;18(7):43. doi:10.1007/s11926-016-0591-y

146. Collins JA, Kapustina M, Bolduc JA, et al. Sirtuin 6 (SIRT6) regulates redox homeostasis and signaling events in human articular chondrocytes. *Free Radical Biology and Medicine*. 2021;166:90-103. doi:10.1016/j.freeradbiomed.2021.01.054

147. Wu Y, Chen L, Wang Y, et al. Overexpression of Sirtuin 6 suppresses cellular senescence and NF-κB mediated inflammatory responses in osteoarthritis development. *Sci Rep*. 2015;5:17602. doi:10.1038/srep17602

148. Ailixiding M, Aibibula Z, Iwata M, et al. Pivotal role of Sirt6 in the crosstalk among ageing, metabolic syndrome and osteoarthritis. *Biochemical and Biophysical Research Communications*. 2015;466(3):319-326. doi:10.1016/j.bbrc.2015.09.019

CHAPTER 2: THE COMBINATION OF MITOGENIC STIMULATION AND DNA DAMAGE INDUCES CHONDROCYTE SENESCENCE[1]

2.1 INTRODUCTION

Osteoarthritis (OA) is a disease characterized by joint pain and progressive degradation of articular cartilage and other tissues of the joint[1,2]. As the most common chronic disease of the articular joint, OA produces a substantial burden on society and the economy[3,4]. Despite increasing knowledge about factors contributing to the progression of OA, there are no approved disease-modifying therapies[5], leading to high rates of total joint replacement[6]. Risk factors for OA include obesity, joint injury, and genetic predisposition, with the most dominant risk factor being aging[7,8]. Cellular senescence has been described as a key phenotype associated with aging[9], and there is mounting evidence that the accumulation of senescent cells in the joint during both aging and in response to injury contributes to the development of OA[10–14]. Senescent chondrocytes likely contribute to tissue degradation by producing pro-inflammatory and matrix-degrading molecules known collectively as the senescence-associated secretory phenotype (SASP)[15,16]. Significant advances have begun to unravel the role of senescence in OA and the therapeutic implications of such findings, including the potential for senolytic therapy as a potential disease-modifying therapy[13,17]. However, there has been less progress in understanding the underlying biologic processes that drive the accumulation of senescent cells in the joint space. With clinical trials that target senescent cells in the joint underway (e.g. NCT03513016), it is imperative to identify the physiological contexts that promote senescence induction[18]. The goal of this study was to investigate the mechanisms of senescence induction in articular cartilage through the use of explants from healthy equine and human cadaveric donors.

---

[1] The following chapter was published in Osteoarthritis and Cartilage.

Copp ME, Flanders MC, Gagliardi R, et al. The combination of mitogenic stimulation and DNA damage induces chondrocyte senescence. *Osteoarthritis and Cartilage*. 2021;29(3):402-412. doi:10.1016/j.joca.2020.11.004

Senescent cells display stable cell cycle arrest even in an environment that would normally promote cell division, which distinguishes the senescent phenotype from quiescence[19]. Indeed, there is evidence that a pro-growth environment – termed expansion signals to account for stimuli associated with proliferation or cellular hypertrophy – drives senescence induction in cells harboring strong growth arrest (reviewed in [20]). The upregulation of metabolic processes associated with an ongoing stress response, combined with absence of division, result in abnormally high lysosomal activity in senescent cells. This feature has been used to identify senescence through detection of β-galactosidase activity at the sub-optimal pH of 6.0 – the senescence-associated β-galactosidase (SA-β-gal) assay[21,22]. We recently used cartilage explants from $p16^{tdTomato}$ knock-in senescence reporter mice[23] to show that transforming growth factor beta (TGF-β1) and basic fibroblastic growth factor (bFGF), both of which are released from cartilage tissue in response to injury and degradation, were potent inducers of senescence by the measure of *$p16^{Ink4a}$* promoter activity[24]. In this study, we implement a quantitative flow-cytometry-based assay of SA-β-gal activity to demonstrate that the combination of cellular damage (by irradiation) and cell-expansion stimuli (through culture with growth factors) induces a senescent phenotype.

2.2 MATERIALS & METHODS

2.2.1 Acquisition of equine cartilage explants

Cartilage isolation was performed under IACUC approval at the North Carolina State University College of Veterinary Medicine from donor horses that were euthanized for reasons outside of this study. Horses were between 4 and 7 years of age and included 3 geldings and 4 non-parous mares. A series of 6 mm biopsy punches were taken from the femoral trochlear ridges of thoroughbred horses without known patellofemoral disease or any macroscopic signs of cartilage damage.

2.2.2 Acquisition of human cartilage explants

Tali from cadaveric ankle joints were obtained from organ donors within 24 hours of death through the Gift of Hope Organ and Tissue Donor Network (Itasca, IL). A tissue repository for donor material supported by the Material Transfer Agreement has been established within the Department of Pediatrics (Dr. Chubinskaya, Director) and has been approved by the Research and Clinical Trials Administration Office at Rush University Medical Center (Chicago, IL), ORA 08082803IRB01AM2. An

exemption for IRB approval was granted on February 15, 2016 according to the Deceased Subjects Rule. Samples were shipped overnight with ice packs to the University of North Carolina at Chapel Hill. Ankle tissue was used instead of knee tissue due to greater availability, but donor-matched comparisons of chondrocytes from ankle and femoral cartilage have shown a similar response to stimuli in culture[25]. Donors had no history of joint disease and ankle tissue was screened with a modified Collins grade on a 4-point scale[26]. Only ankle joints with grades of 0 – 2 (eliminating joints with evidence of erosion to the subchondral bone in any region) were used to avoid the confounding factor of extensive cartilage degeneration. Explants of 5 mm were taken from the talar surface for culture. Tissue was used from a total of 31 donors – 22 males and 9 females ranging from 38 to 73 years of age. Donor information is included in a table alongside the appropriate figures.

2.2.3 Explant culture for senescence induction

The experimental layout is provided as a schematic in **Figure 2.1**. Harvested equine explants were allowed to recover in 6-well plates for 3-7 days in the following control medium: DMEM/F12 medium (11330, Thermo Fisher Scientific, Waltham, MA), 10% fetal bovine serum (Seradigm 1500-500; VWR International, West Chester, PA, USA), penicillin and streptomycin (15140; Thermo Fisher Scientific), gentamicin (15750; Thermo Fisher Scientific), and amphotericin B (A2942; MilliporeSigma, Burlington, MA, USA). Half of the explants from each horse donor were irradiated with 10 Gy using a RS2000 Biological Irradiator, with the other half remaining as experimental controls. Post irradiation, the explants were cultured in the same control medium for 7 – 10 days before digestion for monolayer culture. Human cartilage explants were cultured in the same way as with equine explants, with the exception that mitogenic stimulation was included as an additional experimental factor. Mitogenic stimulus conditions were applied immediately after irradiation and consisted of control medium with the addition of 1 ng/mL TGF-β1 and 5 ng/mL basic fibroblastic growth factor (bFGF) (PHG9204 and PHG0264; Thermo Fisher Scientific).

2.2.4 Monolayer culture of primary chondrocytes for maturation of senescent phenotype

Following senescence induction in explant culture, chondrocytes were isolated from cartilage by enzymatic digestion with Pronase (1 hour) and subsequently with Collagenase P (overnight) as described previously[27]. The approximate yield was 100,000 cells per 5 mm diameter x ~1.5 mm depth explant.

Isolated chondrocytes were resuspended in 1 mL of media and plated in 12-well plates at a concentration of $6.4x10^4$ cells per cm^2. All cells (including those from the growth factor treated explants) were cultured in control medium, with media being changed every 2-3 days. The chondrocytes were cultured in monolayer for 10 – 12 days without passaging before SA-β-Gal flow cytometry analysis. Images of chondrocytes at the end of monolayer culture were taken with an EVOS FL microscope (Life Technologies, Carlsbad, CA).

2.2.5 Flow Cytometry Analysis of SA-β-gal

SA-β-gal activity in the chondrocytes after senescence induction and monolayer culture was evaluated using the CellEvent™ Senescence Green Flow Cytometry Assay Kit (C10840; Thermo Fisher Scientific). This kit utilizes the same principle as the traditional colorimetric SA-β-gal assay in that excessive galactosidase activity is detected at the sub-optimal pH of 6.0. In this case, the CellEvent™ probe contains two galactosidase moieties and cleavage releases a fluorescent signal that is retained in the cytoplasm for detection by flow cytometry. As consistent with the manufacturer recommendations, the working solution was prepared by diluting the CellEvent™ Senescence Green Probe (1,000X) into the CellEvent™ Senescence Buffer that had been warmed to 37°C. Chondrocytes to be analyzed were washed twice with 1x PBS (14190136, Gibco), incubated at 37°C for 5 minutes in Trypsin-EDTA (T4174; Sigma-Aldrich, St. Louis, MO), and neutralized with 50 µg/mL Soybean Trypsin Inhibitor (17075029, Thermo Fisher Scientific) with EDTA (46-034-CI, Corning, Corning, NY). The mixture was centrifuged at 800 xg for 6 minutes, washed with PBS, and fixed with 2% paraformaldehyde in PBS (1:1 volume of cells in PBS and 4% solution made from 16% stock, 43368, Alfa Aesar, Haverhill, MA) for 10 minutes at room temperature. Fixed cells were washed with 1% bovine serum albumin (A7906; Sigma Aldrich) in PBS and resuspended in 100 µL of the working solution. The chondrocytes were incubated with the dye at 37°C for 2 hours at 300 rpm in a ThermoMixer C (Eppendorf, Hamburg, Germany). After incubation, the chondrocytes were washed with 1 mL of PBS and resuspended in 200 µL of PBS. The stained cells were filtered with a 30-µm strainer to achieve a single-cell suspension. Flow cytometry analysis was performed using an Attune NxT (Thermo Fisher Scientific) with a 488 nm laser, and analysis performed using FCS Express 8 software (De Novo Software, Glendale, CA, USA).

2.2.6 Immunofluorescence

After explant digestion, cells were plated into 8-well chamber slides (Nunc Lab-Tek II, Thermo Fisher Scientific 154534) at the same density as other monolayer cultures. After 12 days, cells were fixed in 1% paraformaldehyde and permeabilized with 0.25% Triton X-100 to prepare for immunofluorescence. Cells were blocked with a solution of 1% BSA, 0.1% Tween, and 22.5 mg/ml glycine and then incubated overnight at 4°C with primary antibodies (p16: CINtec®, pre-diluted, Roche Diagnostics; γH2AX: sc-517348, 1:100, Santa Cruz Biotechnology). The CINtec® p16 antibody has been extensively characterized through its approved use in the evaluation of cervical biopsy specimens. Goat anti-mouse secondary antibodies (Thermo Fisher Scientific R37120) and NucBlue™ nuclear stain (Thermo Fisher Scientific R37605) were applied according to manufacturer recommendations. Quantification of p16 was performed using Image J to calculate the corrected total cell fluorescence of 50 cells per condition per donor. Briefly, the area of a cell is multiplied by the area integrated density of the fluorescence signal and this value is normalized to a background region near each analyzed cell. Quantification of γH2AX foci was performed using the “Find Maxima” tool in ImageJ. The number of foci were counted in approximately 100 nuclei per condition per donor. Following previous analysis strategies[28], the percentage of cells with 3 or more foci was calculated as a measure of cells with an ongoing DNA damage response.

2.2.7 Quantitative Polymerase Chain Reaction (qPCR)

After explant digestion, cells were plated into tissue culture plates for the purpose of subsequent RNA isolation and qPCR. After 7-12 days of monolayer culture, cells were washed with PBS and RLT buffer was directly added to lyse cells. RNA was isolated using RNeasy Mini columns (Qiagen 74104) and reverse transcription was performed using qScript XLT cDNA SuperMix (VWR International 95161). Taqman Universal Master Mix (Applied Biosystems 4304437) was used along with Taqman primer probes for the following genes: matrix metalloproteinase 13 (MMP-13, Hs00942584_m1), interleukin-6 (IL6, Hs00985639_m1), insulin-like growth factor binding protein 3 (IGFBP3, Hs00426289_m1), and C-C motif chemokine ligand 2 / monocyte chemoattractant protein 1 (CCL2, Hs00234140_m1), with TATA box binding protein (TBP, Hs00427620_m1) used as a housekeeping gene.

2.2.8 Histology and Chondrocyte Cluster Analysis

Human cartilage explants from 7 male and 2 female donors were fixed at the end of explant culture in 4% paraformaldehyde in PBS for 24 hours at 4°C and processed for paraffin embedding. Additionally, tissues from two sources were immediately fixed without culture: “healthy” tissue (Collins grade 0 or 1, 3 males and 3 females, average age 67.2 years) and de-identified OA waste tissue procured from total knee replacements performed at University of North Carolina Hospitals (3 males and 4 females, average age 67.6 years). Individual donor information is provided in Figure 2.5C and 2.5E. Sections of 5 µm thickness were collected on Superfrost™ Plus slides (12-550-15; Thermo Fisher Scientific). Slides were stained with Hematoxylin (nuclei) and Eosin (cytoplasm) to detect cell cluster formation in explants. Representative bright field images were taken with an Olympus BX60 microscope. Chondrocyte cluster analysis was assessed throughout the depth of cross-sectional histological sections that began at the superficial zone and extended into the middle zone. The number of chondrocytes in singlet, doublet, and triplet or more (triplet^{+}) clusters were counted and quantified using ImageJ.

2.2.9 Statistical Analyses

Statistical analysis and plotting were performed using Prism 8 (GraphPad, La Jolla, CA, USA) and flow cytometry data was processed with FCS Express 8 (De Novo Software, Glendale, CA, USA). Data are plotted as individual points with the mean shown. The error bars indicate the 95% confidence interval (CI) and these values are noted in parentheses on the appropriate plots. Outliers were identified using Grubbs test with $\alpha = 0.05$ and were excluded from subsequent analysis. Data from individual donors were excluded if the flow cytometry event count for any condition was less than 800 events. Outliers and excluded data are noted in the figure legends. Mean fluorescence intensity (MFI) data were normalized to the control condition for each donor to account for subtle differences in flow cytometry settings between days. Normalized MFI data in each treatment group were analyzed using a one-sample t-test against a hypothetical value of one and thus plots show a dotted line to represent this comparison. The percentage of SA-β-gal high cells was determined by introducing a cutoff at the mean plus two times the standard deviation of the control group. By Shapiro-Wilk test, these data were consistent with being sampled from a Gaussian distribution. Thus, this outcome measure was analyzed using a paired Student’s t-test (equine) or Two-Way ANOVA with Tukey’s Multiple Comparisons Test (human). Sample

size was determined by analyzing preliminary data on three donors for the effect size and variability. It was estimated that 5-10 equine donors and 10-20 human donors would be required to detect a doubling in the main outcome measure (percentage of SA-β-gal high cells), which we determined to be biologically meaningful. With this goal, we collected as many donors as feasible in the allocated experimental timeframe. Using a post-hoc effect size calculation in SAS (POWER procedure), we determined the minimum difference that could have been detected given the actual data (sample size, mean, standard deviation) at 0.9 power and alpha = 0.05. The minimum detectable difference was 17.72 for comparison of equine explants (control vs. irradiation) and 4.11 for comparison of human explants (control 10% vs. irradiated with growth factors).

2.3 RESULTS

2.3.1 Induction of senescence in equine cartilage explants

Cartilage explants harvested from the equine stifle (patellofemoral joint) were induced to senescence in explant culture with irradiation followed by culture in monolayer for maturation of the senescent phenotype (overview of experimental design illustrated in **Figure 2.1**). Chondrocytes from explants that had been irradiated revealed an enlarged and flattened morphology as compared to chondrocytes from control explants (**Figure 2.2A**). Flow cytometry for SA-β-gal activity was used to quantify the induction of senescence in the cartilage explants. A representative SA-β-gal flow plot from one equine donor is included, showing the shift in SA-β-gal fluorescence between chondrocytes cultured from the control and irradiated equine explants (**Figure 2.2B**). The region two standard deviations above the control mean fluorescence intensity (MFI) was delineated on the SA-β-gal flow plot and was used in this study to indicate the population of SA-β-gal high cells. Chondrocytes irradiated in explant culture had significantly increased SA-β-gal activity as compared to chondrocytes from control explants (2.40-fold increase, CI 0.22 to 2.58; $p = 0.027$ by one-sample t-test compared to a hypothetical value of 1; **Figure 2.2C**). The percentage of cells with high SA-β-gal activity also significantly increased in the irradiated condition as compared to control (mean difference: 21.57%, CI 10.48 to 32.65%; $p = 0.0031$ by paired t-test; **Figure 2.2D**). A table listing the age and sex of the equine donors is provided (**Figure 2.2E**).

2.3.2 Induction of senescence in human cartilage explants

Unlike equine cartilage explants, preliminary studies indicated that irradiation alone was insufficient to induce robust senescence in human articular cartilage explants. We hypothesized that mitogenic stimulation of damaged chondrocytes would initiate the senescence phenotype and tested this by supplementing the 10% FBS media with growth factors TGF-β1 and bFGF after irradiation. Cartilage explants harvested from cadaveric human ankles of 14 donors were cultured as described for the horse explants, with the only difference being the inclusion of growth factors during explant culture as an additional variable (**Figure 2.1**). As compared to control chondrocytes, cells digested from irradiated explants cultured with growth factors showed an enlarged morphology and the presence of bi-nucleated cells, which has been associated with senescence[29] (**Figure 2.3A**). Experiments testing the incorporation of EdU to mark cells in S phase showed that growth factor treatment during explant culture initiated cell cycle entry that persisted in monolayer culture under control conditions (**Supplemental Figure 2.1**). A representative SA-β-gal flow cytometry plot illustrates the robust shift in SA-β-gal fluorescence with both irradiation and growth factor treatment (**Figure 2.3B**). Chondrocytes from irradiated explants treated with TGF-β1 and bFGF showed significantly higher SA-β-gal MFI values as compared to the non-irradiated 10% FBS control (1.44 mean fold increase, CI 1.26 to 1.63; $p = 0.0002$ by one-sample t-test compared to a hypothetical value of 1; **Figure 2.3C**). By this measure, chondrocytes from irradiated explants without growth factors also showed a moderate increase in SA-β-gal MFI values as compared to the non-irradiated control (1.17 mean fold increase, CI 1.03 to 1.31; $p = 0.025$). When the percentage of SA-β-gal high cells was analyzed by Two-way ANOVA, both irradiation and media condition, as well as the interaction, were significant factors in senescence induction. Using Tukey's multiple comparison test, the irradiated explants cultured with growth factors were significantly different than all other conditions ($p<0.005$ to all conditions) (**Figure 2.3D**). A table listing the age and sex of the donors used in the irradiation experiments is provided (**Figure 2.3E**).

2.3.3 Additional markers of the senescence phenotype

Chondrocytes isolated from explants cultured in all four conditions (control or irradiation, 10% serum media or with the inclusion of growth factors) were plated in monolayer culture to perform additional analysis of the senescence phenotype. Analysis of γH2AX foci by immunofluorescence

indicated that both irradiation and TGF-β1/bFGF treatment were required to initiate a persistent DNA damage response (**Figure 2.4A and B**, 10.0% of cells with 3 or more foci, CI 5.0. to 15.0., all other conditions upper bound CI of ≤ 4.5.%). Quantification of p16 protein by immunofluorescence also showed the highest signal with the combination of irradiation and growth factors (**Figure 2.4C**). The confidence interval for this group did not overlap with the confidence interval of the baseline condition (**Figure 2.4D**, CI 13.5 to 23.2 arbitrary units per cell compared to upper bound of 10.3). Finally, qPCR analysis for 4 SASP factors was used to compare the group with the highest senescence induction (irradiation with growth factors) to the baseline control group of no irradiation with 10% serum media. This analysis showed an average fold increase of 1.29, 2.19, 1.99, and 1.68 for MMP-13, IL6, IGFBP3, and CCL2, respectively (**Figure 2.4E**). Of these genes, IGFBP3 and CCL2 had confidence intervals with lower bounds above 1 (1.01 to 2.97 for IGFBP3 and 1.04 to 2.32 for CCL2).

2.3.4 Cluster formation in response to senescence-inducing conditions

H&E staining of cartilage at the end of explant culture revealed an increase in the presence of chondrocyte clusters in conditions that also resulted in senescence induction – irradiation with growth factor treatment (**Figure 2.5A**). There was a statistically significant increase in the percentage of chondrocyte clusters in a triplet^{+} formation for the irradiation plus growth factors group as compared to all three of the other conditions ($p<0.0005$, Two-way ANOVA with Tukey's multiple comparison test; **Figure 2.5B**). The same analysis of clusters was applied to uncultured healthy cartilage (Collins grade 0 or 1) or waste OA tissue from total joint replacement. OA cartilage showed a significant increase in the percentage of clusters that are in triplet^{+} formation (28.49 with CI 22.9 to 34.08 vs. 9.69 with CI 7.01 to 12.37, $p=0.0006$ by t-test; **Figure 2.5D**).

2.4 DISCUSSION

This study demonstrates that treatment of articular cartilage explants with mitogenic stimuli in the context of DNA damage reliably induces high levels of SA-β gal activity (summarized in **Fig. 6**). By maintaining cell-matrix interactions, this approach provides a physiologically relevant setting to investigate the initiation of senescence. Detailed characterization of the origins of cellular senescence within cartilage may provide insight into why senescent cells accumulate to pathological levels in the joint space with age

and in response to joint injury. Greater understanding of senescence induction will also support the emerging therapeutic approach to target senescent cells with senolytics[30,31], which has shown promising results in animal models for post-traumatic and age-related OA[13].

The most widely used biomarker for senescence is SA-β-gal, which distinguishes senescent cells based on high lysosomal activity[32]. Traditionally, SA-β-gal activity is detected cytochemically using 5-bromo-4-chloro-3-indolyl-β-D-galactoside (X-gal) as a substrate and by discriminating negative from positive cells by visualization of blue color in cell culture images[33]. This manual process means that only a limited number of cells can be analyzed, and the readout is subjective and binary in nature. Conversely, the SA-β-gal flow cytometry approach utilized in this study provides a quantitative readout that captures the full range of lysosomal activity and is capable of analyzing tens of thousands of cells in a short time frame. Prior studies using a related but distinct flow cytometry readout of β-galactosidase activity revealed enhanced sensitivity as compared to the more widely used cytochemical method[33]. We also performed additional experiments to confirm that potential "false positive" signals due to confluency[34], autofluorescence[35], or the presence of dead cell did not interfere with the reported conclusion that irradiation and growth factor treatment increased true SA-β-gal activity **(Supplemental Figure 2.2)**.

Full characterization of the senescent state incorporates numerous orthogonal biomarkers[36]. Thus, we assayed the extent to which three additional features of senescence are present in chondrocytes induced by the combination of DNA damage and mitogenic stimulation. First, the combination resulted in an increased number of cells with widespread γH2AX foci at the end of the monolayer culture period, indicating a persistent DNA damage response as consistent with some forms of senescence induction. Note that 10 Gy irradiation initiates a strong acute DNA damage response in chondrocytes (approximately 50% at 30-120 minutes after irradiation in monolayer culture, **Supplemental Figure 2.3**), but growth factors are required to induce a stable DNA damage response in a substantial percentage of the chondrocytes (approximately 10%). Second, we quantified the level of $p16^{INK4a}$ protein by immunofluorescence and showed that this senescence biomarker is highest in cells that are exposed to irradiation and growth factors. This is consistent with our previous finding that human chondrocytes have higher expression of $p16^{INK4a}$ with aging, although DNA damage was not explicitly measured in that study[37]. Third, we investigated whether our senescence-inducing conditions also resulted in higher SASP

gene expression as compared to the control condition. While the specific components of the SASP vary based on cell type and induction stimulus, we elected to analyze expression of 4 SASP factors that are relevant to OA and had been examined in our previous work that treated murine cartilage with the same growth factor cocktail[24]. In that system, the senescence reporter allele $p16^{tdTom}$ allows for separation of senescent cells that enables a direct comparison to non-senescent cells from the same population. Results from that study showed that senescent chondrocytes express have higher expression of Igfbp3, Ccl2, and Il6 (but not Mmp-13). Similarly, the current study showed an increase in IGFBP3 and CCL2, with a trend towards increased IL6 and no change in MMP-13. The observed fold increase is modest, likely because the bulk population was investigated and the SA-β-gal activity results indicate that only a subset of chondrocytes become senescent in response to the applied conditions. It is important to recognize that each of the four measures (SA-β-gal, γH2AX foci, p16 immunofluorescence, and SASP) may not score the same subset of cells as "senescent" due to varied sensitivity of the assays and the heterogeneity of senescent population[36]. However, when assessed across the population of cells derived from each culture condition, these orthogonal measures provide support for the conclusion that the mitogenic stimulation and DNA damage combine to induce senescence in human chondrocytes.

The cartilage utilized in this study originated from the equine stifle and from cadaveric human cartilage explants. The horse is a representative model of naturally occurring human osteoarthritis due to the similarities between human and equine articular cartilage and subchondral bone thickness[38]. Further, spontaneous joint injury is common in horses and post-traumatic OA is an important challenge in veterinary care[39,40]. In contrast to human explants, high levels of senescence were induced in equine explants without the addition of growth factors, perhaps because the cartilage from relatively young horses showed a significant mitogenic response to the serum-containing medium. It is possible that a higher dose of irradiation would be sufficient to induce senescence in human explants without growth factor stimulation, although this was not tested in the current study. The dose of 10 Gy was chosen based on the induction of senescence in other cell types[28]. Further, 10 Gy was shown to induce a level of DNA damage in porcine chondrocytes that was similar to advanced OA[41].

Cellular senescence was initially identified as an irreversible phenotype that cells entered upon reaching the limit of normal cell proliferation[42]. While chondrocytes divide in monolayer culture, this cell

type is hypo-replicative when surrounded by healthy cartilage matrix *in vivo*[43], suggesting that replicative senescence is unlikely to occur at a high rate during cartilage homeostasis. However, the growth factors that are released from degrading matrix during early OA provide a potent mitogenic stimulus, as evidenced by the emergence of chondrocyte "clusters". Increased numbers and sizes of cell clusters are characteristic of OA articular cartilage and these clusters are often localized in fissures and clefts of the upper cartilage layer[44–46]. bFGF is released from damaged cartilage tissue and has been identified near chondrocyte clusters[47]. There is also evidence of an interactive effect with TGF-β in cluster formation[48], which is of particular interest given the finding that TGF-β is a key mediator of senescence in certain contexts[49].

In this study, conditions that resulted in the highest rates of cluster formation in human explants (irradiation plus growth factors) also showed the highest rates of senescence upon maturation of the phenotype in monolayer culture. While further investigation will be required to determine the extent to which cell cycle entry plays a causal role in senescence induction, our observations that mitogenic stimulation of damaged chondrocytes induces senescence is consistent with the concept that cellular senescence arises from the coordination of two conflicting processes – cell expansion and cell-cycle arrest[20,50,51]. For example, studies in other quiescent and post-mitotic cell types show that the accumulation of DNA damage may not result in dysfunction until cell division is initiated[52,53]. Our analysis of uncultured OA tissue demonstrated a similar frequency of clusters as found in explants cultured with senescence-inducing stimuli. Thus, an important area of future investigation will be to determine the extent to which cell cycle entry during OA progression initiates signaling pathways that result in subsequent senescence. One recent finding illustrates this possibility by demonstrating that Cellular Communication Network Factor 1 (CCN1, aka CYR61) increases during OA and plays a functional role in stimulating cluster formation, while inhibiting this pathway reduced the expression of senescence markers[54].

There are currently no cures for OA, and the development of effective treatments has been limited by an insufficient understanding of disease initiation and progression. This *in vitro* system establishes a set of physiological cues that induces senescence within both equine and human cartilage tissue, which will enable future mechanistic studies on senescence induction, the role of senescent

chondrocytes in cartilage dysfunction, and the use of senolytic compounds to target senescent cells as a potential treatment for OA.

2.5 ACKNOWLEDGEMENTS

The authors thank Mrs. Julie Long and members of the Central Procedures Laboratory at the North Carolina State University College of Veterinary Medicine for help in isolating equine cartilage explants as well as members of Dr. Richard Loeser's laboratory at the University of North Carolina at Chapel Hill (UNC) for help in isolating human cartilage explants. The authors also would like to acknowledge the Gift of Hope Tissue and Organ Donor Bank and donor's families as well as Dr. Arkady Margulis, MD, for tissue procurement. The authors appreciate assistance from the UNC Animal Histopathology & Laboratory Medicine Core and UNC Flow Cytometry Cores, which are supported in part by a National Cancer Institute Center Core Support Grant (5P30CA016086) to the UNC Lineberger Comprehensive Cancer Center. Figures 2.1 and 2.6 of the manuscript were created using BioRender.com and exported under a paid subscription.

2.6 CONTRIBUTIONS

The conception and design of this study was done by MEC and BOD. Collection and analysis of data conducted by MEC, MCF, GAS and BOD. Study materials provided by RG, JMG, RFL, LVS, and SC. MEC drafted the article and RFL, LVS, SC, and BOD contributed to the critical revision of the article. All authors have read and approved the final manuscript. BOD takes responsibility for the integrity of the work as a whole.

2.7 ROLE OF THE FUNDING SOURCES

None of the funding sources had a role in the study or in the decision to publish. Pilot funding was provided through a Functional Tissue Engineering Seed Grant to LVS/BOD by the Comparative Medicine Institute based at North Carolina State University (NCSU). The project described was also supported by an NC TraCS grant to BOD/LVS as part of North Carolina National Center for Advancing Translational Sciences (NCATS), National Institutes of Health, through Grant Award Number UL1TR002489. Support

was also provided by a grant from the National Institute on Aging (RO1 AG044034 to RFL). The content is solely the responsibility of the authors and does not necessarily represent the official views of the NIH. Matching funds for the NC TraCS award were provided by the UNC Thurston Arthritis Research Center, the NCSU Office of Research and Innovation, and NCSU Comparative Medicine Institute. Additional support was provided by the UNC Office of the Executive Vice Chancellor and Provost through the Junior Faculty Development Award (BOD) and the Orthoregeneration Network through a Kick-Starter grant (#18-048 to BOD). Procurement of human tissue was supported in part by the Rush University Klaus Kuettner Endowed Chair for Research on Osteoarthritis (SC).

2.8 FIGURES

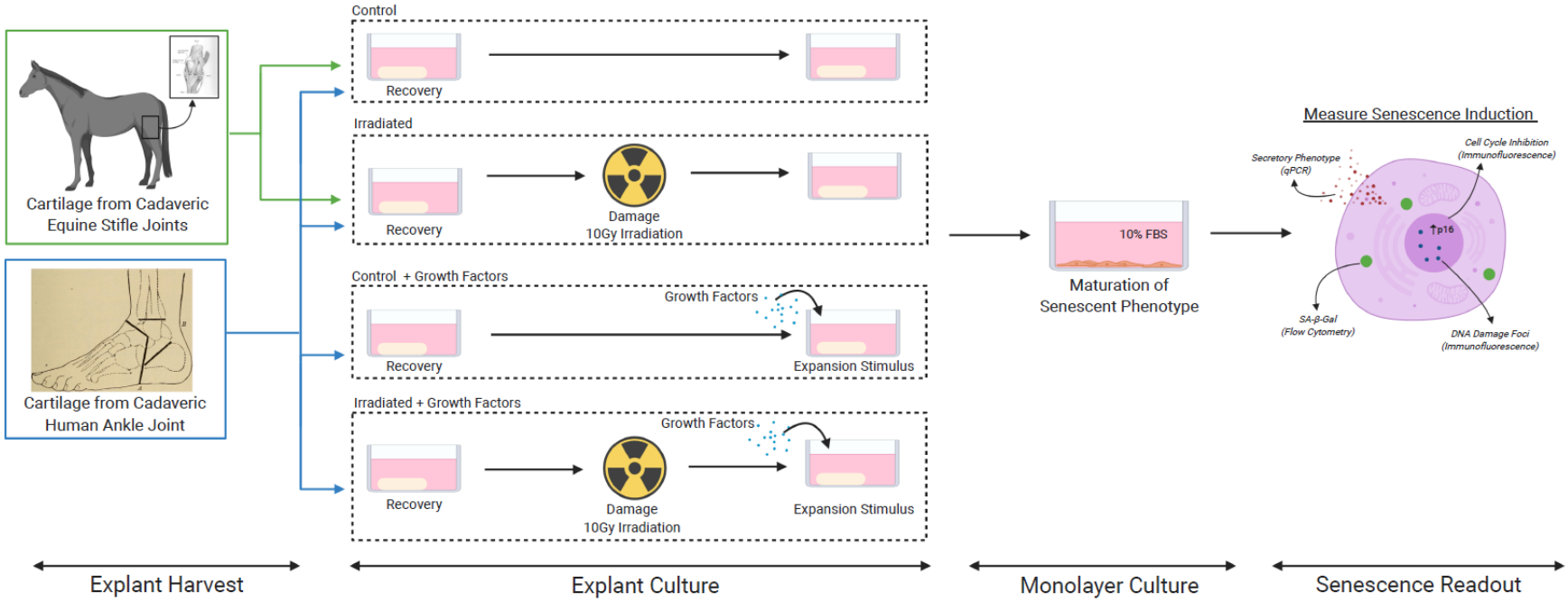

Figure 2.1: Experimental system schematic. Senescence was induced in healthy cadaveric cartilage by damaging explants with irradiation (10 Gy), culturing the explants for 7 to 10 days, followed by enzymatic digestion and culture in monolayer for an additional 10 to 12 days. For human explants the effect of adding the growth factors TGF-β1 and bFGF was investigated. Senescence induction was assessed via SA- β-gal flow cytometry, qPCR, and immunofluorescence. Figure Created with BioRender.com.

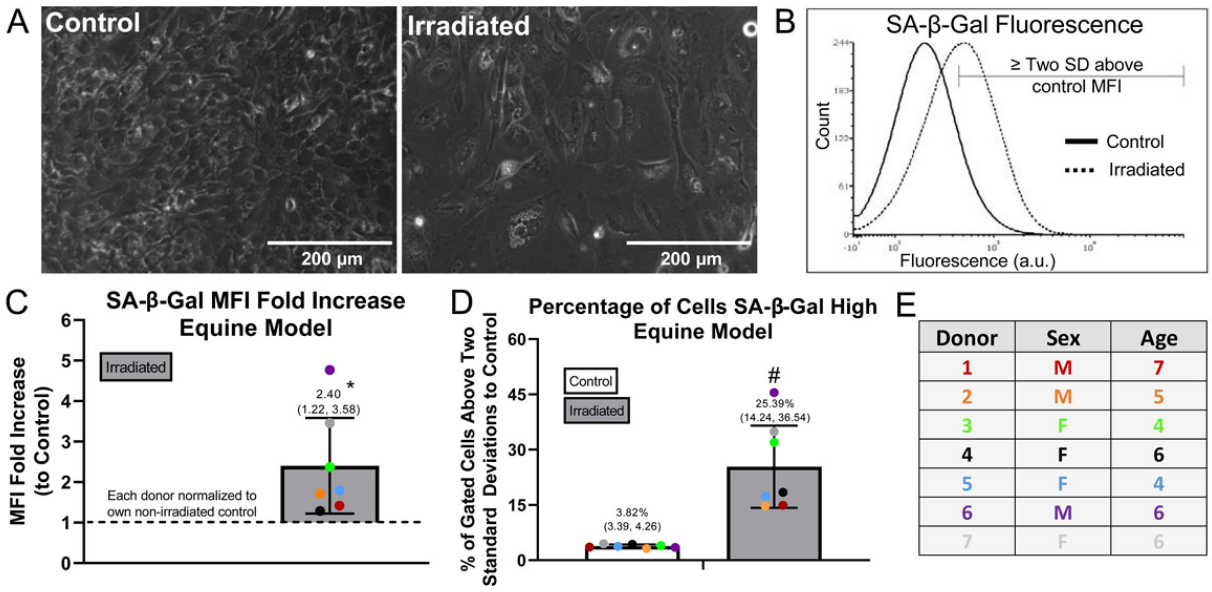

Figure 2.2: Quantification of senescence induction within equine explants. Equine explants were divided into control and irradiated groups, cultured in explant form for 7 to 10 days, digested, and cultured in monolayer for an additional 10 to 12 days in 10% FBS for maturation of the senescence phenotype. (A) Morphology of control and irradiated chondrocytes from Equine Donor 3 after 12 days of monolayer culture; scale bar = 200 µm. (B) Representative SA-β-Gal flow cytometry plot with the region two standard deviations above control MFI marked (Equine Donor 3). (C) SA-β-Gal mean fluorescence intensity (MFI) fold increase above control quantified; (*) indicates significance by one-sample t-test compared to a hypothetical value of 1, p=0.0272. (D) SA-β-Gal flow quantified as percentage of cells SA-β-Gal high. SA-β-Gal high cells delineated as those expressing SA-β-Gal fluorescence above 2 standard deviations from the control MFI; (#) indicates significance by paired t-test, p=0.0031. (E) Information from equine donors included in the analysis (n=7 thoroughbred horses), no horses excluded from analysis.

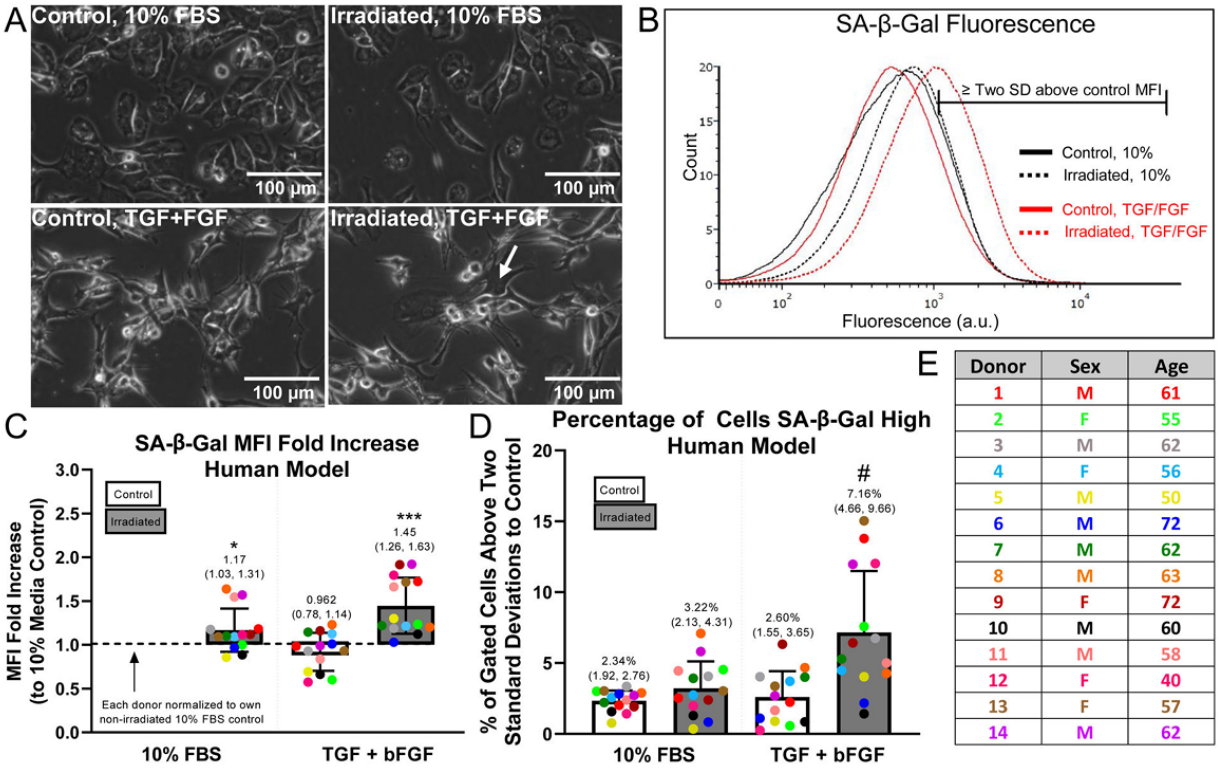

Donor	Sex	Age
1	M	61
2	F	55
3	M	62
4	F	56
5	M	50
6	M	72
7	M	62
8	M	63
9	F	72
10	M	60
11	M	58
12	F	40
13	F	57
14	M	62

Figure 2.3: Quantification of senescence induction within human explants. Human explants were divided into control and irradiated groups, cultured in explant form for 7 days, then cultured in monolayer for an additional 12 days in 10% FBS for maturation of senescence phenotype. Growth factors, 1 ng/mL TGF-β1 and 5 ng/mL bFGF, were added to the 10% FBS in the explant culture to provide a mitogenic stimulus. (A) Morphology of chondrocytes digested from control or irradiated cartilage (treated with or without growth factors) after 12 days of monolayer culture in 10% FBS medium (Human Donor 14); scale bar = 100 µm; arrow indicates bi-nucleated cell. (B) Representative SA-β-Gal flow cytometry plot with the region two standard deviations above control MFI marked (Human Donor 1). (C) SA-β-Gal MFI fold increase above the control 10% condition quantified; (*) indicates significance by one-sample t-test compared to a hypothetical value of 1, p=0.025; (***) indicates significance by one-sample t-test compared to a hypothetical value of 1, p=0.0002. (D) SA-β-Gal flow quantified as the percentage of cells SA-β-Gal high; (#) indicates significance to all other groups by 2-way ANOVA with Tukey's multiple comparison test, p<0.005. (E) Information from human cartilage donors included in the analysis (n=14); three donors excluded due to too few cells (<800 events) in SA-β gal flow cytometry experiment and one outlier identified by Grubbs test and removed from subsequent analysis.

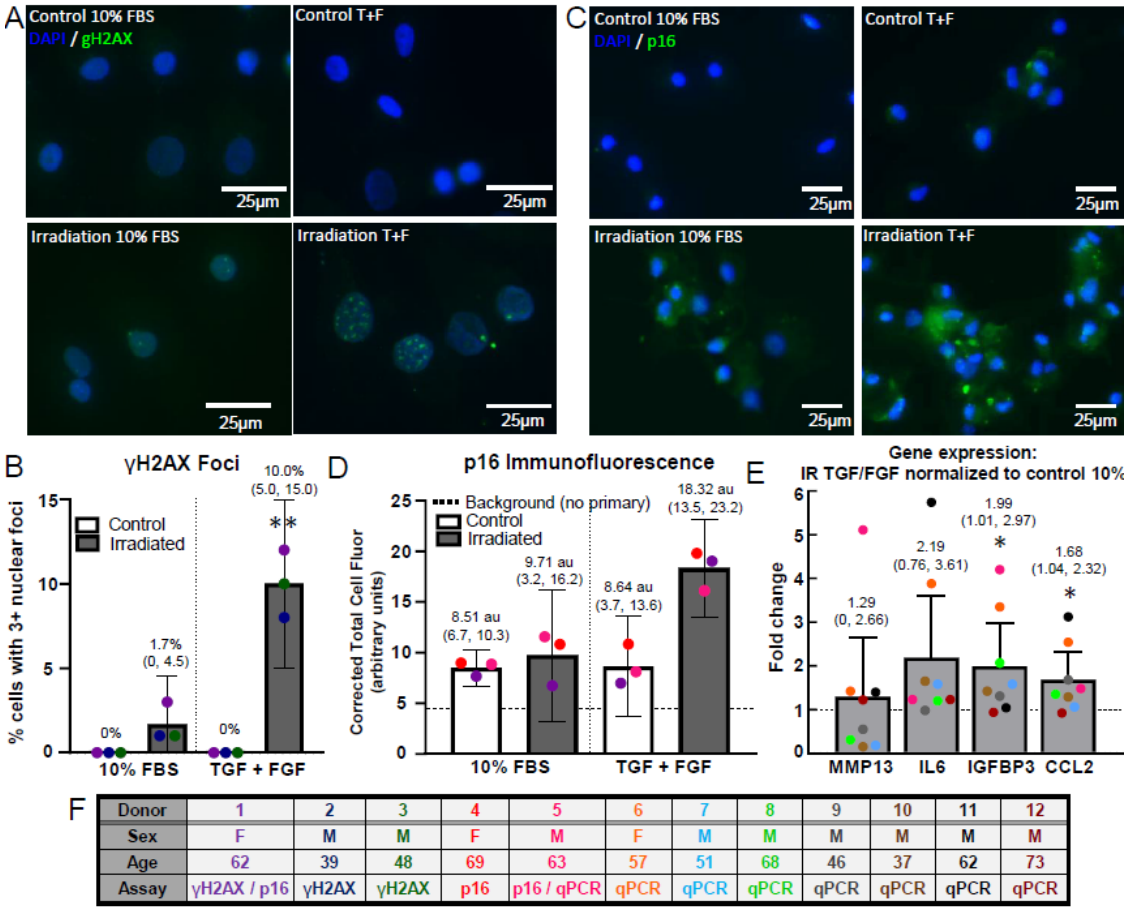

F

Donor	1	2	3	4	5	6	7	8	9	10	11	12
Sex	F	M	M	F	M	F	M	M	M	M	M	M
Age	62	39	48	69	63	57	51	68	46	37	62	73
Assay	γH2AX / p16	γH2AX	γH2AX	p16	p16 / qPCR	qPCR	qPCR	qPCR	qPCR	qPCR	qPCR	qPCR

Figure 2.4: Verification of senescence induction. Control and irradiated explants were either treated with 10% FBS or 10% FBS spiked with TGF and bFGF, then digested and plated in monolayer. (A) γH2AX immunofluorescence was used to identify sustained DNA damage; scale bar = 25 μm. (B) The γH2AX images were analyzed by quantifying the number of nuclei with three or more γH2AX puncta; (***) indicates significance to all other groups by 2-way ANOVA with Tukey's multiple comparison test, $p<0.005$ (n=3) (C) p16 immunofluorescent images at the end of monolayer culture for each condition. (D) The p16 corrected total cell fluorescence normalized to cell area was quantified for each condition. The irradiation + TGF/FGF treated cells had a higher total cell fluorescence compared to the other groups (n=3). (E) qPCR was performed to measure the SASP expression from the chondrocytes at the end of monolayer culture. The fold change in gene expression in the irradiation + TGF/FGF group to the control group for MMP13, IL-6, IGFBP3, and CCL2 is plotted; (*) indicates significance by one-sample t-test compared to a hypothetical value of 1, $p<0.05$. (F) Human donor information. Note that donor numbering and color coding do not match Figure 2.3.

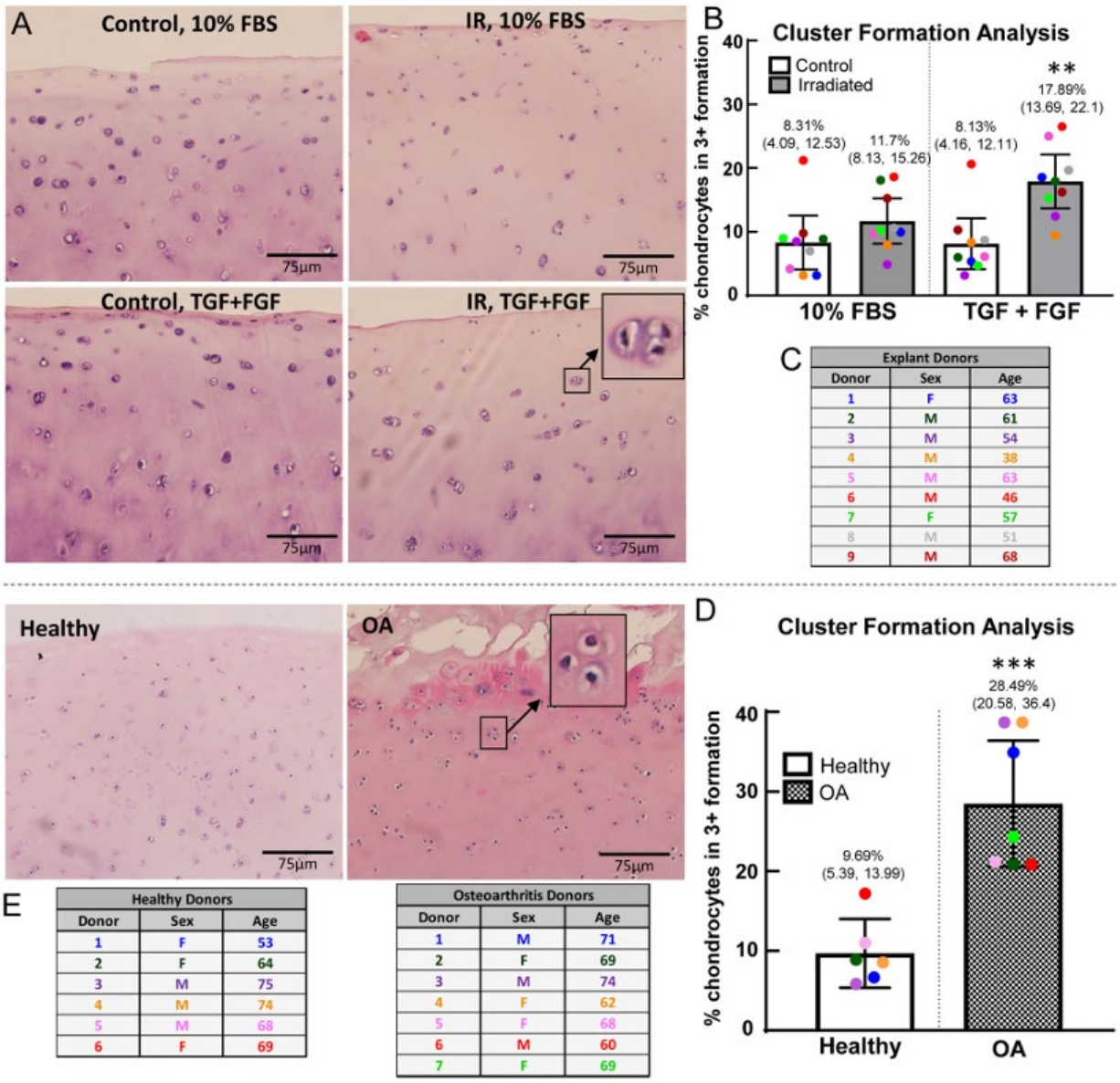

Figure 2.5: Chondrocyte clusters in cartilage explants. The chondrocyte clusters in the superficial and middle zones for the control and experimental conditions were analyzed using ImageJ. (A) H&E staining on control and irradiated explants after explant culture for 7 days, with or without growth factors (Explant Donor 7). H&E staining of healthy and osteoarthritic cartilage (Healthy Donor 4, OA Donor 7). (B) Cell cluster analysis on cultured explants, with percentage of all clusters (including individual cells as a cluster) in triplet^{+} formation; (***) indicates significance by 2-way ANOVA with Tukey's multiple comparison test to all other groups, $p<0.0005$ (C) Table of the human cartilage donors included in the analysis, (n=9). One outlier identified by Grubb's test and removed from analysis. (D) Cell cluster analysis

on healthy and OA cartilage; (***) indicates significance by unpaired t-test, p=0.0006 (E) Table of the human osteoarthritis cartilage donors and healthy cartilage donors included in the analysis (n=6 healthy donors, n=7 OA donors). Average age of healthy donors is 67.2 years (3 males, 3 females); average age of OA donors is 67.6 years (3 males, 4 females). No outliers removed from analysis.

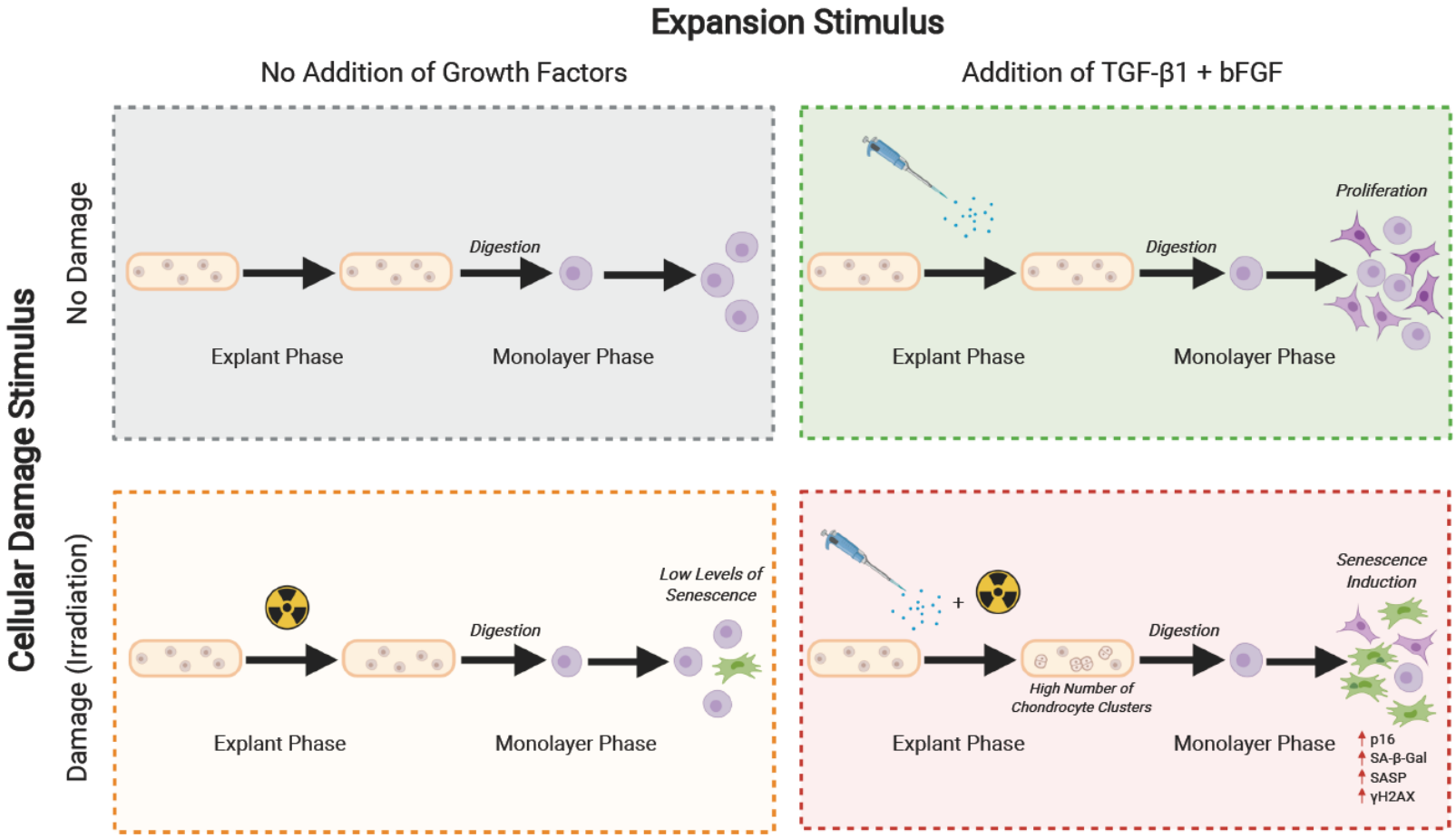

Figure 2.6: Overview of the senescence induction process. The senescence induction phenotype is hypothesized to be a result of conflicting cues from cellular damage stimuli and expansion stimuli. In the context of this study, the expansion stimulus was provided by 10% FBS (equine model) and 10% FBS + bFGF + TGF-β1 (human model), while the cellular damage stimulus was provided by 10 Gy of irradiation. Figure created with BioRender.com.

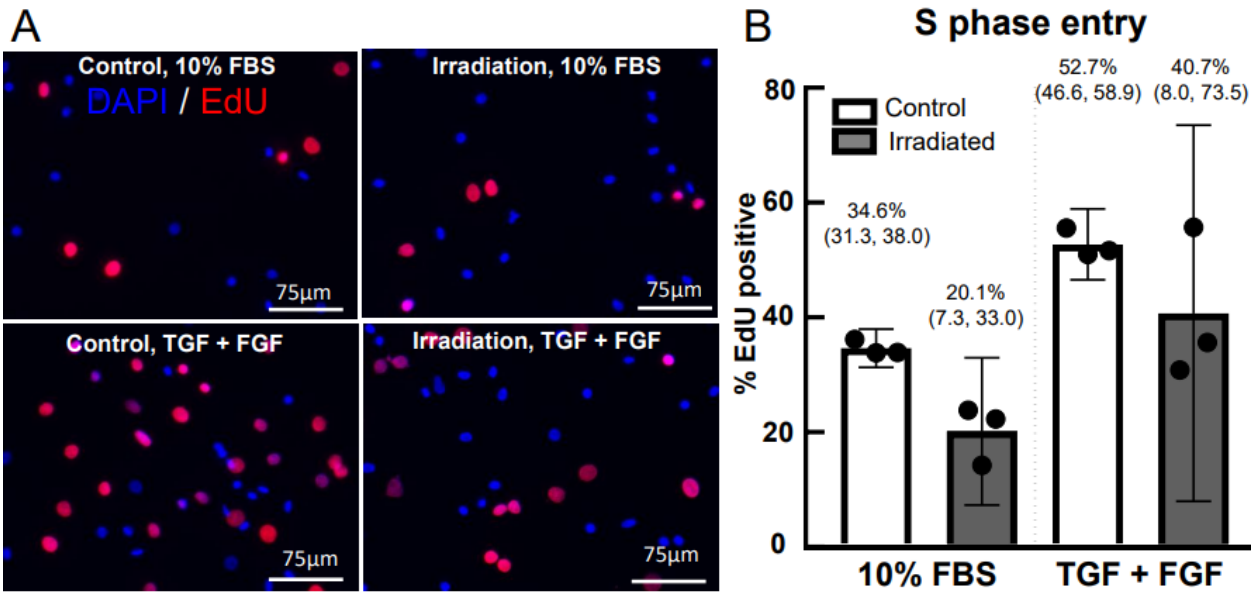

Supplemental Figure 2.1: Validation of mitogenic stimulation by growth factor treatment. EdU incorporation during subsequent monolayer culture in response to the growth factors TGF-β1 and bFGF (during explant culture only). (A) EdU by AF555 at the end of monolayer culture. (B) Percentage of cells with positive signal for EdU. The main effects of irradiation ($p<0.01$) and growth factors ($p<0.05$) provided a significant source of variation by two-way ANOVA (n=3).

Supplemental Figure 2.1: Methods: To assess whether growth factor treatment during explant culture results in greater subsequent S phase entry, a distinct set of cells from three donors were treated with 1 µM EdU (5-ethynyl-2'- deoxyuridine, Click-iT™ EdU, Thermo Fisher Scientific C10338) at each feed for the duration of monolayer culture. Visualization of integrated EdU was obtained by imaging the companion Alexa Fluor™ 555 with an EVOS M5000 imaging system (Thermo Fisher Scientific) and the percentage of positive cells was quantified across 5 randomly selected images per condition per donor using ImageJ imaging software (Fiji).

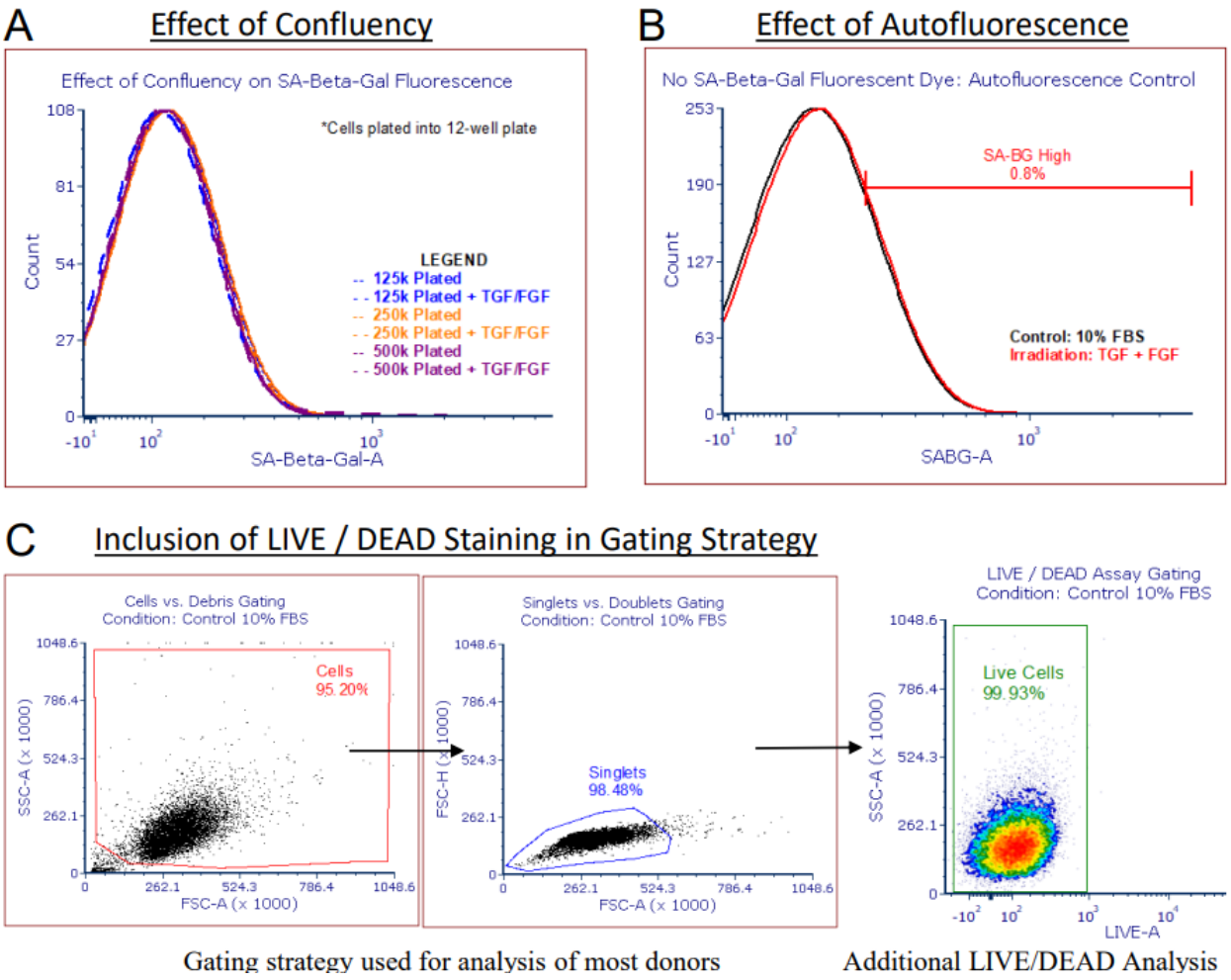

Supplemental Figure 2.2: Validation of SA- β-Gal flow cytometry readout. (A) Differing confluence and cell morphology was achieved through 3 plating densities with and without growth factors (B) Autofluorescence was tested by leaving out the fluorescent SA-β-gal substrate. Senescent cells (Irradiation plus growth factors) were compared the control 10% group. In this experiment, 0.8% of cells from the IR with TGF/FGF would have been deemed as SA-β-gal high based on autofluorescence alone. (C) The default gating strategy did not use an explicit live/dead cell discriminator but applying a fixable live/dead analysis (Thermo Fisher Scientific, L34962) showed that in this case 99.93% of cells reaching analysis are live.

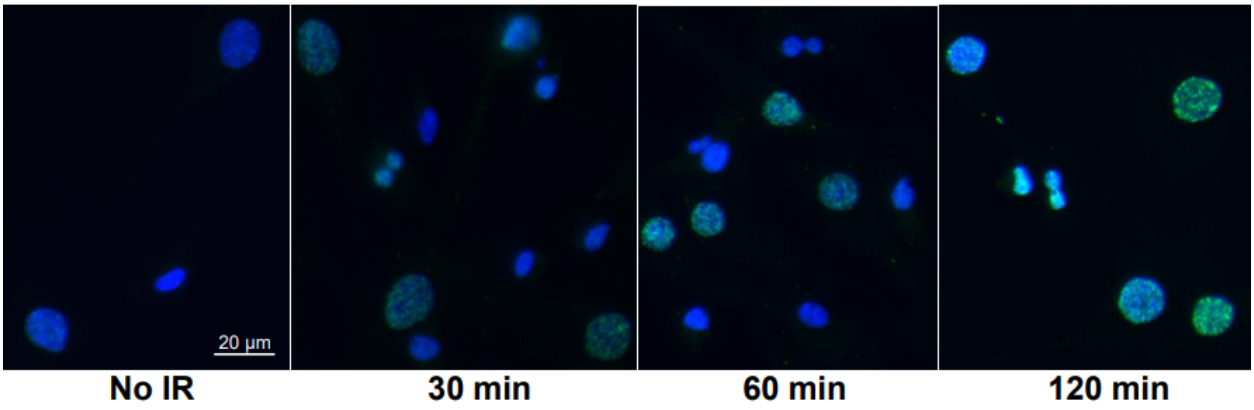

Supplemental Figure 2.3: Acute DNA damage after irradiation. Primary human chondrocytes in monolayer culture were treated with 10 Gy irradiation to initiate DNA damage. At 30, 60, and 120 minutes after irradiation (or a no irradiation control), individual wells were fixed and analyzed by immunofluorescence for γH2AX. The appearance of foci throughout the nucleus indicates a robust DNA damage response.

REFERENCES

1. Loeser RF, Goldring SR, Scanzello CR, Goldring MB. Osteoarthritis: a disease of the joint as an organ. *Arthritis Rheum*. 2012;64(6):1697-1707. doi:10.1002/art.34453

2. Bijlsma JWJ, Berenbaum F, Lafeber FPJG. Osteoarthritis: an update with relevance for clinical practice. *Lancet*. 2011;377(9783):2115-2126. doi:10.1016/S0140-6736(11)60243-2

3. Murphy L, Schwartz TA, Helmick CG, et al. Lifetime risk of symptomatic knee osteoarthritis. *Arthritis Rheum*. 2008;59(9):1207-1213. doi:10.1002/art.24021

4. Gabriel SE, Crowson CS, Campion ME, O'Fallon WM. Direct medical costs unique to people with arthritis. *J Rheumatol*. 1997;24(4):719-725.

5. Oo WM, Yu SPC, Daniel MS, Hunter DJ. Disease-modifying drugs in osteoarthritis: current understanding and future therapeutics. *Expert Opin Emerg Drugs*. 2018;23(4):331-347. doi:10.1080/14728214.2018.1547706

6. Kurtz SM, Ong KL, Lau E, Bozic KJ. Impact of the economic downturn on total joint replacement demand in the United States: updated projections to 2021. *J Bone Joint Surg Am*. 2014;96(8):624-630. doi:10.2106/JBJS.M.00285

7. Loeser RF, Collins JA, Diekman BO. Ageing and the pathogenesis of osteoarthritis. *Nat Rev Rheumatol*. 2016;12(7):412-420. doi:10.1038/nrrheum.2016.65

8. Felson DT. Osteoarthritis: New Insights. Part 1: The Disease and Its Risk Factors. *Ann Intern Med*. 2000;133(8):635. doi:10.7326/0003-4819-133-8-200010170-00016

9. López-Otín C, Blasco MA, Partridge L, Serrano M, Kroemer G. The hallmarks of aging. *Cell*. 2013;153(6):1194-1217. doi:10.1016/j.cell.2013.05.039

10. Martin JA, Buckwalter JA. Human chondrocyte senescence and osteoarthritis. *Biorheology*. 2002;39(1-2):145-152.

11. Price JS, Waters JG, Darrah C, et al. The role of chondrocyte senescence in osteoarthritis. *Aging Cell*. 2002;1(1):57-65. doi:10.1046/j.1474-9728.2002.00008.x

12. Rose J, Söder S, Skhirtladze C, et al. DNA damage, discoordinated gene expression and cellular senescence in osteoarthritic chondrocytes. *Osteoarthr Cartil*. 2012;20(9):1020-1028. doi:10.1016/j.joca.2012.05.009

13. Jeon OH, Kim C, Laberge RM, et al. Local clearance of senescent cells attenuates the development of post-traumatic osteoarthritis and creates a pro-regenerative environment. *Nat Med*. 2017;23(6):775-781. doi:10.1038/nm.4324

14. Philipot D, Guérit D, Platano D, et al. p16INK4a and its regulator miR-24 link senescence and chondrocyte terminal differentiation-associated matrix remodeling in osteoarthritis. *Arthritis Res Ther*. 2014;16(1):R58. doi:10.1186/ar4494

15. Coppé JP, Desprez PY, Krtolica A, Campisi J. The Senescence-Associated Secretory Phenotype: The Dark Side of Tumor Suppression. *Annu Rev Pathol*. 2010;5:99-118. doi:10.1146/annurev-pathol-121808-102144

16. He S, Sharpless NE. Senescence in Health and Disease. *Cell*. 2017;169(6):1000-1011. doi:10.1016/j.cell.2017.05.015

17. Jeon OH, David N, Campisi J, Elisseeff JH. Senescent cells and osteoarthritis: a painful connection. *J Clin Invest*. 2018;128(4):1229-1237. doi:10.1172/JCI95147

18. van Deursen JM. Senolytic therapies for healthy longevity. *Science*. 2019;364(6441):636-637. doi:10.1126/science.aaw1299

19. Sharpless NE, Sherr CJ. Forging a signature of in vivo senescence. *Nature Reviews Cancer*. 2015;15(7):397-408. doi:10.1038/nrc3960

20. Ogrodnik M, Salmonowicz H, Jurk D, Passos JF. Expansion and Cell-Cycle Arrest: Common Denominators of Cellular Senescence. *Trends in Biochemical Sciences*. 2019;44(12):996-1008. doi:10.1016/j.tibs.2019.06.011

21. Debacq-Chainiaux F, Erusalimsky JD, Campisi J, Toussaint O. Protocols to detect senescence-associated beta-galactosidase (SA-betagal) activity, a biomarker of senescent cells in culture and in vivo. *Nat Protoc*. 2009;4(12):1798-1806. doi:10.1038/nprot.2009.191

22. Itahana K, Campisi J, Dimri GP. Methods to detect biomarkers of cellular senescence: the senescence-associated beta-galactosidase assay. *Methods Mol Biol*. 2007;371:21-31. doi:10.1007/978-1-59745-361-5_3

23. Liu JY, Souroullas GP, Diekman BO, et al. Cells exhibiting strong p16INK4a promoter activation in vivo display features of senescence. *PNAS*. 2019;116(7):2603-2611. doi:10.1073/pnas.1818313116

24. Sessions GA, Copp ME, Liu JY, Sinkler MA, D'Costa S, Diekman BO. Controlled induction and targeted elimination of p16INK4a-expressing chondrocytes in cartilage explant culture. *FASEB J*. 2019;33(11):12364-12373. doi:10.1096/fj.201900815RR

25. Collins JA, Arbeeva L, Chubinskaya S, Loeser RF. Articular chondrocytes isolated from the knee and ankle joints of human tissue donors demonstrate similar redox-regulated MAP kinase and Akt signaling. *Osteoarthritis Cartilage*. 2019;27(4):703-711. doi:10.1016/j.joca.2018.12.010

26. Muehleman C, Bareither D, Huch K, Cole AA, Kuettner KE. Prevalence of degenerative morphological changes in the joints of the lower extremity. *Osteoarthr Cartil*. 1997;5(1):23-37. doi:10.1016/s1063-4584(97)80029-5

27. Forsyth CB, Pulai J, Loeser RF. Fibronectin fragments and blocking antibodies to alpha2beta1 and alpha5beta1 integrins stimulate mitogen-activated protein kinase signaling and increase collagenase 3 (matrix metalloproteinase 13) production by human articular chondrocytes. *Arthritis Rheum*. 2002;46(9):2368-2376. doi:10.1002/art.10502

28. Rodier F, Coppé JP, Patil CK, et al. Persistent DNA damage signalling triggers senescence-associated inflammatory cytokine secretion. *Nat Cell Biol*. 2009;11(8):973-979. doi:10.1038/ncb1909

29. Leikam C, Hufnagel A, Schartl M, Meierjohann S. Oncogene activation in melanocytes links reactive oxygen to multinucleated phenotype and senescence. *Oncogene*. 2008;27(56):7070-7082. doi:10.1038/onc.2008.323

30. Muñoz-Espín D, Serrano M. Cellular senescence: from physiology to pathology. *Nat Rev Mol Cell Biol*. 2014;15(7):482-496. doi:10.1038/nrm3823

31. Xu M, Pirtskhalava T, Farr JN, et al. Senolytics improve physical function and increase lifespan in old age. *Nat Med*. 2018;24(8):1246-1256. doi:10.1038/s41591-018-0092-9

32. Lee BY, Han JA, Im JS, et al. Senescence-associated β-galactosidase is lysosomal β-galactosidase. *Aging Cell*. 2006;5(2):187-195. doi:10.1111/j.1474-9726.2006.00199.x

33. Noppe G, Dekker P, Koning-Treurniet C de, et al. Rapid flow cytometric method for measuring senescence associated β-galactosidase activity in human fibroblasts. *Cytometry Part A*. 2009;75A(11):910-916. doi:10.1002/cyto.a.20796

34. Yang NC, Hu ML. The limitations and validities of senescence associated-beta-galactosidase activity as an aging marker for human foreskin fibroblast Hs68 cells. *Exp Gerontol*. 2005;40(10):813-819. doi:10.1016/j.exger.2005.07.011

35. Bertolo A, Baur M, Guerrero J, Pötzel T, Stoyanov J. Autofluorescence is a Reliable in vitro Marker of Cellular Senescence in Human Mesenchymal Stromal Cells. *Sci Rep*. 2019;9(1):2074. doi:10.1038/s41598-019-38546-2

36. Gorgoulis V, Adams PD, Alimonti A, et al. Cellular Senescence: Defining a Path Forward. *Cell*. 2019;179(4):813-827. doi:10.1016/j.cell.2019.10.005

37. Diekman BO, Sessions GA, Collins JA, et al. Expression of p16INK 4a is a biomarker of chondrocyte aging but does not cause osteoarthritis. *Aging Cell*. 2018;17(4). doi:10.1111/acel.12771

38. McIlwraith CW, Frisbie DD, Kawcak CE. The horse as a model of naturally occurring osteoarthritis. *Bone Joint Res*. 2012;1(11):297-309. doi:10.1302/2046-3758.111.2000132

39. McIlwraith CW, Fortier LA, Frisbie DD, Nixon AJ. Equine Models of Articular Cartilage Repair. *Cartilage*. 2011;2(4):317-326. doi:10.1177/1947603511406531

40. Goodrich LR, Nixon AJ. Medical treatment of osteoarthritis in the horse – A review. *The Veterinary Journal*. 2006;171(1):51-69. doi:10.1016/j.tvjl.2004.07.008

41. Chen AF, Davies CM, De Lin M, Fermor B. Oxidative DNA damage in osteoarthritic porcine articular cartilage. *J Cell Physiol*. 2008;217(3):828-833. doi:10.1002/jcp.21562

42. Hayflick L, Moorhead PS. The serial cultivation of human diploid cell strains. *Experimental Cell Research*. 1961;25(3):585-621. doi:10.1016/0014-4827(61)90192-6

43. Aigner T, Hemmel M, Neureiter D, et al. Apoptotic cell death is not a widespread phenomenon in normal aging and osteoarthritis human articular knee cartilage: a study of proliferation, programmed cell death (apoptosis), and viability of chondrocytes in normal and osteoarthritic human knee cartilage. *Arthritis Rheum*. 2001;44(6):1304-1312. doi:10.1002/1529-0131(200106)44:6<1304::AID-ART222>3.0.CO;2-T

44. Lotz MK, Otsuki S, Grogan SP, Sah R, Terkeltaub R, D'Lima D. Cartilage Cell Clusters. *Arthritis Rheum*. 2010;62(8):2206-2218. doi:10.1002/art.27528

45. Lee GM, Paul TA, Slabaugh M, Kelley SS. The incidence of enlarged chondrons in normal and osteoarthritic human cartilage and their relative matrix density. *Osteoarthritis and Cartilage*. 2000;8(1):44-52. doi:10.1053/joca.1999.0269

46. Mankin H, Dorfman H, Lippiello L, Zarins A. Biochemical and Metabolic Abnormalities in Articular Cartilage from Osteo-Arthritic Human Hips: II. Correlation of Morphology with Biochemical and Metabolic Data. *The Journal of Bone & Joint Surgery*. 1971;53(3):523-537.

47. Vincent T, Hermansson M, Bolton M, Wait R, Saklatvala J. Basic FGF mediates an immediate response of articular cartilage to mechanical injury. *PNAS*. 2002;99(12):8259-8264. doi:10.1073/pnas.122033199

48. Quintavalla J, Kumar C, Daouti S, Slosberg E, Uziel-Fusi S. Chondrocyte cluster formation in agarose cultures as a functional assay to identify genes expressed in osteoarthritis. *J Cell Physiol*. 2005;204(2):560-566. doi:10.1002/jcp.20345

49. Acosta JC, Banito A, Wuestefeld T, et al. A complex secretory program orchestrated by the inflammasome controls paracrine senescence. *Nat Cell Biol*. 2013;15(8):978-990. doi:10.1038/ncb2784

50. Blagosklonny MV. Geroconversion: irreversible step to cellular senescence. *Cell Cycle*. 2014;13(23):3628-3635. doi:10.4161/15384101.2014.985507

51. Serrano M, Lin AW, McCurrach ME, Beach D, Lowe SW. Oncogenic ras provokes premature cell senescence associated with accumulation of p53 and p16INK4a. *Cell*. 1997;88(5):593-602. doi:10.1016/s0092-8674(00)81902-9

52. Flach J, Bakker ST, Mohrin M, et al. Replication stress is a potent driver of functional decline in ageing haematopoietic stem cells. *Nature*. 2014;512(7513):198-202. doi:10.1038/nature13619

53. Sousa-Victor P, Gutarra S, García-Prat L, et al. Geriatric muscle stem cells switch reversible quiescence into senescence. *Nature*. 2014;506(7488):316-321. doi:10.1038/nature13013

54. Feng M, Peng H, Yao R, et al. Inhibition of cellular communication network factor 1 (CCN1)-driven senescence slows down cartilage inflammaging and osteoarthritis. *Bone*. 2020;139:115522. doi:10.1016/j.bone.2020.115522

CHAPTER 3: COMET ASSAY FOR QUANTIFICATION OF THE INCREASED DNA DAMAGE BURDEN IN PRIMARY HUMAN CHONDROCYTES WITH AGING AND OSTEOARTHRITIS[1]

3.1 INTRODUCTION

Osteoarthritis (OA) is a degenerative disorder characterized by joint pain and the progressive degradation of articular cartilage and other tissues of the joint. Aging is the strongest risk factor for the development of OA, but the mechanisms that drive this relationship remain unclear[1]. Previous studies have shown that OA chondrocytes exhibit high levels of DNA damage and that this may contribute to heterogeneous gene expression and dysfunction[2,3]. However, the degree to which chondrocytes accumulate DNA damage during "normal aging" has not been reported in the literature. Chondrocytes and other hypo-replicative cells may be particularly susceptible to acquiring sites of persistent DNA damage with age, as they cannot take advantage of the efficient and accurate DNA repair mechanisms that are restricted to S phase[4,5]. It is important to quantify this burden, as DNA damage is a central mediator of numerous aspects of aging, including cell senescence[6,7]. A widely established method for measuring DNA damage in individual cells is the comet assay, which is sufficiently sensitive to serve as an effective biomonitoring tool for assessing the effect of various environmental exposures[8]. The alkaline comet assay uses gel electrophoresis of single nuclei and fluorescence microscopy to visualize damaged DNA in the "comet tail" as compared to intact DNA in the "comet head"[9]. The comet tail is caused by relaxation of supercoiled DNA loops due to strand breaks, which results in greater migration through the agarose gel when an electric field is applied. The alkaline comet assay detects single-stand breaks (SSBs) and double-strand breaks (DSBs), as well as abasic sites and other forms of damage that can be converted into strand breaks under alkaline conditions[9]. To gain additional information on the type of damage present in a given

[1] The following chapter was published in Aging Cell.

Copp ME, Chubinskaya S, Bracey DN, Shine J, Sessions G, Loeser RF, Diekman BO. Comet assay for quantification of the increased DNA damage burden in primary human chondrocytes with aging and osteoarthritis. Aging Cell. n/a: e13698.

cell, a “two-tailed” version of the comet uses sequential electrophoresis steps in orthogonal directions under neutral pH and then alkaline pH buffer conditions[10]. The goal of this study was to use the comet assay to quantify the DNA damage present in chondrocytes obtained from cadaveric donors of a wide age range, and to compare the extent of this damage to OA chondrocytes taken at the time of joint replacement. Lastly, we treated chondrocytes from young donors with irradiation to identify the dose of DNA damage that was required to recapitulate the baseline levels found in older donors.

3.2 RESULTS

3.2.1 DNA damage increases with age in primary human chondrocytes.

Cadaveric donors without a history of OA served as the source of normal cartilage from the ankle (talus) and the knee (femur). Tissue was obtained from organ donors within 24 hours of death through the Gift of Hope Organ and Tissue Donor Network (Itasca, IL) and shipped overnight to the University of North Carolina at Chapel Hill (UNC). Tissue was graded according to the 0-4 point Collins scale and only cartilage from regions that were macroscopically normal were used[11]. Cartilage was dissected away from the underlying bone and chondrocytes were isolated by enzymatic digestion with Pronase for 1 hour and subsequently with Collagenase P overnight[12], followed by plating at ~$1x10^5$ cells/cm^2 for a recovery period of ~2-7 days before cryopreservation (12648010, ThermoFisher). Cryopreserved cells were thawed and plated for ~2-3 days to recover before performing the comet assay in batches that represented all groups being compared.

DNA damage in primary human chondrocytes from young (<45 years) and older (>70 years) donors was assessed using the comet assay. Chondrocytes were trypsinized and $5x10^4$ chondrocytes were mixed with 1% Low Melting Agarose (A0701, MilliporeSigma) at a 1:10 volume ratio and applied to a Superfrost slide (12-550-15, ThermoFisher) pre-coated with 1% normal melting agarose (20-240, Apex). The slides were placed in the lysis solution (2.5 M NaCl, 0.1 M disodium EDTA, 10 mM Tris base, 0.2 M NaOH, 0.1% sodium lauryl sarcosinate, 1% Triton X-1000, pH 10) overnight at 4 ^oC. After lysis, slides were immersed at 4 ^oC in an alkaline electrophoresis solution (200 mM NaOH, 1 mM disodium EDTA, pH > 13) for 45 minutes followed by electrophoresis at 1 V/cm and 300 mA for 20 minutes. Samples were washed twice with dH_20, dried and stained with NucBlue™ nuclear stain (R37605, Thermo Fisher Scientific). Approximately 100

randomly selected cells per condition were imaged under an EVOS M5000 microscope (AMF5000, Thermo Fisher Scientific) and analyzed in ImageJ using the OpenComet plugin software. Representative wide-field images of chondrocyte comets from young, older, and OA donors are provided in **Supplementary Figure 3.1.** Chondrocytes from older donors revealed a wide distribution in the percentage of DNA found in the comet tail, whereas most chondrocytes from younger donors exhibited low or moderate levels of DNA damage (**Figure 3.1A**). The driving factor in the distribution of tail DNA percentage was donor age, with a Collins grade between 0-2 showing no effect on the tail DNA percentage (**Figure 3.1A**). The tail DNA percentage was averaged across all cells for a given donor and grouped according to age, with the older donors showing a significant increase in DNA damage compared to young donors (**Figure 3.1B**, unpaired t-test $p < 0.0001$).

3.2.2 Two-tailed comet indicates that chondrocytes from older donors harbor damage in the form of strand breaks.

We assessed the type of DNA damage in chondrocytes from three >70 year-old donors using a two-tailed comet assay, where strand breaks are represented by a tail in the “x direction” due to a first electrophoresis under neutral pH conditions, and base damage is represented by a tail in the “y direction” due to a second electrophoresis with alkaline pH (the slide is rotated 90° between runs). We followed a published protocol[10], with a modification to perform lysis II at 37 degrees to avoid precipitation. A custom script was written using CellProfiler™ to calculate the “x” and “y” distance in pixels between the centroid of the head and the centroid of all stained DNA. The DNA damage present in chondrocytes from older donors is predominantly in the form of strand breaks rather than base damage (**Figure 3.1C**). While some investigators suggest that neutral pH conditions detect only DSBs and not SSBs[10,13,14], here is strong experimental and theoretical support for the interpretation that all strand breaks are detected at neutral pH and alkali conditions additionally detect base damage[15–17]. The data from the IR control are consistent with this latter interpretation, as the expected ratio of SSB:DSB is ~20:1[18] and therefore the abundant SSBs would bias the tails strongly towards the y-direction if neutral conditions only detected DSBs. As expected given the complexity of damage in response to IR[19], 10 Gy did cause both strand breaks and base damage. Other controls show that young chondrocytes treated with ellipticine have strand breaks as expected for this DSB-inducing agent[20], methyl methanesulfonate (MMS) shows acute base damage due to direct

alkylation[21], and overnight recovery after MMS treatment reveals the SSBs that are generated during failed base excision repair (BER)[21].

3.2.3 Osteoarthritis accelerates DNA damage as compared to age-matched normal donors.

OA cartilage was obtained from intact areas of the femur at the time of total knee replacement surgeries performed at the UNC Medical Center. Tissue was handled in a manner consistent with the cadaveric donors by storing in saline at 4 °C for 24-48 hours before dissociation and cell isolation. Using donors between 50-60 years old, chondrocytes derived from OA cartilage showed higher levels of DNA damage as compared to chondrocytes derived from femoral and ankle cartilage of cadaveric donors (**Figure 3.1D**, Tukey's multiple comparison test, $p<0.0001$; individual cell data in **Supplementary Figure 3.2**). Cadaveric tissue from both the knee and ankle were used to address the possibility that anatomical site may alter the level of DNA damage, but there was no effect (**Figure 3.1D**).

3.2.4 Linear increase in DNA damage with age.

Compiling data from the comet assay on cadaveric talar chondrocytes from 25 donors between 34 and 78 years of age revealed a linear increase in the percentage of DNA in the comet tail (**Figure 3.2A**, $R^2 = 0.865$ by linear regression, $p < 0.0001$). OA chondrocytes plotted on the same figure fall above the trendline (**Figure 3.2A**, red dots) and femoral chondrocytes from cadaveric donors fell slightly below the trendline (**Figure 3.2A**, blue dots). Of note, the four cadaveric donors in which both ankle and femur cartilage were available demonstrate a similar burden of DNA damage across these two anatomical sites.

3.2.5 High doses of irradiation are required to match the level of age-associated DNA damage.

Chondrocytes of young donors with low baseline levels of damage (39, 40, and 45 years of age) were treated with increasing levels of irradiation: 0 Gy, 1.25 Gy, 2.5 Gy, 5 Gy, and 10 Gy. Cells cultured in well plates were placed directly in a RS2000 Biological Irradiator. Following irradiation, the media was replaced and the cells were allowed to recover to allow for repair of acute DNA damage, with the comet assay performed after 48 hours to assess the persistent damage. The irradiated chondrocytes showed a corresponding increase in the level of DNA damage as assessed by the percent of DNA in comet tails (**Figure 3.2B**). The chondrocytes from these donors reached an average of 26.4 percent DNA in comet tail at 10 Gy of irradiation. This level of damage is comparable to that found in chondrocytes from either OA

donors between the ages of 50-60 years (mean of 28.5% DNA in comet tail) or cadaveric donors between the ages of 70-80 years (mean of 29.9% DNA in comet tail).

3.3 DISCUSSION

This study quantified DNA damage in primary human chondrocytes, with a particular emphasis on the effects of aging and OA. Our goal was to assess baseline damage and minimize the effects of acute changes due to tissue isolation, storage, or enzymatic digestion. Thus, we plated chondrocytes in monolayer to allow for recovery, which also removes dead or dying cells that are unable to successfully plate down. Chondrocytes were then routinely cryopreserved and thawed in batches containing multiple samples from each group (e.g. young and older; normal and OA) to facilitate direct comparisons, with trial experiments confirming that cryopreservation did not significantly alter the level of DNA damage. The single cell electrophoresis comet assay was sufficiently sensitive to detect increased DNA damage in older donors as compared to young. Assessing the percentage DNA in the “comet tail” of donors between the ages of 34 and 78 showed a linear increase with age, although the progression to end-stage OA appears to accelerate this process. The finding of significant DNA damage in OA chondrocytes is consistent with previous studies in human and porcine cartilage[2,3]. While the increased DNA damage with “normal” aging has not been previously reported for chondrocytes, our results are consistent with studies in peripheral blood mononuclear cells that have shown an increase of ~1% per year in damage by the comet assay[22].

Ionizing irradiation was used to contextualize the extent of damage measured by the comet assay. Remarkably, 10 Gy irradiation was required for young chondrocytes to reach the levels of DNA damage found in aged and OA chondrocytes. This high level of baseline damage is likely to have phenotypic consequences, as we have shown that 10 Gy irradiation is sufficient to induce senescence in human chondrocytes when coupled with growth factor activation[23]. Markers of senescence increase with age in both human and murine chondrocytes[24], and the presence of senescent cells in the joint has been implicated in OA pathophysiology[25]. This is consistent with evidence in other tissue systems that supports DNA damage as a key driver of the cellular dysfunction that emerges during aging[6,7]. It will be important to further dissect the mechanisms by which chondrocytes accumulate such high levels of damage. For example, the relative contribution of increased susceptibility to damage and slower repair is unknown, but

there is evidence in other cell types that aging results in a compromised capacity for repair[26]. Further, hypo-replicative cell types such as chondrocytes may downregulate global DNA repair and prioritize the maintenance of genomic regions required for cell identity[5,27,28].

3.4 FIGURES

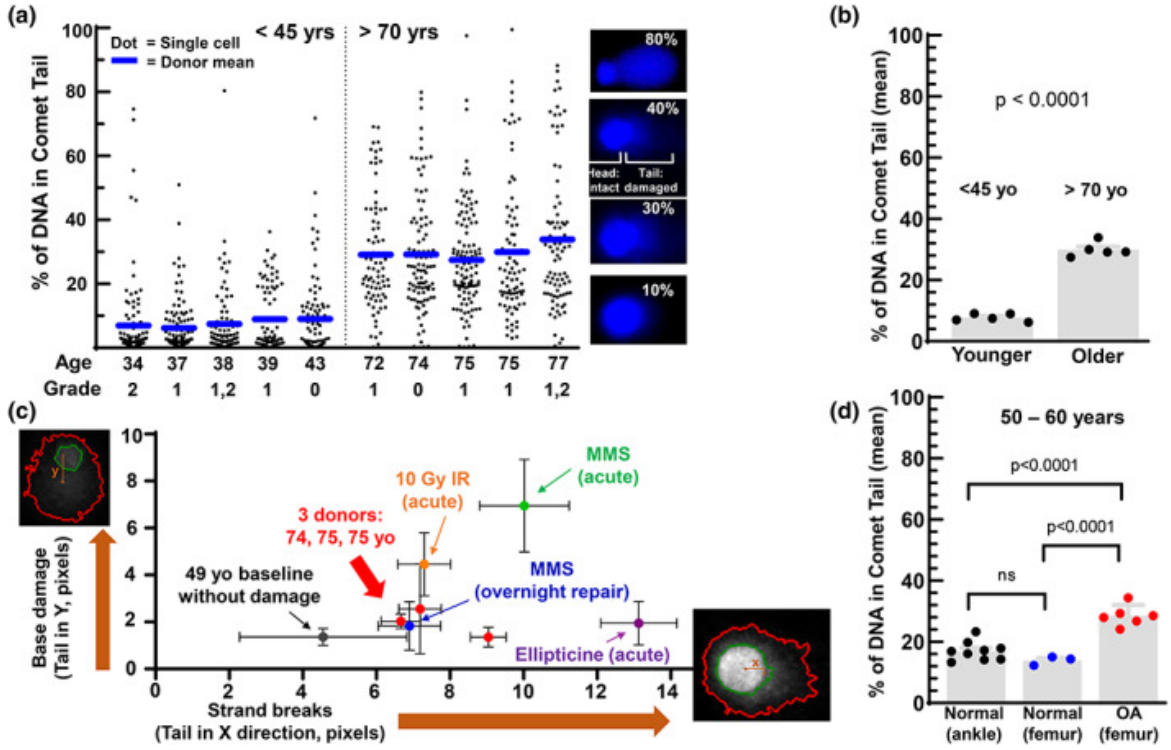

Figure 3.1: DNA damage in chondrocytes with aging and osteoarthritis. (A) Percent DNA in comet tail for chondrocytes from cadaveric donors of various ages with Collins grade shown. Dots are individual cells, with the mean shown as blue bars. Example cells with given % DNA in tail shown, with wide-field images in Supplemental Figure 3.2. (B) Donor mean % DNA in comet tail for those younger than 45 years of age (mean: 7.7%) and older than 70 years of age (mean: 29.9%). Stats by t-test. (C) Two-tailed comet using distance between centroid of comet head (green outline) and centroid of entire region including the tail (red outline). Strand breaks show up in x direction under neutral conditions and base damage is detected under alkaline conditions during the second electrophoresis (y direction). Chondrocytes from 49 yo serve as low damage control and were treated to induce damage. Ellipticine: 1h with 1 μM; MMS acute: 30 min with 0.5 mM; MMS repair: treatment removed before overnight repair; IR: 10 Gy applied to cells in gel on comet slide 15 min before lysis. Mean ± SEM both directions. ~100 cells per group. (D) Cadaveric tissue from donors with no clinical history of OA as compared to cartilage from end-stage OA at total knee replacement. All donors between 50-60 years of age. Mean tail DNA percent in the normal ankle is 17.5%, in normal femur is 13.9%, and in OA tissue is 28.5%. Stats by ANOVA with Tukey's post-hoc. Single-cell analysis for panel D shown in Supplemental Figure 3.2.

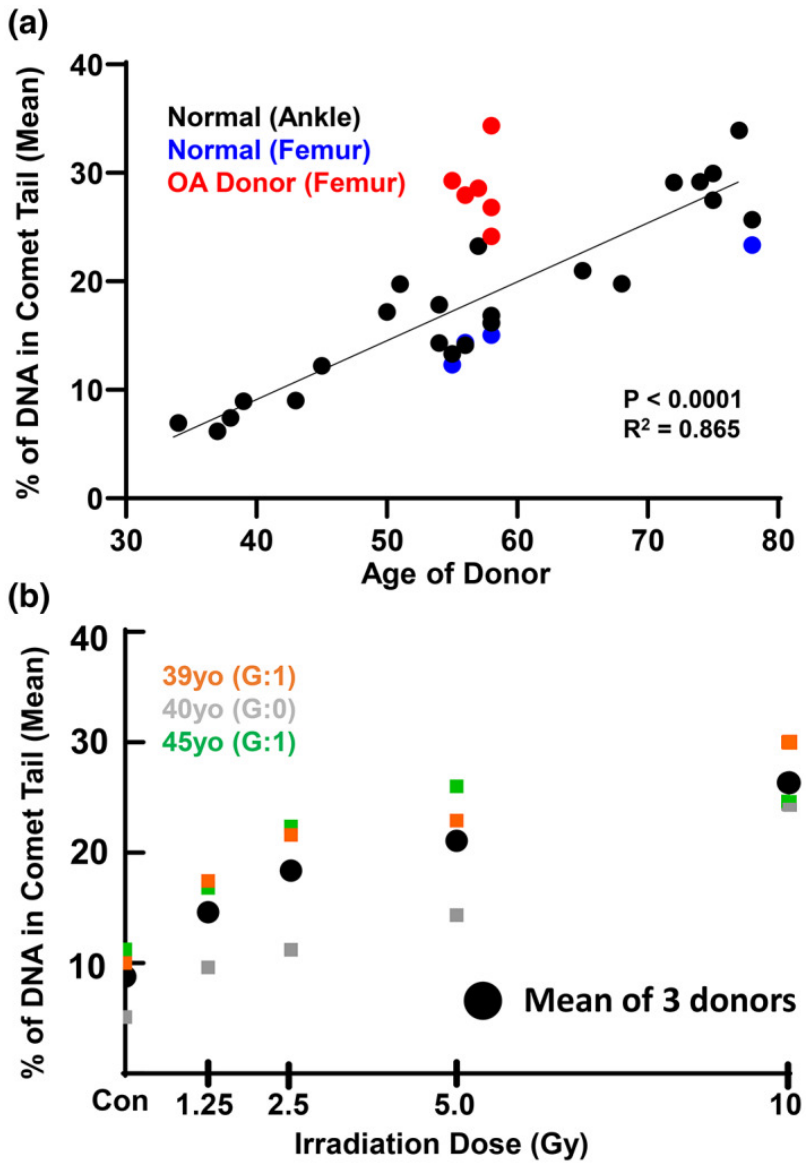

Figure 3.2: Linearity of DNA damage increase with age and comparison to damage from irradiation. (A) Linear regression for the 23 normal ankles, with p value and R^2 shown. OA donors (red) are plotted next to the normal donors and fall above the regression line. Cadaveric femur (blue) was available from four donors. Data are from Figure 3.1B and 3.1D, with the addition of 4 donors: 45 yo (grade 1,2), 65 yo (grade 0,1), 68 yo (grade 1,2), and 78 yo (grade 1). (B) DNA damage with increasing irradiation dose from 0 to 10 Gy. The average percent DNA in comet tail from the chondrocytes treated with 10 Gy of irradiation was 26.4%.

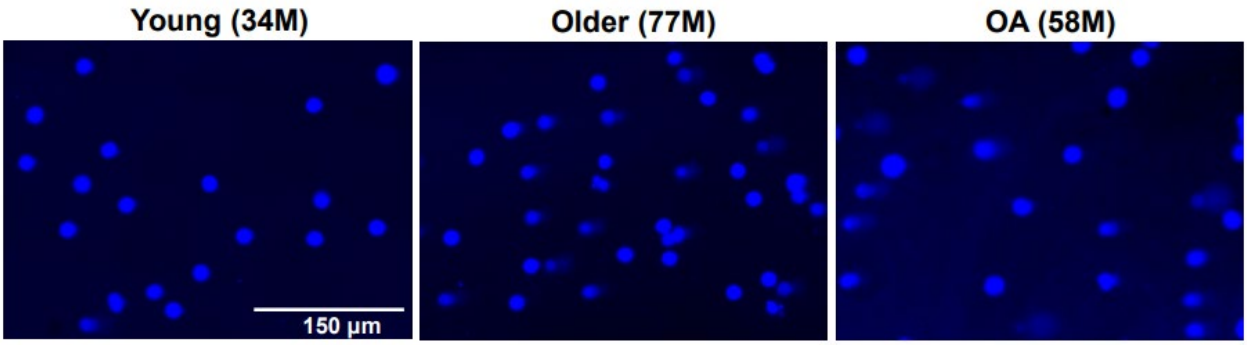

Supplemental Figure 3.1: Representative wide-field images of chondrocyte comets. Chondrocytes from young (34 y.o. male), older (77 y.o. male), and end-stage osteoarthritis (58 y.o. male) were analyzed by alkaline comet assay. Images are representative of those used to quantify the % of DNA in tail in Figure 3.1.

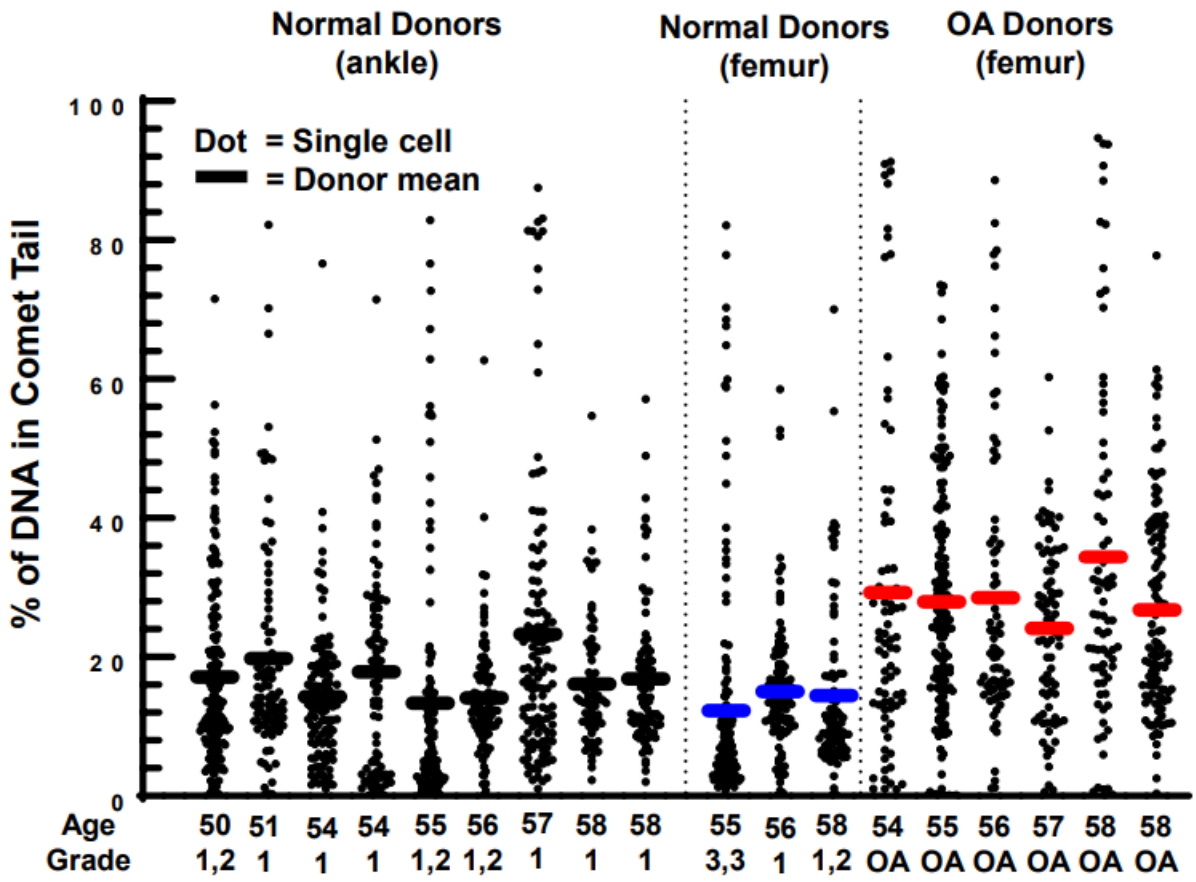

Supplemental Figure 3.2: Individual cell analysis of donors aged 50-60 years. Percent DNA in comet tails from chondrocytes derived from OA femur cartilage compared to cadaveric femur or ankle donors. Age and Collins grade are shown for each donor (multiple numbers indicate a distinct score for the two joints of a given donor, which were combined). The mean % of DNA in comet tail for each donor is plotted in Figure 3.1D.

3.5 ACKNOWLEDGEMENTS

The authors thank members of Dr. Richard Loeser's laboratory at the University of North Carolina at Chapel Hill for help in isolating human cartilage. The authors would also like to acknowledge the Gift of Hope Tissue and Organ Donor Bank, the families of tissue donors, as well as Mrs. Arnavaz Hakimiyan for tissue procurement. Support for this work was provided by the National Institutes of Health (R56 AG066911 to BOD, RO1 AG044034 to RFL). Procurement of human tissue was supported in part by the Rush University Klaus Kuettner Endowed Chair for Research on Osteoarthritis (SC). None of the funding sources had a role in the study or in the decision to publish.

REFERENCES

1. Loeser RF, Collins JA, Diekman BO. Ageing and the pathogenesis of osteoarthritis. *Nat Rev Rheumatol*. 2016;12(7):412-420. doi:10.1038/nrrheum.2016.65

2. Chen AF, Davies CM, De Lin M, Fermor B. Oxidative DNA damage in osteoarthritic porcine articular cartilage. *J Cell Physiol*. 2008;217(3):828-833. doi:10.1002/jcp.21562

3. Rose J, Söder S, Skhirtladze C, et al. DNA damage, discoordinated gene expression and cellular senescence in osteoarthritic chondrocytes. *Osteoarthr Cartil*. 2012;20(9):1020-1028. doi:10.1016/j.joca.2012.05.009

4. Arnoult N, Correia A, Ma J, et al. Regulation of DNA repair pathway choice in S and G2 phases by the NHEJ inhibitor CYREN. *Nature*. 2017;549(7673):548-552. doi:10.1038/nature24023

5. Reid DA, Reed PJ, Schlachetzki JCM, et al. Incorporation of a nucleoside analog maps genome repair sites in postmitotic human neurons. *Science*. 2021;372(6537):91-94. doi:10.1126/science.abb9032

6. Schumacher B, Pothof J, Vijg J, Hoeijmakers JHJ. The central role of DNA damage in the ageing process. *Nature*. 2021;592(7856):695-703. doi:10.1038/s41586-021-03307-7

7. Yousefzadeh M, Henpita C, Vyas R, Soto-Palma C, Robbins P, Niedernhofer L. DNA damage—how and why we age? Simon M, Tyler JK, eds. *eLife*. 2021;10:e62852. doi:10.7554/eLife.62852

8. Milić M, Ceppi M, Bruzzone M, et al. The hCOMET project: International database comparison of results with the comet assay in human biomonitoring. Baseline frequency of DNA damage and effect of main confounders. *Mutat Res Rev Mutat Res*. 2021;787:108371. doi:10.1016/j.mrrev.2021.108371

9. Olive PL, Banáth JP. The comet assay: a method to measure DNA damage in individual cells. *Nat Protoc*. 2006;1(1):23-29. doi:10.1038/nprot.2006.5

10. Cortés-Gutiérrez EI, Fernández JL, Dávila-Rodríguez MI, López-Fernández C, Gosálvez J. Two-Tailed Comet Assay (2T-Comet): Simultaneous Detection of DNA Single and Double Strand Breaks. *Methods Mol Biol*. 2017;1560:285-293. doi:10.1007/978-1-4939-6788-9_22

11. Muehleman C, Bareither D, Huch K, Cole AA, Kuettner KE. Prevalence of degenerative morphological changes in the joints of the lower extremity. *Osteoarthr Cartil*. 1997;5(1):23-37. doi:10.1016/s1063-4584(97)80029-5

12. Forsyth CB, Pulai J, Loeser RF. Fibronectin fragments and blocking antibodies to alpha2beta1 and alpha5beta1 integrins stimulate mitogen-activated protein kinase signaling and increase collagenase 3 (matrix metalloproteinase 13) production by human articular chondrocytes. *Arthritis Rheum*. 2002;46(9):2368-2376. doi:10.1002/art.10502

13. Lu Y, Liu Y, Yang C. Evaluating In Vitro DNA Damage Using Comet Assay. *JoVE (Journal of Visualized Experiments)*. 2017;(128):e56450. doi:10.3791/56450

14. Enciso M, Sarasa J, Agarwal A, Fernández JL, Gosálvez J. A two-tailed Comet assay for assessing DNA damage in spermatozoa. *Reprod Biomed Online*. 2009;18(5):609-616. doi:10.1016/s1472-6483(10)60003-x

15. Afanasieva K, Zazhytska M, Sivolob A. Kinetics of comet formation in single-cell gel electrophoresis: Loops and fragments. *ELECTROPHORESIS*. 2010;31(3):512-519. doi:10.1002/elps.200900421

16. Collins AR, Oscoz AA, Brunborg G, et al. The comet assay: topical issues. *Mutagenesis*. 2008;23(3):143-151. doi:10.1093/mutage/gem051

17. Gradzka I, Iwaneńko T. A non-radioactive, PFGE-based assay for low levels of DNA double-strand breaks in mammalian cells. *DNA Repair (Amst)*. 2005;4(10):1129-1139. doi:10.1016/j.dnarep.2005.06.001

18. Roots R, Holley W, Chatterjee A, Rachal E, Kraft G. The influence of radiation quality on the formation of DNA breaks. *Adv Space Res*. 1989;9(10):45-55. doi:10.1016/0273-1177(89)90422-5

19. Nikjoo H, O'Neill P, Wilson WE, Goodhead DT. Computational approach for determining the spectrum of DNA damage induced by ionizing radiation. *Radiat Res*. 2001;156(5 Pt 2):577-583. doi:10.1667/0033-7587(2001)156[0577:cafdts]2.0.co;2

20. Pommier Y, Schwartz RE, Kohn KW, Zwelling LA. Formation and rejoining of deoxyribonucleic acid double-strand breaks induced in isolated cell nuclei by antineoplastic intercalating agents. *Biochemistry*. 1984;23(14):3194-3201. doi:10.1021/bi00309a013

21. Wyatt MD, Pittman DL. Methylating Agents and DNA Repair Responses: Methylated Bases and Sources of Strand Breaks. *Chem Res Toxicol*. 2006;19(12):1580-1594. doi:10.1021/tx060164e

22. Møller P. Effect of age and sex on the level of DNA strand breaks and oxidatively damaged DNA in human blood cells. *Mutat Res Genet Toxicol Environ Mutagen*. 2019;838:16-21. doi:10.1016/j.mrgentox.2018.11.010

23. Copp ME, Flanders MC, Gagliardi R, et al. The combination of mitogenic stimulation and DNA damage induces chondrocyte senescence. *Osteoarthritis and Cartilage*. 2021;29(3):402-412. doi:10.1016/j.joca.2020.11.004

24. Diekman BO, Sessions GA, Collins JA, et al. Expression of p16INK 4a is a biomarker of chondrocyte aging but does not cause osteoarthritis. *Aging Cell*. 2018;17(4). doi:10.1111/acel.12771

25. Jeon OH, Kim C, Laberge RM, et al. Local clearance of senescent cells attenuates the development of post-traumatic osteoarthritis and creates a pro-regenerative environment. *Nat Med*. 2017;23(6):775-781. doi:10.1038/nm.4324

26. Chen Y, Geng A, Zhang W, et al. Fight to the bitter end: DNA repair and aging. *Ageing Res Rev*. 2020;64:101154. doi:10.1016/j.arr.2020.101154

27. Nouspikel T, Hanawalt PC. DNA repair in terminally differentiated cells. *DNA Repair*. 2002;1(1):59-75. doi:10.1016/S1568-7864(01)00005-2

28. Wu W, Hill SE, Nathan WJ, et al. Neuronal enhancers are hotspots for DNA single-strand break repair. *Nature*. 2021;593(7859):440-444. doi:10.1038/s41586-021-03468-5

CHAPTER 4: SIRT6 ACTIVATION RESCUES THE AGE-RELATED DECLINE IN DNA DAMAGE REPAIR IN PRIMARY HUMAN CHONDROCYTES[1]

4.1 INTRODUCTION

Osteoarthritis (OA) is a chronic joint disease affecting approximately 13% of the US adult population and is characterized by the degradation of articular cartilage, synovial inflammation, and subchondral bone remodeling[1-3]. As no disease-modifying therapies for OA have been FDA approved to date[4], the main options available to OA patients are pain management and eventual total joint replacement, leading to extensive societal and economic burdens[5]. While a number of risk factors have been associated with OA – obesity, biological sex, joint injury, and genetics – the leading risk factor is older age[6]. While progress continues to be made, the biological mechanisms linking aging and OA prevalence remain largely unknown[7].

Hypo-replicative cell types such as neurons, hematopoietic stem cells, and chondrocytes tend to accumulate sites of persistent DNA damage during aging, due at least in part to the lack of access to repair mechanisms that are only present in S phase[8-10]. As measured by the alkaline comet assay[11,12], we showed that chondrocytes isolated from older cadaveric donors, despite no known history of OA or macroscopic cartilage damage, harbor high levels of DNA damage[13]. One objective of this study was to determine whether a reduced efficiency of DNA damage repair with aging is one potential cause of DNA damage accumulation.

Sirtuin 6 (SIRT6) is nuclear-localized NAD(+)-dependent deacetylase that has been shown to play numerous important roles in cellular processes that become dysregulated with aging[14-17]. SIRT6

[1] The following chapter was published on BioRxiv.

Copp ME, Shine J, Brown HL, et al. SIRT6 activation rescues the age-related decline in DNA damage repair in primary human chondrocytes. Published online February 28, 2023:2023.02.27.530205. doi:10.1101/2023.02.27.530205

quickly localizes to sites of DNA damage and initiates chromatin remodeling to facilitate the recruitment and activity of proteins involved in DNA repair[18-22]. Prior work has indicated that SIRT6 is a critical factor in joint tissue homeostasis[23-26], and the level and/or enzymatic activity of SIRT6 decreases with age and in the context of OA[25,27]. Small molecules can be used to either increase or decrease the deacetylase activity of SIRT6: MDL-800 is an allosteric activator that increases activity by ~22-fold[28], whereas EX-527 is an inhibitor that stabilizes the closed conformation of sirtuins[29] and blocks 67% of recombinant SIRT6 activity within 15 minutes[25]. The second objective of this study was to examine how modulating SIRT6 activity impacts the repair of DNA.

Prior work completed in our lab has demonstrated that primary human chondrocytes accumulate damage in a linear manner with age, predominantly driven by strand breaks to the DNA[13]. The third objective of this study was to determine the extent to which MDL-800 can reduce DNA damage that has accumulated over decades in chondrocytes from older donors. Similarly, we investigated whether murine chondrocytes show a similar increase in DNA damage with age and whether MDL-800 treatment is sufficient to reverse damage in this important model species.

In this study, we use irradiation as an acute model of DNA damage to show that the DNA repair efficiency of chondrocytes deteriorates throughout life but can be enhanced by activating SIRT6. Further, SIRT6 activation was sufficient to reduce the accumulated DNA damage that arises with aging in human and murine chondrocytes. These findings support DNA damage repair as one beneficial aspect of SIRT6 and promote the activation of SIRT6 as a possible point of intervention to mitigate age-related OA.

4.2 RESULTS:

4.2.1 Decreased DNA damage repair efficiency with aging in primary human chondrocytes

To investigate how aging impacts the repair capacity of chondrocytes, we used irradiation to apply an acute bolus of damage to cells and monitored DNA damage by the comet assay at time points of 15, 30, 45, 60, 120, and 240 minutes after damage. This irradiation model allowed us to apply nearly instantaneous damage to the cells and conduct a precise time-course study of repair by transferring the slides directly to the lysis buffer (experimental approach in **Figure 4.4**). Importantly, chondrocytes from distinct age ranges of young (≤45 years old), middle (50-65 years old), and older (>70 years old) had a

similar amount of DNA damage immediately after irradiation, indicating that this bolus of damage was sufficient to overcome the background differences in accumulated damage. The ability of the chondrocytes to resolve DNA damage from this equal starting point over the course of 4 hours was impaired in the middle-aged and older donors as compared to the young donors (**Figure 4.1A**). The older donors had a significantly higher percentage of DNA in comet tails as compared to the middle and/or younger donors at 60, 120, and 240 minutes ($p<0.05$, multiple comparisons test). By 4 hours post-irradiation, most of the damage was resolved in chondrocytes from younger donors, whereas the average percentage of DNA in comet tails remained elevated for both middle-aged and older donors. Additional insight can be gained by assessing the distribution of damage within individual cells for each donor, as shown for representative young, middle, and older donors (**Figure 4.1B**). Of note, there was a bifurcated response in the older donors, with a significant fraction of cells retaining very high levels of damage (dotted line at 60% of damage in comet tails). When quantified across all donors, 27.6% of chondrocytes in the older group retained this high level of damage at 4 hours, whereas this percentage was 12.5% and 2.6% for middle and younger donors, respectively (**Figure 4.1C**). Analysis of chondrocytes with <15% DNA in comet tails at 4 hours showed that 68.7%, 49.6%, and 41.3% of cells from young, middle, and older donors, respectively, repaired the damage from irradiation to near-baseline levels (**Figure 4.5**).

4.2.2 SIRT6 activation and inhibition affects the repair efficiency of chondrocytes.

As SIRT6 is critical in the DNA repair process of cells, we sought to study how modulating SIRT6 activity impacts the repair of DNA. Using the same irradiation and comet assay system to study repair efficiency, chondrocytes from middle-aged donors were pre-treated for 2 hours with MDL-800 (activator), EX-527 (inhibitor), or DMSO (vehicle control). Following irradiation, the slides were placed back into media baths with their respective treatments for recovery (15 to 240 minutes post-irradiation), such that the cells were receiving SIRT6 activation/inhibition for the entirety of the study (experimental approach in **Figure 4.4**). When assessed by repeated measures two-way ANOVA without consideration of EX-527 treatment, MDL-800 treated groups showed lower DNA damage as compared to DMSO in middle-aged donors (**Figure 4.1A**, main effects p-value = 0.005). Similarly, when DMSO and MDL-800 were compared in chondrocytes from older donors (>70 years), there was reduced damage with MDL-800 treatment at 30, 60, 120, and 240 minutes (**Figure 4.6A**). Further, MDL-800 reduced the percentage of cells with high

damage (>60% DNA in comet tails) at 4 hours from 20.1% to 4.9% (**Figure 4.6B**). When EX-527 was also considered in the ANOVA for middle-aged donors, this inhibitor showed strong effects with significantly more DNA damage as compared to the DMSO and/or MDL-800 groups at baseline, 60, 120, and 240 minutes of repair (**Figure 4.2A**). The all-cell plot shows a striking increase in the percentage of individual cells that retain high levels of DNA damage in the EX-527 group (**Figure 4.2B**) – at 4 hours, 37.2% of cells still had greater than 60% of the DNA in comet tails. When comparing the percentage of cells with low levels of DNA damage, MDL-800 treatment significantly increased the likelihood that cells are able to restore near-baseline levels of damage at two- and four-hours post-irradiation (**Figure 4.5B**).

4.2.3 SIRT6 activation decreases DNA damage associated with older age.

Having shown that SIRT6 activity affects the repair capacity of chondrocytes in response to an acute bolus of damage, we wanted to test whether MDL-800 could also repair long-standing naturally accumulated damage. In previous studies, we have established that there is higher DNA damage in chondrocytes from older donors, with a linear regression showing that donors at age 40 have ~10% DNA in comet tails and donors at age 75 have ~27%[13]. Here, we treated chondrocytes isolated from older cadaveric donors for 48 hours with either 20 μM of MDL-800 or vehicle control (DMSO). The MDL-800 treated chondrocytes showed significantly lower levels of DNA damage (mean: 11.3% of DNA in comet tails) as compared to the DMSO groups (21.3%) (**Figure 4.3A**, p=0.0031, paired t-test).

4.2.4 MDL-800 treatment reduces DNA damage in aged murine chondrocytes.

Mice are a commonly used model species for investigations of mammalian aging and thus we sought to determine whether DNA damage also accumulates with age in murine chondrocytes. Chondrocytes from the proximal femur were isolated and then treated with MDL-800 (20 μM) or DMSO control for 48 hours before comet analysis. DNA damage increased in the DMSO-treated groups with age, with the percentage of DNA in comet tails approximately doubling from 4 to 22 months of age (**Figure 4.3B**). MDL treatment consistently lowered DNA damage in all age groups, with significant reductions at 8, 14, and 22 months of age (**Figure 4.3B**, $p<0.05$, multiple comparisons test).

4.3 DISCUSSION

In the present study, we found that (1) advanced age negatively impacts the ability of chondrocytes to repair DNA damage, (2) modulating SIRT6 activity affects the repair capacity of chondrocytes, and (3) activating SIRT6 with MDL-800 can aid in repairing DNA damage that had accumulated over decades. The first two findings made use of irradiation to initiate a bolus of damage. This system was particularly valuable in that the level of damage immediately following irradiation was consistent across all ages and treatment groups, allowing us to directly compare the progressive reduction in DNA damage over time.

There is growing evidence that the efficiency of DNA damage repair declines with age (reviewed in [30] and [31]). Previous work has largely been performed in fibroblasts and lymphocytes, but the current study confirms that aging also affects the repair of DNA damage in primary human chondrocytes. We used the alkaline comet assay to provide a sensitive and quantitative measure of DNA damage levels. Upon placement in a lysis solution, single strand breaks (SSBs), double strand breaks (DSBs), and other forms of damage (i.e., abasic sites) relax the supercoiled DNA loops of the nucleus, enabling easier movement of the DNA through the agarose gel when an electric field is applied[11,12]. As a result, damaged DNA produces a “comet tail” while intact DNA remains in the “comet head”. One advantage of this assay is the single-cell nature of the readout. This allowed us to observe that chondrocytes from older donors had a larger percentage of cells that showed very little repair and instead retained a high damage burden at four hours post-irradiation. This finding aligns with a previous study in lymphocytes that showed the primary difference with age in response to irradiation was the increased subset of cells that retained high damage[32].

SIRT6 is involved in numerous biological processes with relevance to aging[33], including a role in multiple DNA damage repair pathways[18,19,34-36]. Given the selectivity of MDL-800 for SIRT6[28], we were able to show that activation of SIRT6 is sufficient to repair approximately half of the accumulated damage in chondrocytes from older human donors and from older mice. For human chondrocytes, 48 hours of treatment with MDL-800 lowered the percentage of DNA in comet tails from 21.3% to 11.3%. Based on the linear regression calculated from 25 donors ranging in age from 34 to 78 years old in Copp et al.[13], MDL-800 treatment was able to eliminate the equivalent of ~34 years’ worth of damage is erased.

Cellular senescence is a phenotypic state characterized by stable cell cycle arrest in response to intrinsic or extrinsic stress[37]. The accumulation of senescent cells has been associated with numerous aging-related diseases and likely plays a role in OA pathogenesis[38,39]. However, less is known regarding the biological processes and environmental cues that prime chondrocytes to become senescent. Evidence supports the notion that DNA damage is a potential causative factor that drives senescence and other features of aging[40,41], and other studies have linked DNA damage with chondrocyte dysfunction during OA[42]. Our previous work also supports a causal role for DNA damage in chondrocyte senescence, as the application of 10 Gy irradiation (which recapitulates the level of DNA damage in older donors[13]) is capable of inducing senescence in cartilage explants when paired with a mitogenic stimulus[43]. A recent study demonstrated that Sirt6 deficiency exaggerated chondrocyte senescence and OA, while intra-articular injection of adenovirus-Sirt6 or the introduction of nanoparticles releasing MDL-800 mitigated OA caused by destabilization of the medial meniscus surgery[25]. When paired with the results of the current study, an intriguing hypothesis for future work is that SIRT6 activation prevents senescence and OA through enhanced DNA damage repair capacity.

In conclusion, the findings presented here support the hypothesis that the efficiency of DNA damage repair declines with age in chondrocytes and that SIRT6 activation improves repair both in response to an acute irradiation challenge and in the context of age-related damage accumulation. These results emphasize the critical role of SIRT6 in DNA repair and support further studies investigating the use of MDL-800 (or alternative SIRT6 activators) in mitigating senescence induction and ameliorating OA development.

4.4 MATERIALS AND METHODS

4.4.1 Isolation and culture of primary human chondrocytes.

Primary human chondrocytes were isolated from the ankle cartilage of cadaveric donors without a history of OA and with grades between 0 and 2 on the modified Collins grade[44]. For the study presented in **Figure 4.1**, ages of donors were in three groups: younger (40, 44, 45 years old); middle-aged (56, 56, 63 years old); older (73, 75, 76 years old). For the study presented in **Figure 4.2**, the donors used were middle-aged (51, 54, 54, 55, 56, 56, 60, 63). For the study presented in **Figure 4.3A**, the ages of the

donors were 74, 75, 75, and 76. To isolate the primary chondrocytes, full-thickness cartilage shards were digested with 2 mg/ml Pronase (1 hour) followed by overnight incubation with 3.6 mg/ml Collagenase P at 37^{o}C in 5% serum media[45]. The isolated chondrocytes were plated at a concentration of ~1x10^{5} cells per cm^{2} in DMEM/F12 supplemented with 10% FBS, penicillin and streptomycin, gentamicin, and amphotericin B to recover from isolation and frozen in Recovery™ Cell Culture Freezing Medium. Chondrocytes were plated for ~2-3 days before harvest for resuspension in comet gels for irradiation.

4.4.2 Isolation of primary murine chondrocytes.

The cartilaginous head of the proximal femur (i.e., the femoral cap of the hip) was used as the source of chondrocytes from C57BL/6 mice at various ages. Chondrocytes were isolated via pronase (2 mg/ml, 1 hour in serum-free media) and collagenase P (500 µg/ml, overnight in 10% serum) from mice aged 4, 8, 14, and 22 months of age (n=3 each). Chondrocytes were cultured for ~3 days to recover before treatment.

4.4.3 SIRT6 Activation and Inhibition Treatment.

The small molecule MDL-800 (Sigma) was used at a concentration of 20 µM to activate SIRT6. Conversely, EX-527 (Selleck) was used at a concentration of 10 µM to inhibit SIRT6 activity. When testing the effect of SIRT6 modulation on DNA repair following acute damage (**Figure 4.2**), primary chondrocytes were pre-treated with either DMSO (vehicle control, concentration matching the DMSO used with MDL-800), MDL-800, or EX-527 for 2 hours prior to harvest for irradiation experiments. For experiments testing the reduction of accumulated DNA damage in chondrocytes from older cadaveric donors and mice, cells were treated with DMSO or 20 µM MDL-800 for 48 hours.

4.4.4 Acute Irradiation Repair Model and Comet Assay Protocol.

A schematic depicting the irradiation repair model is shown in **Figure 4.4**. After trypsinization, chondrocytes were prepared for the comet assay as described[13], with adjustments made to measure DNA damage levels at specific time points following irradiation. Briefly, cells were mixed 1:10 with 1% low melting agarose and coated onto a Superfrost slide. The slides were placed in a media bath and irradiated with 10 Gy X-ray (RS2000 Biological Irradiator), with one slide not irradiated as a control group. The slides were moved to an incubator with their appropriate media for various amounts of time for recovery and then added to a lysis solution at the indicated time point – immediate (no recovery after IR),

15 min., 30 min., 60 min., 120 min., and 240 min. The lysis solution was prepared by mixing 2.5 M NaCl, 0.1 M disodium EDTA, 10 mM Tris base, 0.2 M NaOH, 0.1% sodium lauryl sarcosinate, and 1% Triton X-1000, and adjusting the solution to a pH of 10. After overnight incubation in the lysis solution at 4°C, the slides were added to an alkaline electrophoresis solution (200 mM NaOH, 1 mM disodium EDTA, pH > 13) for 30 minutes. Next, the slides were placed into an electrophoresis chamber and an electric field of 1 V/cm for 20 minutes was applied. Slides were washed with dH_2O and stained with NucBlue™ (R37605; Thermo Fisher Scientific). Fluorescence images were captured with an EVOS M5000 microscope (AMF5000; Thermo Fisher Scientific). Image analysis and comet quantification were performed for approximately 100 cells per condition using the OpenComet plugin software in ImageJ.

4.4.5 Statistical Analysis

Comet data were analyzed and plotted using GraphPad Prism 9. Statistical analysis was performed using paired t-test, two-way ANOVA, or two-way repeated measures ANOVA. Multiple comparison test used either Sidak's (two treatment groups) or Tukey's (three treatment groups) within each time point.

4.5 ABBREVIATIONS

OA – osteoarthritis

SIRT6 – Sirtuin 6

DNA: deoxyribonucleic acid

DSB: double strand breaks

SSB: single strand breaks

IR: irradiation

4.6 AUTHOR CONTRIBUTIONS

Conception and experimental design of this study was completed by MEC and BOD, with input from JAC. Data collection and analysis was done by MEC, JS, HLB, KRN, and BOD. Study materials were provided by SC and RFL. MEC drafted the manuscript and BOD and RFL provided critical revision and edits. All authors have approved of the final article provided herein.

4.7 ACKNOWLEDGEMENTS

We appreciate the work of Dr. Richard Loeser's laboratory members for help in isolating human cartilage. We acknowledge the Gift of Hope Tissue and Organ Donor Bank, the families of tissue donors, and Mrs. Arnavaz Hakimiyan for tissue procurement. Procurement of human tissue supported in part by the Rush University Klaus Kuettner Endowed Chair for Research on Osteoarthritis (SC). Funding sources had no role in the study or in the decision to publish.

4.8 FUNDING

Support provided by National Institutes of Health: R56 AG066911 to BOD; RO1 AG044034 to RFL.

4.9 FIGURES

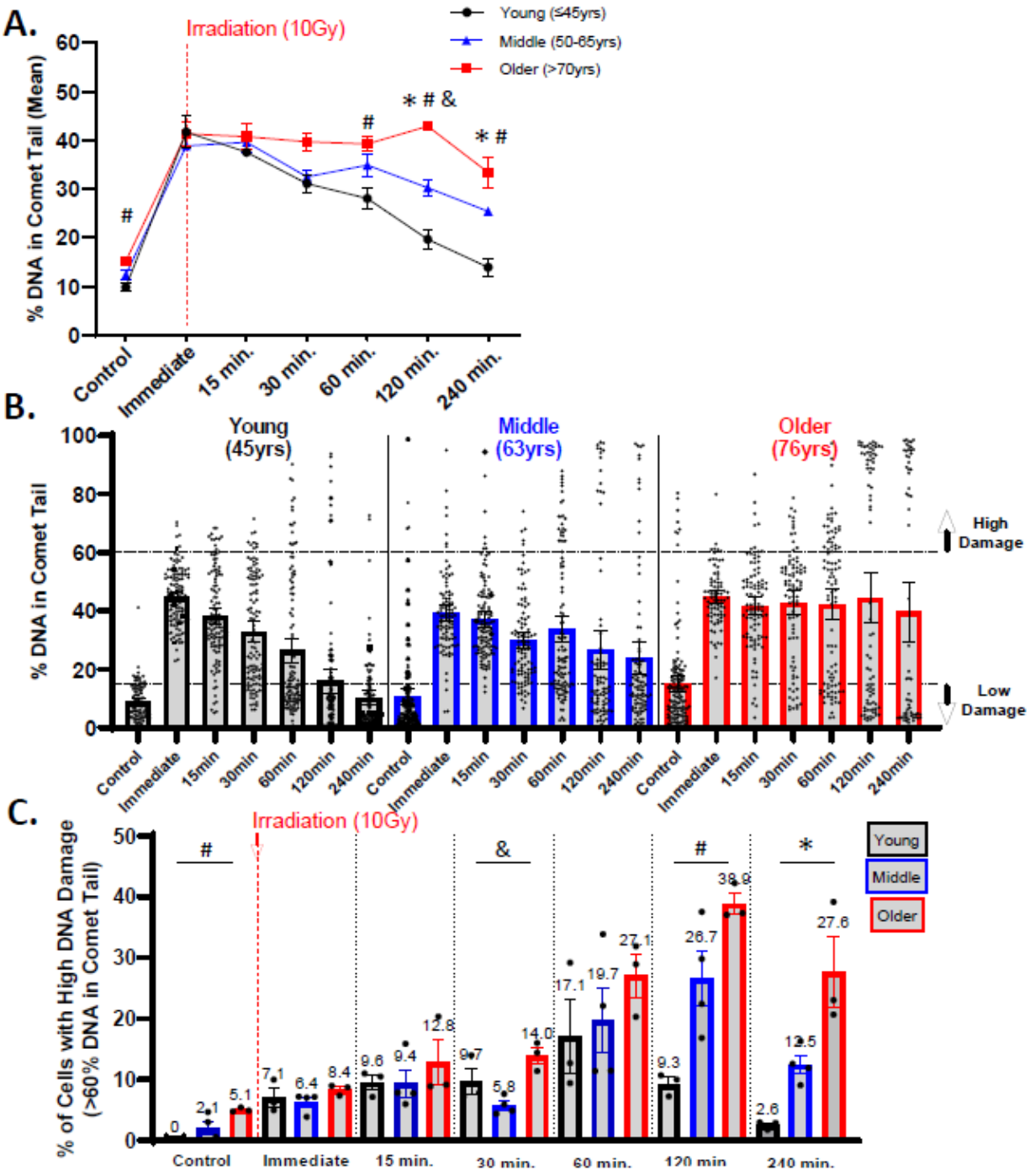

Figure 4.1: Repair after acute DNA damage in chondrocytes from different aged donors. Primary human chondrocytes from young (n=3, ≤45 years), middle-aged (n=4, 50-65 years), and older (n=3, >70 years) were prepared in gels on microscope slides and irradiated with 10 Gy(or not for control). Slides were transferred to media for repair after irradiation and then lysis buffer at various time points. (A) The

percentage of DNA in comet tails for all cells were averaged for each donor, and the mean of all donors per age group is shown (mean + SEM). Repair time, age, and their interaction were significant sources of variation (2-way repeated measures ANOVA). Significant differences between groups at each time point (Tukey's multiple comparisons test, $p<0.05$) are denoted by symbols: (*) = young vs. middle, (#) = young vs. old, (&) = middle vs. old. (B) Plots showing all individual cells of representative young, middle, and older donors. (C) The percentage of cells with high levels of DNA damage (>60% of DNA in comet tails). Statistics same as in B.

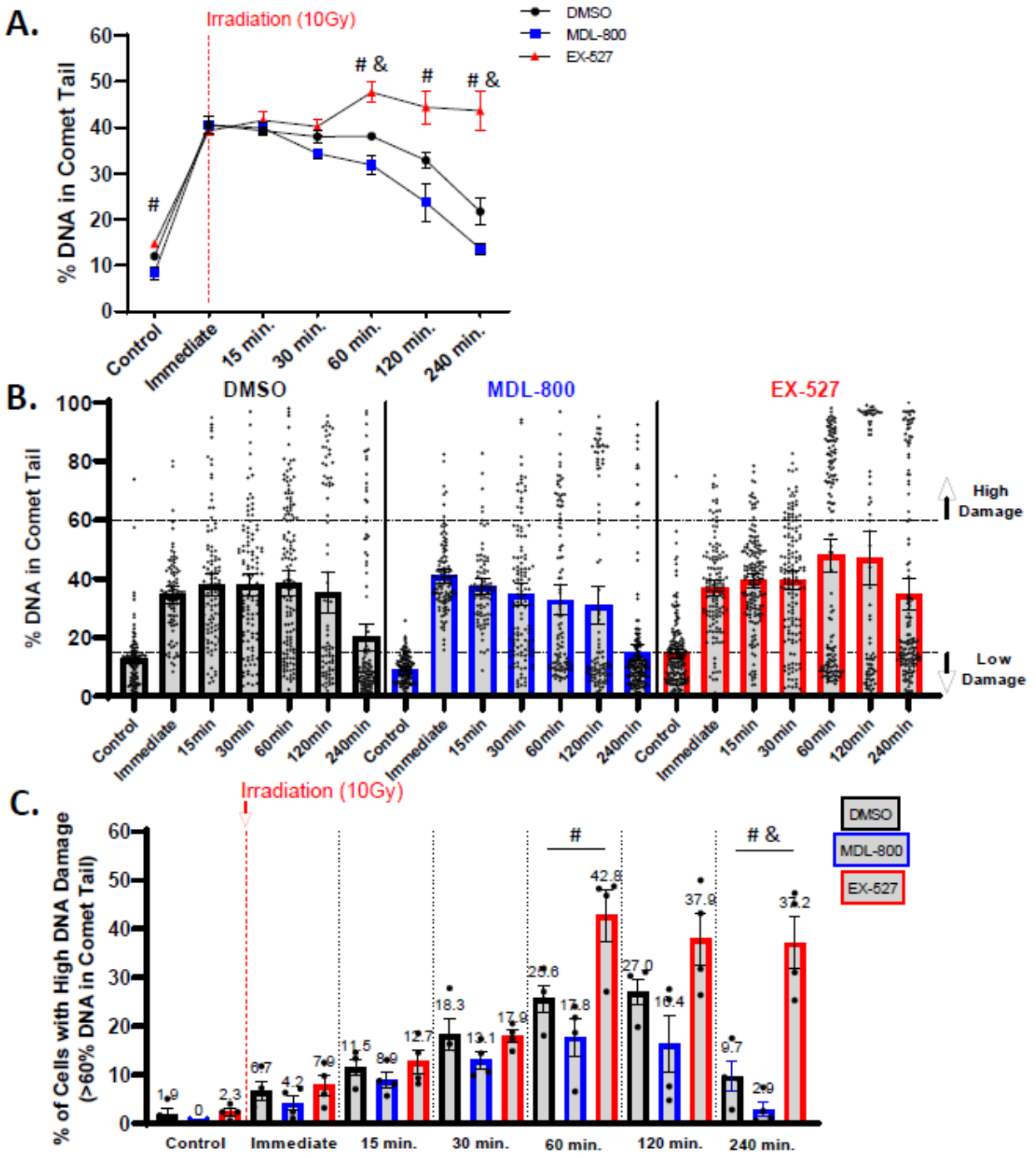

Figure 4.2: Effect of SIRT6 activation and inhibition on chondrocyte repair efficiency. Chondrocytes from middle-aged donors were pre-treated with 20 μM MDL-800, 10 μM EX-527, or vehicle (DMSO) for 2 hours before trypsinization, gel encapsulation, and irradiation. Treatment continued during the repair phase. (A) The percentage of DNA in comet tails for all cells were averaged for each donor, and the mean of all donors per condition is shown (mean + SEM). Repair time, treatment, and their interaction

were significant sources of variation (2-way repeated measures ANOVA). Significant differences between groups at each time point (Tukey's multiple comparisons test, $p<0.05$) are denoted by symbols: (*) = DMSO vs. MDL, (#) = MDL vs. EX, (&) = DMSO vs. EX). (B) Plots show all individual cells of a representative donor treated with DMSO, MDL-800, or EX-527. (C) The percentage of cells with high levels of DNA damage (>60% of DNA in comet tails). Statistics as in B.

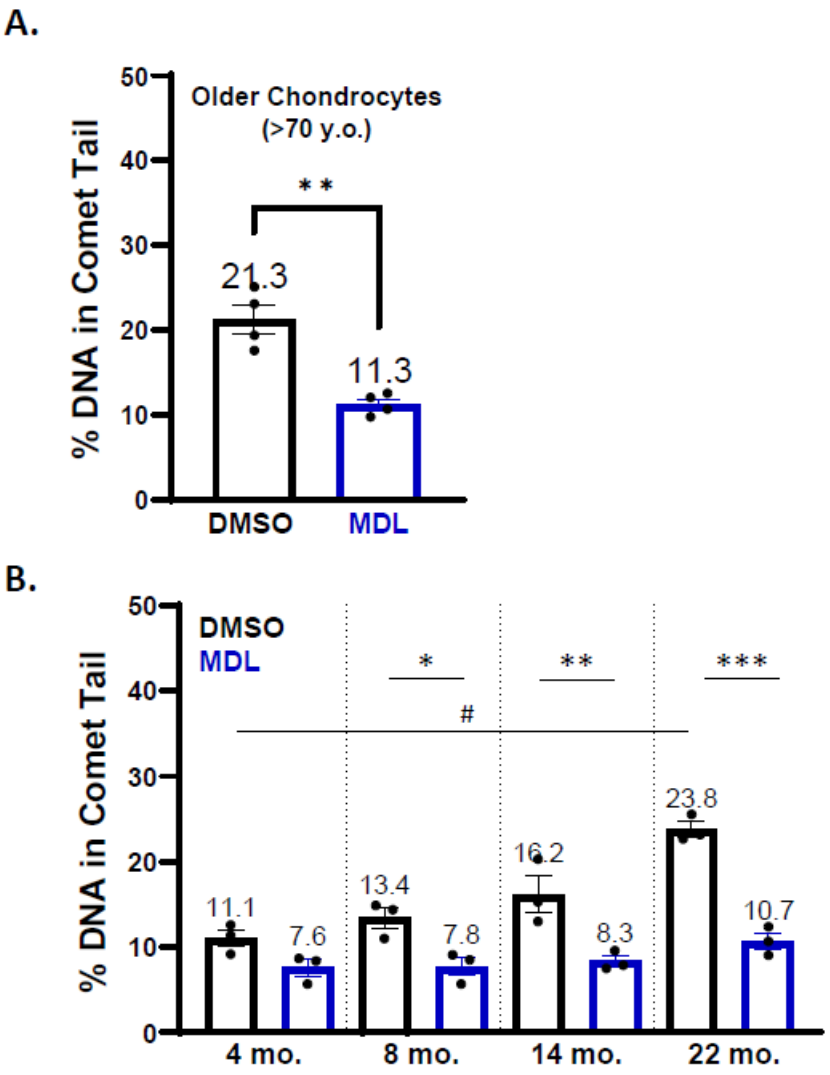

Figure 4.3: SIRT6 activation in chondrocytes from older human donors and mice. (A) Chondrocytes derived from cadaveric ankle cartilage of older donors (>70 years) were treated with 20 μM MDL-800 or vehicle (DMSO) for 48 hours. Stats by paired t-test. (B) Chondrocytes from the proximal femur of mice were isolated and treated for 48 hours with DMSO or 20 μM MDL-800. Analysis by two-way ANOVA showed significant effects of age, treatment, and their interaction. Significant differences between groups at each time point (Sidak'smultiple comparisons test, $p<0.001$) are denoted by # symbol, with differences between treatments denoted by *.

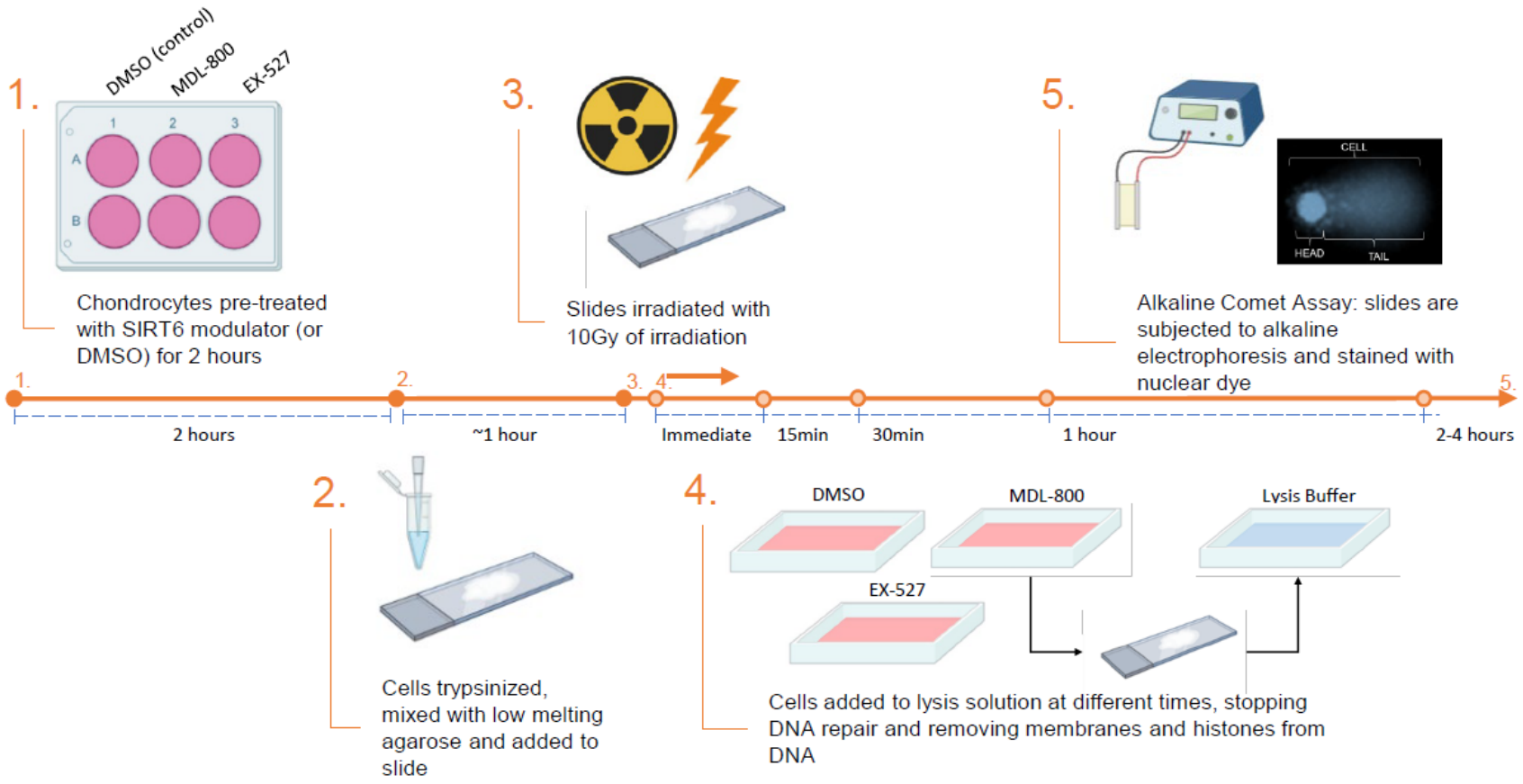

Figure 4.4: Experimental design for the results shown in Figure 4.2. For the data in Figure 4.1, there was no pre-treatment and steps 2-5 were completed as shown (with 10% serum media used for the repair phase).

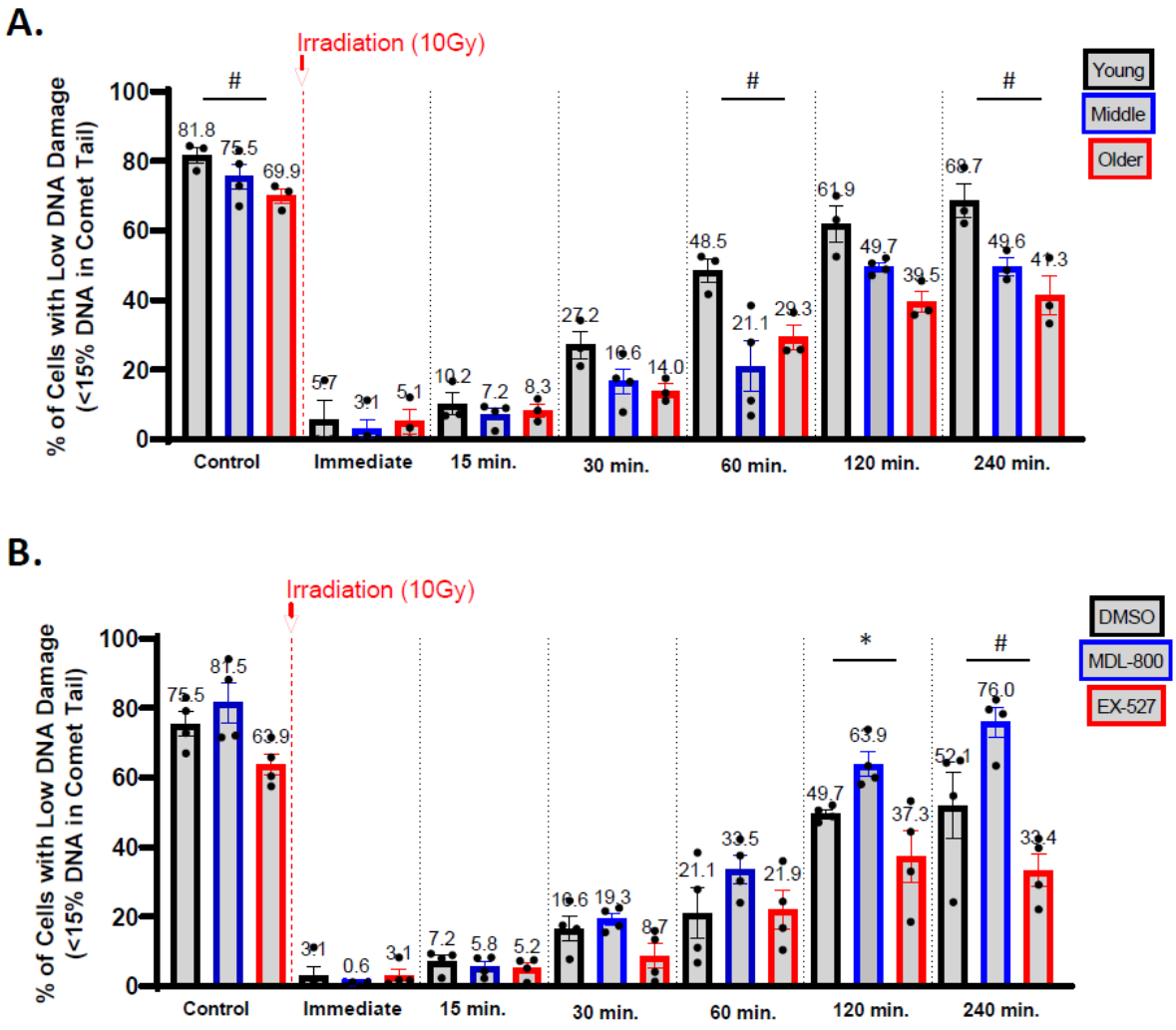

Figure 4.5: Efficacy of chondrocytes to restore low levels of DNA damage after acute damage. (A) Primary human chondrocytes from young, middle, and older donors prepared as described in Figure 4.1. The percentage of cells with low levels of DNA damage (<15% of DNA in comet tail) were plotted and the mean of all donors per age group is shown (mean + SEM). Repair time, age, and their interaction were significant sources of variation (2-way repeated measures ANOVA). Significant differences between groups at each time point (Tukey's multiple comparisons test, $p<0.05$) are denoted by symbols: (*) = young vs. middle, (#) = young vs. old, (&) = middle vs. old. (B) Chondrocytes from middle-aged donors were pre-treated with 20 μM MDL-800, 10 μMEX-527, or vehicle (DMSO) for 2 hours before trypsinization, gel encapsulation, and irradiation. The percentage of cells with low levels of DNA damage (<15% of DNA in comet tails). Statistics similar toA, but with significant differences denoted by symbols: (*) = DMSO vs. MDL, (#) = MDL vs. EX, (&) = DMSO vs. EX).

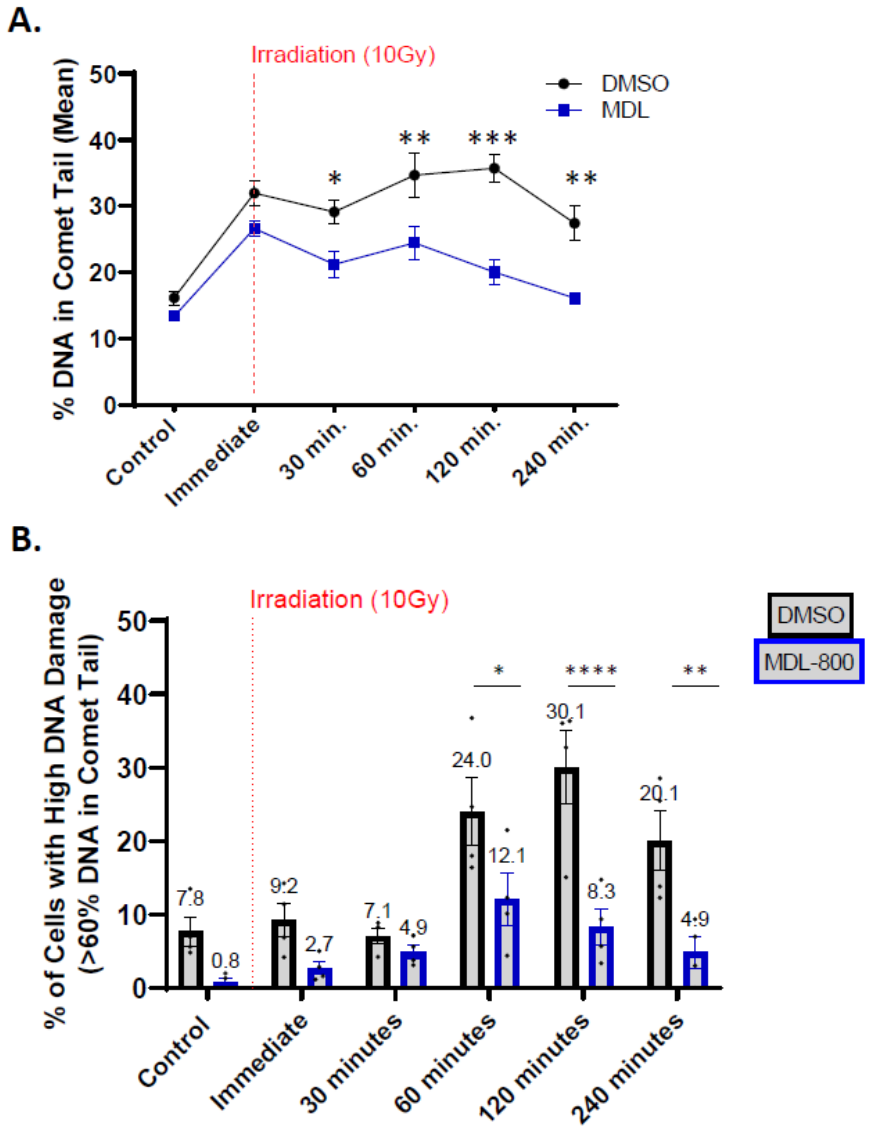

Figure 4.6: Effect of SIRT6 activation and inhibition on older chondrocyte repair efficiency. Chondrocytes from older donors (n=4, >70 years) were pre-treated with 20 μM MDL-800, 10 μMEX-527, or vehicle (DMSO) for 2 hours before trypsinization, gel encapsulation, and irradiation. Treatment continued during the repair phase. (A) The percentage of DNA in comet tails for all cells were averaged for each condition, and the mean of all donors per age group is shown (mean + SEM). Repair time, treatment, and their interaction were significant sources of variation (2-way repeated measures ANOVA). Significant differences between groups at each time point (Tukey's multiple comparisons test, $p<0.05$) are denoted by symbols: (*) = DMSO vs. MDL. (B) The percentage of cells with high levels of DNA damage (>60% of DNA in comet tails). Statistics as in A.

REFERENCES

1. Bijlsma JW, Berenbaum F, Lafeber FP. Osteoarthritis: an update with relevance for clinical practice. Lancet. 2011;377(9783):2115-26. doi: 10.1016/S0140-6736(11)60243-2. PubMed PMID: 21684382.

2. Loeser RF, Goldring SR, Scanzello CR, Goldring MB. Osteoarthritis: a disease of the joint as an organ. Arthritis Rheum. 2012;64(6):1697-707. doi: 10.1002/art.34453. PubMed PMID: 22392533; PMCID: PMC3366018.

3. Cisternas MG, Murphy L, Sacks JJ, Solomon DH, Pasta DJ, Helmick CG. Alternative Methods for Defining Osteoarthritis and the Impact on Estimating Prevalence in a US Population-Based Survey. Arthritis Care Res (Hoboken). 2016;68(5):574-80. doi: 10.1002/acr.22721. PubMed PMID: 26315529; PMCID: PMC4769961.

4. Oo WM, Yu SP, Daniel MS, Hunter DJ. Disease-modifying drugs in osteoarthritis: current understanding and future therapeutics. Expert Opin Emerg Drugs. 2018;23(4):331-47. Epub 2018/11/13. doi: 10.1080/14728214.2018.1547706. PubMed PMID: 30415584.

5. Zhao X, Shah D, Gandhi K, Wei W, Dwibedi N, Webster L, Sambamoorthi U. Clinical, humanistic, and economic burden of osteoarthritis among noninstitutionalized adults in the United States. Osteoarthritis Cartilage. 2019;27(11):1618-26. Epub 20190709. doi: 10.1016/j.joca.2019.07.002. PubMed PMID: 31299387.

6. Felson DT, Lawrence RC, Dieppe PA, Hirsch R, Helmick CG, Jordan JM, . . . Fries JF. Osteoarthritis: new insights. Part 1: the disease and its risk factors. Ann Intern Med. 2000;133(8):635-46. PubMed PMID: 11033593.

7. Loeser RF, Collins JA, Diekman BO. Ageing and the pathogenesis of osteoarthritis. Nat Rev Rheumatol. 2016;12(7):412-20. doi: 10.1038/nrrheum.2016.65. PubMed PMID: 27192932; PMCID: PMC4938009.

8. Wu W, Hill SE, Nathan WJ, Paiano J, Callen E, Wang D, . . . Nussenzweig A. Neuronal enhancers are hotspots for DNA single-strand break repair. Nature. 2021;593(7859):440-4. Epub 2021/03/27. doi: 10.1038/s41586-021-03468-5. PubMed PMID: 33767446.

9. Reid DA, Reed PJ, Schlachetzki JCM, Nitulescu, II, Chou G, Tsui EC, . . . Gage FH. Incorporation of a nucleoside analog maps genome repair sites in postmitotic human neurons. Science. 2021;372(6537):91-4. Epub 2021/04/03. doi: 10.1126/science.abb9032. PubMed PMID: 33795458.

10. Beerman I, Seita J, Inlay MA, Weissman IL, Rossi DJ. Quiescent hematopoietic stem cells accumulate DNA damage during aging that is repaired upon entry into cell cycle. Cell Stem Cell. 2014;15(1):37-50. Epub 2014/05/13. doi: 10.1016/j.stem.2014.04.016. PubMed PMID: 24813857; PMCID: PMC4082747.

11. Olive PL, Banath JP. The comet assay: a method to measure DNA damage in individual cells. Nat Protoc. 2006;1(1):23-9. Epub 2007/04/05. doi: 10.1038/nprot.2006.5. PubMed PMID: 17406208.

12. Afanasieva K, Sivolob A. Physical principles and new applications of comet assay. Biophys Chem. 2018;238:1-7. Epub 2018/04/29. doi: 10.1016/j.bpc.2018.04.003. PubMed PMID: 29704770.

13. Copp ME, Chubinskaya S, Bracey DN, Shine J, Sessions G, Loeser RF, Diekman BO. Comet assay for quantification of the increased DNA damage burden in primary human chondrocytes

with aging and osteoarthritis. Aging Cell. 2022;21(9):e13698. Epub 2022/08/24. doi: 10.1111/acel.13698. PubMed PMID: 35996812.

14. Roichman A, Kanfi Y, Glazz R, Naiman S, Amit U, Landa N, . . . Cohen HY. SIRT6 Overexpression Improves Various Aspects of Mouse Healthspan. J Gerontol A Biol Sci Med Sci. 2017;72(5):603-15. doi: 10.1093/gerona/glw152. PubMed PMID: 27519885.

15. Tasselli L, Zheng W, Chua KF. SIRT6: Novel Mechanisms and Links to Aging and Disease. Trends Endocrinol Metab. 2017;28(3):168-85. Epub 20161109. doi: 10.1016/j.tem.2016.10.002. PubMed PMID: 27836583; PMCID: PMC5326594.

16. Toiber D, Sebastian C, Mostoslavsky R. Characterization of nuclear sirtuins: molecular mechanisms and physiological relevance. Handb Exp Pharmacol. 2011;206:189-224. doi: 10.1007/978-3-642-21631-2_9. PubMed PMID: 21879451.

17. Mostoslavsky R, Chua KF, Lombard DB, Pang WW, Fischer MR, Gellon L, . . . Alt FW. Genomic instability and aging-like phenotype in the absence of mammalian SIRT6. Cell. 2006;124(2):315-29. doi: 10.1016/j.cell.2005.11.044. PubMed PMID: 16439206.

18. Mao Z, Hine C, Tian X, Van Meter M, Au M, Vaidya A, . . . Gorbunova V. SIRT6 promotes DNA repair under stress by activating PARP1. Science. 2011;332(6036):1443-6. Epub 2011/06/18. doi: 10.1126/science.1202723. PubMed PMID: 21680843; PMCID: PMC5472447.

19. Xu Z, Zhang L, Zhang W, Meng D, Zhang H, Jiang Y, . . . Mao Z. SIRT6 rescues the age related decline in base excision repair in a PARP1-dependent manner. Cell Cycle. 2015;14(2):269-76. Epub 2015/01/22. doi: 10.4161/15384101.2014.980641. PubMed PMID: 25607651; PMCID: PMC4614943.

20. Toiber D, Erdel F, Bouazoune K, Silberman DM, Zhong L, Mulligan P, . . . Mostoslavsky R. SIRT6 recruits SNF2H to DNA break sites, preventing genomic instability through chromatin remodeling. Mol Cell. 2013;51(4):454-68. Epub 2013/08/06. doi: 10.1016/j.molcel.2013.06.018. PubMed PMID: 23911928; PMCID: PMC3761390.

21. Hou T, Cao Z, Zhang J, Tang M, Tian Y, Li Y, . . . Zhu WG. SIRT6 coordinates with CHD4 to promote chromatin relaxation and DNA repair. Nucleic Acids Res. 2020;48(6):2982-3000. doi: 10.1093/nar/gkaa006. PubMed PMID: 31970415; PMCID: PMC7102973.

22. Onn L, Portillo M, Ilic S, Cleitman G, Stein D, Kaluski S, . . . Toiber D. SIRT6 is a DNA double-strand break sensor. Elife. 2020;9. Epub 20200129. doi: 10.7554/eLife.51636. PubMed PMID: 31995034; PMCID: PMC7051178.

23. Dvir-Ginzberg M, Mobasheri A, Kumar A. The Role of Sirtuins in Cartilage Homeostasis and Osteoarthritis. Curr Rheumatol Rep. 2016;18(7):43. doi: 10.1007/s11926-016-0591-y. PubMed PMID: 27289467.

24. Wu Y, Chen L, Wang Y, Li W, Lin Y, Yu D, . . . Pan Z. Overexpression of Sirtuin 6 suppresses cellular senescence and NF-kappaB mediated inflammatory responses in osteoarthritis development. Sci Rep. 2015;5:17602. Epub 2015/12/08. doi: 10.1038/srep17602. PubMed PMID: 26639398; PMCID: PMC4671011.

25. Ji ML, Jiang H, Li Z, Geng R, Hu JZ, Lin YC, Lu J. Sirt6 attenuates chondrocyte senescence and osteoarthritis progression. Nat Commun. 2022;13(1):7658. Epub 2022/12/11. doi: 10.1038/s41467-022-35424-w. PubMed PMID: 36496445; PMCID: PMC9741608.

26. Nagai K, Matsushita T, Matsuzaki T, Takayama K, Matsumoto T, Kuroda R, Kurosaka M. Depletion of SIRT6 causes cellular senescence, DNA damage, and telomere dysfunction in

human chondrocytes. Osteoarthritis Cartilage. 2015;23(8):1412-20. Epub 2015/03/31. doi: 10.1016/j.joca.2015.03.024. PubMed PMID: 25819580.

27. Collins JA, Kapustina M, Bolduc JA, Pike JFW, Diekman BO, Mix K, . . . Loeser RF. Sirtuin 6 (SIRT6) regulates redox homeostasis and signaling events in human articular chondrocytes. Free Radic Biol Med. 2021;166:90-103. Epub 2021/02/19. doi: 10.1016/j.freeradbiomed.2021.01.054. PubMed PMID: 33600943; PMCID: PMC8009856.

28. Huang Z, Zhao J, Deng W, Chen Y, Shang J, Song K, . . . Zhang J. Identification of a cellularly active SIRT6 allosteric activator. Nat Chem Biol. 2018;14(12):1118-26. Epub 2018/10/31. doi: 10.1038/s41589-018-0150-0. PubMed PMID: 30374165.

29. Gertz M, Fischer F, Nguyen GT, Lakshminarasimhan M, Schutkowski M, Weyand M, Steegborn C. Ex-527 inhibits Sirtuins by exploiting their unique NAD+-dependent deacetylation mechanism. Proc Natl Acad Sci U S A. 2013;110(30):E2772-81. Epub 20130709. doi: 10.1073/pnas.1303628110. PubMed PMID: 23840057; PMCID: PMC3725051.

30. Gorbunova V, Seluanov A, Mao Z, Hine C. Changes in DNA repair during aging. Nucleic Acids Res. 2007;35(22):7466-74. Epub 20071002. doi: 10.1093/nar/gkm756. PubMed PMID: 17913742; PMCID: PMC2190694.

31. Chen Y, Geng A, Zhang W, Qian Z, Wan X, Jiang Y, Mao Z. Fight to the bitter end: DNA repair and aging. Ageing Res Rev. 2020;64:101154. Epub 2020/09/26. doi: 10.1016/j.arr.2020.101154. PubMed PMID: 32977059.

32. Singh NP, Danner DB, Tice RR, Brant L, Schneider EL. DNA damage and repair with age in individual human lymphocytes. Mutat Res. 1990;237(3-4):123-30. doi: 10.1016/0921-8734(90)90018-m. PubMed PMID: 2233818.

33. Chang AR, Ferrer CM, Mostoslavsky R. SIRT6, a Mammalian Deacylase with Multitasking Abilities. Physiol Rev. 2020;100(1):145-69. Epub 2019/08/23. doi: 10.1152/physrev.00030.2018. PubMed PMID: 31437090; PMCID: PMC7002868.

34. Mao Z, Tian X, Van Meter M, Ke Z, Gorbunova V, Seluanov A. Sirtuin 6 (SIRT6) rescues the decline of homologous recombination repair during replicative senescence. Proc Natl Acad Sci U S A. 2012;109(29):11800-5. Epub 2012/07/04. doi: 10.1073/pnas.1200583109. PubMed PMID: 22753495; PMCID: PMC3406824.

35. Tian X, Firsanov D, Zhang Z, Cheng Y, Luo L, Tombline G, . . . Gorbunova V. SIRT6 Is Responsible for More Efficient DNA Double-Strand Break Repair in Long-Lived Species. Cell. 2019;177(3):622-38 e22. Epub 2019/04/20. doi: 10.1016/j.cell.2019.03.043. PubMed PMID: 31002797; PMCID: PMC6499390.

36. Simon M, Yang J, Gigas J, Earley EJ, Hillpot E, Zhang L, . . . Gorbunova V. A rare human centenarian variant of SIRT6 enhances genome stability and interaction with Lamin A. EMBO J. 2022;41(21):e110393. Epub 20221010. doi: 10.15252/embj.2021110393. PubMed PMID: 36215696; PMCID: PMC9627671.

37. He S, Sharpless NE. Senescence in Health and Disease. Cell. 2017;169(6):1000-11. doi: 10.1016/j.cell.2017.05.015. PubMed PMID: 28575665.

38. Coryell PR, Diekman BO, Loeser RF. Mechanisms and therapeutic implications of cellular senescence in osteoarthritis. Nat Rev Rheumatol. 2021;17(1):47-57. Epub 2020/11/20. doi: 10.1038/s41584-020-00533-7. PubMed PMID: 33208917; PMCID: PMC8035495.

39. Jeon OH, David N, Campisi J, Elisseeff JH. Senescent cells and osteoarthritis: a painful connection. J Clin Invest. 2018;128(4):1229-37. Epub 2018/04/03. doi: 10.1172/JCI95147. PubMed PMID: 29608139; PMCID: PMC5873863.

40. Yousefzadeh M, Henpita C, Vyas R, Soto-Palma C, Robbins P, Niedernhofer L. DNA damage-how and why we age? Elife. 2021;10. Epub 2021/01/30. doi: 10.7554/eLife.62852. PubMed PMID: 33512317; PMCID: PMC7846274.

41. Schumacher B, Pothof J, Vijg J, Hoeijmakers JHJ. The central role of DNA damage in the ageing process. Nature. 2021;592(7856):695-703. Epub 2021/04/30. doi: 10.1038/s41586-021-03307-7. PubMed PMID: 33911272.

42. Rose J, Soder S, Skhirtladze C, Schmitz N, Gebhard PM, Sesselmann S, Aigner T. DNA damage, discoordinated gene expression and cellular senescence in osteoarthritic chondrocytes. Osteoarthritis Cartilage. 2012;20(9):1020-8. doi: 10.1016/j.joca.2012.05.009. PubMed PMID: 22659602.

43. Copp ME, Flanders MC, Gagliardi R, Gilbertie JM, Sessions GA, Chubinskaya S, . . . Diekman BO. The combination of mitogenic stimulation and DNA damage induces chondrocyte senescence. Osteoarthritis Cartilage. 2021;29(3):402-12. Epub 2020/11/24. doi: 10.1016/j.joca.2020.11.004. PubMed PMID: 33227437; PMCID: PMC7925350.

44. Muehleman C, Bareither D, Huch K, Cole AA, Kuettner KE. Prevalence of degenerative morphological changes in the joints of the lower extremity. Osteoarthritis Cartilage. 1997;5(1):23-37. Epub 1997/01/01. doi: 10.1016/s1063-4584(97)80029-5. PubMed PMID: 9010876.

45. Forsyth CB, Pulai J, Loeser RF. Fibronectin fragments and blocking antibodies to alpha2beta1 and alpha5beta1 integrins stimulate mitogen-activated protein kinase signaling and increase collagenase 3 (matrix metalloproteinase 13) production by human articular chondrocytes. Arthritis Rheum. 2002;46(9):2368-76. Epub 2002/10/02. doi: 10.1002/art.10502. PubMed PMID: 12355484.

CHAPTER 5: EFFECT OF CONTINUAL MDL-800 TREATMENT ON SENESCENCE INDUCTION IN PRIMARY HUMAN AND MURINE CHONDROCYTES

5.1 INTRODUCTION

Cells can transition into a condition of stable cell cycle arrest, known as cellular senescence, in response to various intrinsic and extrinsic stimuli. These may include an extended period of proliferation in culture or in response to DNA damaging agents, such as irradiation, reactive oxygen species, or chemotherapy agents[1,2]. Despite the manner of induction, senescent cells share a common underlying etiology – DNA damage[3]. Advanced age has been associated with both the accumulation of senescent cells[4–6] and higher levels of DNA damage[7,8]. Our group has previously shown that the combination of mitogenic stimulation in addition to cellular damage reliably induces senescence in healthy human articular cartilage[9]. In an alternate setting, prolonged growth factor treatment promotes the development of senescent chondrocytes in young murine hip cartilage explants[10].

In the context of osteoarthritis (OA), senescent cells have been shown to contribute to disease pathogenesis[11–13], while the selective removal of senescent chondrocytes mitigates cartilage degradation in mice[14]. Although therapeutic approaches using senolytics have shown promise within murine models of OA, translation into the clinical setting has not had the same success[15]. Alternative approaches aimed at reducing DNA damage have the potential to prevent the accumulation of senescent cells within the joint space and inhibit the development of OA. The primary objective of this work was to test whether maintaining low levels of DNA damage in chondrocytes blocks senescence induction.

Studies have identified SIRT6 as a key regulator of DNA repair and cellular senescence[16,17]. **Chapter 4** established that the efficiency of DNA repair declines with age in chondrocytes, but could be restored with SIRT6 activation[18]. MDL-800 – a selective small molecule allosteric activator of SIRT6[19] – was used for these studies and shown to be capable of reducing DNA damage accumulated over decades of life[18]. To evaluate the effect of lowering DNA damage on senescence induction, we used several different model systems of senescence induction and assessed the impact of MDL-800 treatment

on senescence burden. In two *in vitro* model systems using human cartilage explants[9] and murine hip explants[10], treatment with MDL-800 provided a protective effect and minimized senescence induction compared to DMSO vehicle control groups.

Mice are a frequently used model species for investigations of mammalian aging and osteoarthritis. We sought to determine whether SIRT6 activation lowered DNA damage, inhibited senescence induction, and prevented cartilage degradation *in vivo* by performing intra-articular (IA) injections of MDL-800 into $p16^{tdTomato}$ reporter mice. This mouse strain has a tdTomato fluorescent protein "knocked-in" to the endogenous $p16^{INK4a}$ promoter, enabling the quantification of p16-high (senescent) cells via flow cytometry[20]. As this study was being conducted, another group demonstrated that Sirt6 deficiency exacerbated chondrocyte senescence and OA progression, while IA injection of either adenovirus-Sirt6 or MDL-800 nanoparticles mitigated PTOA resulting from destabilization of the medial meniscus (DMEM) surgery[21]. In the present study, we show that repeated MDL-800 injection consistently maintained low levels of DNA damage but did not significantly impact the percentage of senescent cells.

Osteoarthritis in humans and mice is associated with altered mechano-sensation in the form of allodynia, a painful response to an innocuous stimulus[22]. The gold standard method for evaluating this change in sensitivity is via use of von Frey fibers[23]. Using the von Frey assay, we show that repeated MDL-800 treatment slightly increased the 50% pain threshold in mice, compared to control matched limbs. Ongoing studies are using histological measures to quantify the effect of MDL-800 treatment on cartilage degradation. Taken together, strategies that seek to activate SIRT6 in chondrocytes remain a promising therapeutic option for treating OA but will require further investigation.

5.2 RESULTS

5.2.1 SIRT6 modulation alters the extent of senescence induction in a human cartilage explant model.

To identify how SIRT6 modulation impacts the induction of senescence, we used the human explant model described in **Chapter 2**[9] in conjunction with MDL-800 (activation) or EX-527 (inhibition) treatment. This experimental design allowed us to investigate how SIRT6 activity altered senescent cell accumulation in a physiologically relevant, and reliable, senescence induction model (experimental approach in Figure 5.1A). The readout for senescence was SA-β-gal flow cytometry. Consistent with

previous data, the irradiated groups (DMSO, MDL-800, EX-527) showed higher levels of SA-β-gal mean fluorescent intensity (MFI) compared to their non-irradiated controls. While non-significant, MDL-800 exhibited a slight protective effect from irradiation, with the SA-β-gal MFI fold increase to the DMSO group only increasing from 0.9 to 1.1 (Figure 5.1B), and the percent of cells SA-β-gal high increasing from 1.9% to 3.7% (Figure 5.1C). Conversely, inhibiting SIRT6 activity significantly increased the senescence readout compared to DMSO and MDL-800 groups. The percent of SA-β-gal high cells averaged to 10.0% in the irradiation plus EX-527 condition, compared to 5.5% and 3.7% in the DMSO and MDL-800 conditions, respectively (Figure 5.1C, $p < 0.05$, Tukey's multiple comparison test).

5.2.2 MDL-800 treatment reduces DNA damage and senescence induction in murine hip explant model.

To explore the effect of MDL-800 treatment on DNA damage and senescence induction in murine chondrocytes, our lab used a previously described[10] mouse hip explant senescence induction model. Over the course of three weeks, mouse hips cartilage explants were treated with growth factors (1ng/mL TGF-β1 and 5ng/mL bFGF) and either (DMSO, vehicle control) or MDL-800 (20 μM). To address donor variability, the two hip cartilage explants isolated from each mouse were split between treatment groups to enable direct comparison between matched samples. At the end of explant culture, the mouse hips were enzymatically digested, and the isolated chondrocytes analyzed by comet assay and flow cytometry (n = 6 $p16^{tdTom}$ reporter mice). The comet analysis revealed that MDL-800 treated hips showed a significant reduction in DNA damage compared to DMSO treated hips (readout % DNA in comet tail, $p < 0.05$, paired t-test; Figure 5.2A). Flow cytometry showed a significant drop in % p16-positive in the MDL-800 group (14.2%), compared to the DMSO control (21.0%) ($p < 0.05$, paired t-test; Figure 5.2B). To see if DNA damage correlated with senescence induction, we plotted the % DNA in comet tail versus the % p16-positive cells and found a positive correlation (R^2=0.589, slope significantly non-zero, p=0.004; Figure 5.2C).

5.2.3 Repeated IA injection of MDL-800 reduces DNA damage but does not impact senescence levels.

With the *in vitro* data showing support for MDL-800 treatment mitigating senescence induction and lowering DNA damage, we sought to evaluate the effect of *in vivo* SIRT6 activation in mice. To confirm that MDL-800 reduced DNA damage within chondrocytes following intra-articular (IA) injection, we

performed a single injection of either DMSO or MDL-800 (1µg in 10µL) in 4 mice and dissociated the cartilage after 48 hours for comet analysis. The limbs injected with MDL-800 showed significantly lower levels of % DNA in their comet tails (10.7%) than donor-matched DMSO limbs (17.4%) ($p < 0.01$, paired t-test, Figure 5.3A). To investigate the effect of consistently lowering DNA damage on senescence burden, we injected 4-month-old $p16^{tdTom}$ reporter mice every 2 weeks with MDL-800 (left hindlimb) and DMSO (right hindlimb) for a total of 8 injections. We also injected age-matched wildtype mice throughout this period to confirm DNA damage was consistently lowered in MDL-800 limbs (experimental approach depicted in Figure 5.3B). A week following the final injection, the chondrocytes from the $p16^{tdTom}$ mouse knees were analyzed by comet assay and flow cytometry. Across all time points – 2 injections, 4 injections, 6 injections, and 8 injections – the MDL-800 treated limbs demonstrated significantly lower levels of DNA damage ($p < 0.01$, paired t-test). The effect of MDL-800 treatment was most notable after the first two injections but remained significant in all proceeding injections (Figure 5.3C). Although damage levels were consistently lowered, the population of senescent chondrocytes were not significantly different between the MDL-800 and DMSO treated limbs. The mean % p16-high in the DMSO group was 6.12% and 5.51% in the MDL-800 group ($n = 12$, $p = 0.33$ (ns), paired t-test; Figure 5.3D).

5.2.4 Impact of repeated MDL-800 treatment on pain threshold.

To ascertain whether repeated MDL-800 injections protected against osteoarthritis-associated pain, mice were subjected to the same injection protocol as described in the prior section. After the 8 injections, the pain threshold of the mice was tested using the Von Frey assay. Two weeks after the last injection, mice were acclimated to the von Frey chambers and filaments on three separate days. The mechanical sensitivity was evaluated using the protocol developed by Cano et al.[23], with one hindlimb of each mouse being tested before testing the other hindlimbs. The MDL-800 limbs showed a slightly higher tolerance to pain (50% Pain Threshold of 1.0) compared to the DMSO treated limbs (0.8), but the effect was not significant ($n = 8$, paired t-test; Figure 5.4B).

5.3 DISCUSSION

With confirmation that MDL-800 treatment improved DNA repair in both human and murine chondrocytes (**Chapter 4**[18]), the next question to address was whether keeping low DNA damage levels

prevented cells from entering the senescent phenotype. Our lab has developed two reliable and physiologically relevant *in vitro* senescence induction models using human cartilage[9] and mouse hip explants[10]. These models enabled us to evaluate the impact of SIRT6 activation (or inhibition) on senescent cell accumulation, with two different readouts of senescence. In the human cartilage explant model, the combination of growth factors (TGF-β1 and bFGF) and irradiation throughout explant culture increased the percentage of cells with elevated expression of SA-β-Gal. SIRT6 activation during this culture procedure slightly reduced SA-β-Gal induction (5.5% in control group to 3.7% in MDL-800 group), while SIRT6 inhibition via EX-527 treatment significantly increased the percentage of SA-β-Gal high cells (10.0%) (Figure 5.1). Although the results suggested a protective response of MDL-800 treatment on senescence induction, the result was not significant. This may be due to the moderate increase in senescence generated by the irradiation, which only provided a narrow dynamic range in which to see a reduction.

As mice are widely used for translational studies, the next step involved testing this effect in a murine senescence induction model. Previous work conducted in our lab has demonstrated that culture of mouse hip cartilage explants for three weeks with TGF-β1 and bFGF dependably induces chondrocytes to become senescent[10]. The benefit of this model is that isolating two hips per mouse allows us to directly test the effect of MDL-800 treatment on a matched control, overcoming donor variability. Using this approach, we found the MDL-800 treatment during the 3 weeks of explant culture significantly reduced DNA damage and limited the percentage of cells with high expression of p16 (Figure 5.2). Notably, the positive correlation found between DNA damage and % p16-high (Figure 5.2C) was suggestive that damage is implicated in the senescence induction process.

To investigate the impact of SIRT6 activation on DNA damage and senescence *in vivo*, we injected MDL-800 into the joint space of $p16^{tdTomato}$ reporter mice. After validating that a single intra-articular (IA) injection of MDL-800 reduced DNA damage for 48 hours, we decided on a repeated treatment approach in 4-month-old mice, with injections every two weeks for a total of 8 injections (~4 months treatment duration). Based on previous experiments, 8-month-old mice show increased levels of DNA damage[18] and p16-positive cells compared to 4-month-old mice (unpublished). By starting with younger mice with low levels of baseline damage, we could identify whether age-accumulated damage

causes chondrocyte senescence. Although DNA damage was consistently lowered throughout the treatment duration, senescence was not reduced in the MDL-800 treated limbs (Figure 5.3). This contrasts with the findings of Ji et al.[21] and Wu et al[24], who both showed a reduction of senescence in response to Sirt6 overexpression. The primary differences between these studies and the one discussed here are (1) the method of Sirt6 activation, and (2) the senescence induction model. The Wu et al. study used lentiviral transfection of Sirt6[24], while the Ji et al. used MDL-800 developed nanoparticles[21]. More notable, both studies used DMM surgery to induce senescence within the joint. In our experimental design, we were dependent on the DNA damage accumulated with age, rather than produced by damage, to initiate the senescence phenotype. Over the 4-month time frame where we modified the DNA damage levels, the increase in p16-positive cells was not nearly as large as that of the injury-induced model. Thus, one explanation for the moderate effects in this study may be due to the limited dynamic range of senescence induction with natural aging. Further iterations of the experimental design could benefit from increasing the treatment duration from 4-months to 8 – 10 months, and thus expanding the amount of time for age-associated senescence to accrue.

Another avenue that could influence the results of the *in vivo* study presented herein is the dosage of MDL-800. In the experiments described in this chapter, 1µg of MDL-800 was delivered in 10µL to the joint by IA injection. This dose was based on the amount used in the *in vitro* experiments, as well as other studies that transitioned from *in vitro* to *in vivo* treatment. Understanding how drugs move into and out of the joint, either through systemic or IA delivery, is an active area of research[25,26]. If repeated injections prove to be an unsuitable approach, other strategies for consistent release of treatment can be considered, such as nanoparticle formulations[21] or slow-release delivery systems[27].

Sirt6 plays a role in metabolism and non-DNA repair processes[28]. While beneficially lowering DNA damage, continuous activation of these alternate pathways via MDL-800 treatment may lead to off-target effects. The dichotomous nature of SIRT6 is exhibited in cancer, which can either be promoted or suppressed by SIRT6 activation depending on the biological context[29]. MDL-800 is among the most potent and selective activators of SIRT6 discovered thus far and is specific for the deacetylase activity of SIRT6[30]. An alternative approach would be to use another confirmed DNA repair booster, such as

nicorandil[31] or cyanidian[32], in place of MDL-800. This would avoid the possible unintentional effects of continuous activation of Sirt6.

While *in vitro* experiments demonstrated a reduction in senescence with MDL-800 treatment, the initial *in vivo* experimental design did not significantly impact the levels of senescent cells. Further alterations of the dosage and/or length of treatment duration will be essential to confidently determine whether Sirt6 activation does, or does not, mitigate senescence induction. Von Frey assessment of these mice demonstrated a mild increase in pain tolerance in the MDL-800 treated limbs, compared to the DMSO limbs. Ongoing histological studies are investigating whether the MDL-800 treatment in the current experimental design impacted cartilage degradation. Altogether, SIRT6 activation as a therapeutic option for OA still has promise, but additional investigation in the translational setting will be critical.

5.4 MATERIALS & METHODS

5.4.1 Human cartilage explant senescence induction model

Primary human cartilage explants were obtained from the tali of cadaveric ankle joints as previously described[9]. For the study presented in Figure 5.1, the ages of the 8 donors used were 42, 44, 45, 45, 57, 60, 68, and 80 years old. All donors were male and had grades between 0 and 2 on the modified Collins grade[33]. The experimental design is depicted in Figure 5.1A. Senescence was induced as outlined in **Chapter 2**, with the addition of pre-feeding the explants with either MDL-800 (20 μM, Sigma) or EX-527 (10 μM, Selleck) for 2 hours before irradiation, and including the SIRT6 treatment during explant culture. At the end of explant culture, chondrocytes were enzymatically isolated, plated in monolayer, and cultured for an additional 12 days in 10% chondrocyte media.

5.4.2 Murine hip explant senescence induction model

Murine hip cartilage explants were cultured for senescence induction as previously described here[10]. Briefly, 3-week-old mice were euthanized, and their hip cartilage explants isolated from the proximal end of the femur. Explants were cultured for 3 weeks in 10% chondrocyte media with growth factors (1 ng/mL TGF-β1 and 5 ng/mL bFGF), as well as either DMSO or 20 μM of MDL-800.

5.4.3 Flow cytometry analysis

In the human cartilage explant model, SA-β-gal activity was assessed using the CellEvent™ Senescence Green Flow Cytometry Assay Kit (C10840; Thermo Fisher Scientific) as discussed in **Chapter 2**. Flow cytometry analysis for tdTomato was the senescence readout for the murine hip explant *in vitro* study (Figure 5.2) and the *in vivo* experiment (Figure 5.3). In both experiments, cartilage explants were digested overnight with collagenase P and flow cytometry analysis conducted on unfixed cells mixed with HBSS with 10 mM EDTA, and 1 µg/mL DAPI. Chondrocytes derived from wildtype mice were used as gating controls. Data was collected with an Attune NxT (Thermo Fisher Scientific) using the 561 nm laser and analyzed using FCS Express (De Novo Software).

5.4.4 Assessing DNA damage with the comet assay

The comet assay was conducted as previously described in **Chapter 3** and **Chapter 4**.

5.4.5 Intra-articular injection of MDL-800

Intra-articular injections of 1 µg MDL-800 in 10 µL of PBS was performed on the left hindlimb knee of $p16^{tdTomato}$ reporter and wildtype mice. The right hindlimb received intra-articular injections of an equivalent dose of DMSO vehicle control in the same volume. The experimental overview of the intra-articular injections is illustrated in Figure 5.3B. Mice were prepared for injection by inducing anesthesia via isoflurane and laying the mouse in a custom-made holder that exposes the patellar tendon for injection. The injection was considered successful when a slight lifting occurred within the joint following injection of the treatment.

5.4.6 Evaluating mechano-sensitivity with the von Frey assay

Two weeks following the last intra-articular injection, mice were acclimated to the holding chambers and von Frey filaments over the course of three separate days. Once the mice were accustomed to the testing procedure, their response to filaments between 0.04 and 4 grams were measured following the protocol previously described[23]. Responses were recorded for all the MDL-800 treated limbs, mice were given a 30-minute period to settle, then the DMSO treated limbs were tested. The 50% pain threshold was generated using the Up-Down Reader software provided here[23].

5.4.7 Statistics

All data analysis and plotting were conducted using GraphPad Prism 9. Statistical analysis was completed using paired t-test, two-way ANOVA, or two-way repeated measures ANOVA. Sidak's multiple comparison test was used when comparing two treatment groups, whereas Tukey's was used when evaluating three treatment groups.

5.5 FIGURES

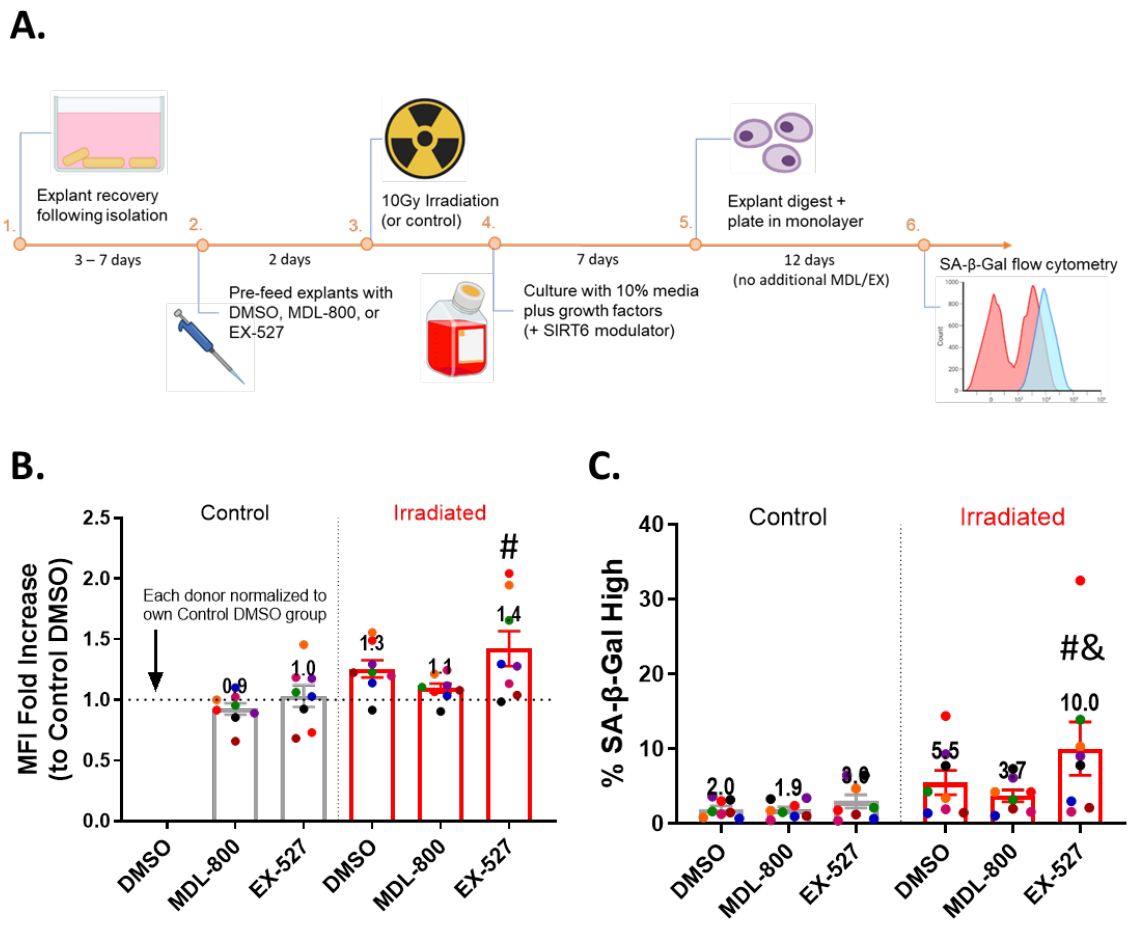

Figure 5.1: SIRT6 modulation alters the extent of senescence induction in a human cartilage explant model. (A) Schematic of experimental design. Explants were collected as full-depth squares from thick ridges of cadaveric talar (lower grade used if available) and treated with 1 ng/mL TGF-β1 and 5 ng/mL bFGF throughout the explant culture (n=8, 42 – 80 years of age, all male donors). (B) SA-β-Gal MFI fold increase above the Control DMSO condition quantified (mean + SEM). Treatment and irradiation were significant sources of variation, but their interaction were not (2-way repeated measures ANOVA). Significant differences between groups at each time point (Tukey's multiple comparisons test, $p<0.05$) are denoted by symbols: (*) = DMSO vs. MDL, (#) = MDL vs. EX, (&) = DMSO vs. EX). (C) SA-β-Gal flow quantified as the percentage of cells SA-β-Gal high, calculating by gating the percent of cells that have an SA-β-Gal MFI above 2 standard deviations from the Control DMSO mean. Treatment and irradiation were significant sources of variation, but their interaction was not (2-way repeated measures ANOVA). Significance indicated same as (B). Individual donors are represented by colored dots.

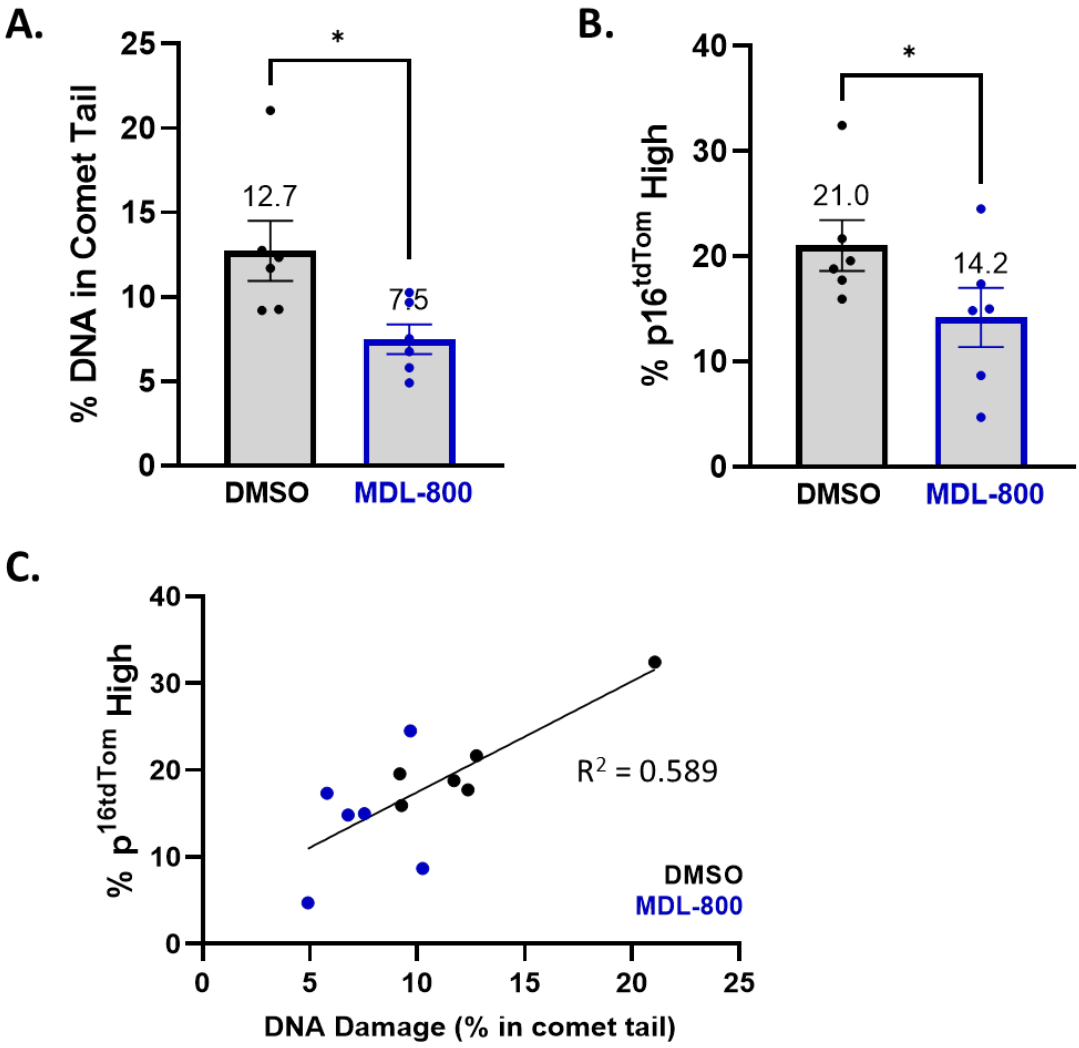

Figure 5.2: Effect of *in vitro* treatment with MDL-800 on DNA damage and senescence induction in mouse hip explant model. Murine hip cartilage explants were induced to senescence over 3-weeks with TGF-β1 and bFGF. Hip explants were treated with either DMSO (vehicle control) or 20 μM MDL-800. After 3 weeks, the chondrocytes were isolated by enzymatic digestion and analyzed via comet analysis and flow cytometry. (A) Explants treated with MDL-800 throughout culture showed a significant reduction in DNA damage compared to DMSO treated hips (paired t-test, p=0.02). (B) Hips treated with MDL-800 showed a significant reduction in $p16^{tdTomato}$ positive cells (p=0.02, paired t-test). (C) There is a correlation between the level of DNA damage and senescence induction (R^2=0.589, slope significantly non-zero, p=0.004).

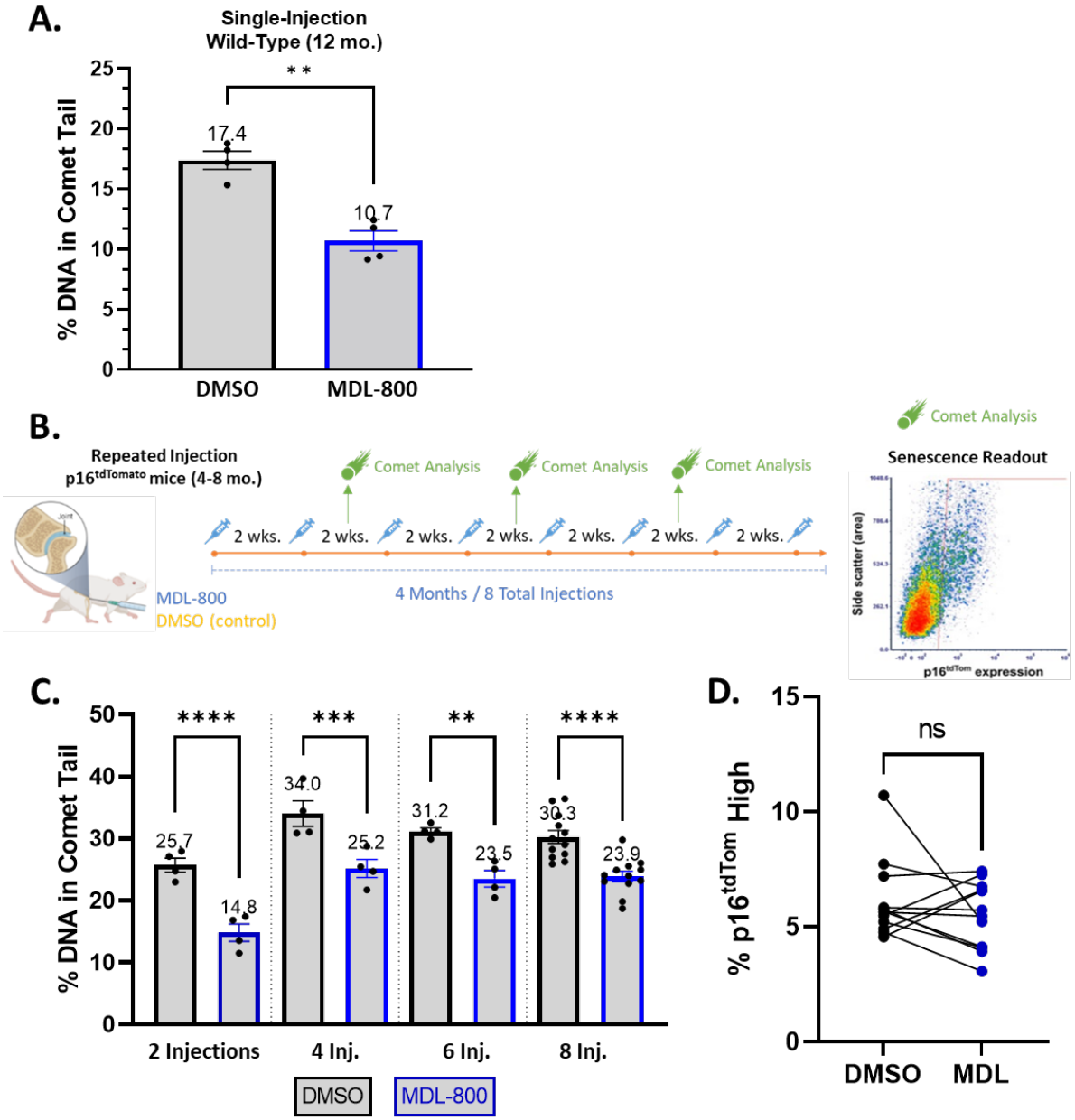

Figure 5.3: Effect of *in vivo* intra-articular MDL-800 treatment on DNA damage and senescence induction. (A) One hindlimb of 12-month-old wildtype mice was injected with 1ug of MDL-800 in 10uL and other injected with matched DMSO. Cartilage dissociated at 48hours for analysis by comet. Chondrocytes isolated from the MDL-800 treated hindlimb showed a significant reduction in % DNA in comet tails, compared to DMSO control (n=4, p=0.005, paired t-test). (B) Experimental design of the repeated *in vivo* MDL-800 injections. One hindlimb of 4-month-old wildtype and $p16^{tdTomato}$ mice were injected with 1ug of MDL-800 in 10uL and the other injected with matched DMSO, every 2 weeks, for a

total of 8 injections. After every second injection, a subset of n=4 wildtype mice were euthanized, and their knee chondrocytes analyzed for DNA damage by comet analysis. A week following the last injection, the $p16^{tdTomato}$ mice were harvested for comet and flow cytometry analysis. (C) MDL-800 significantly kept DNA damage lower in the MDL treated limbs compared to their matched DMSO control limbs (2-way ANOVA, sidak's multiple comparison test, $p<0.01$ for all comparisons). (D) After 8 injections of MDL-800 (or DMSO), $p16t^{dTomato}$ mouse knees were isolated and chondrocytes harvested for flow cytometry. MDL-800 treated limbs showed a moderate, but varied and insignificant, reduction in cells expressing high levels of tdTomato (n=12, paired t-test, p=0.33).

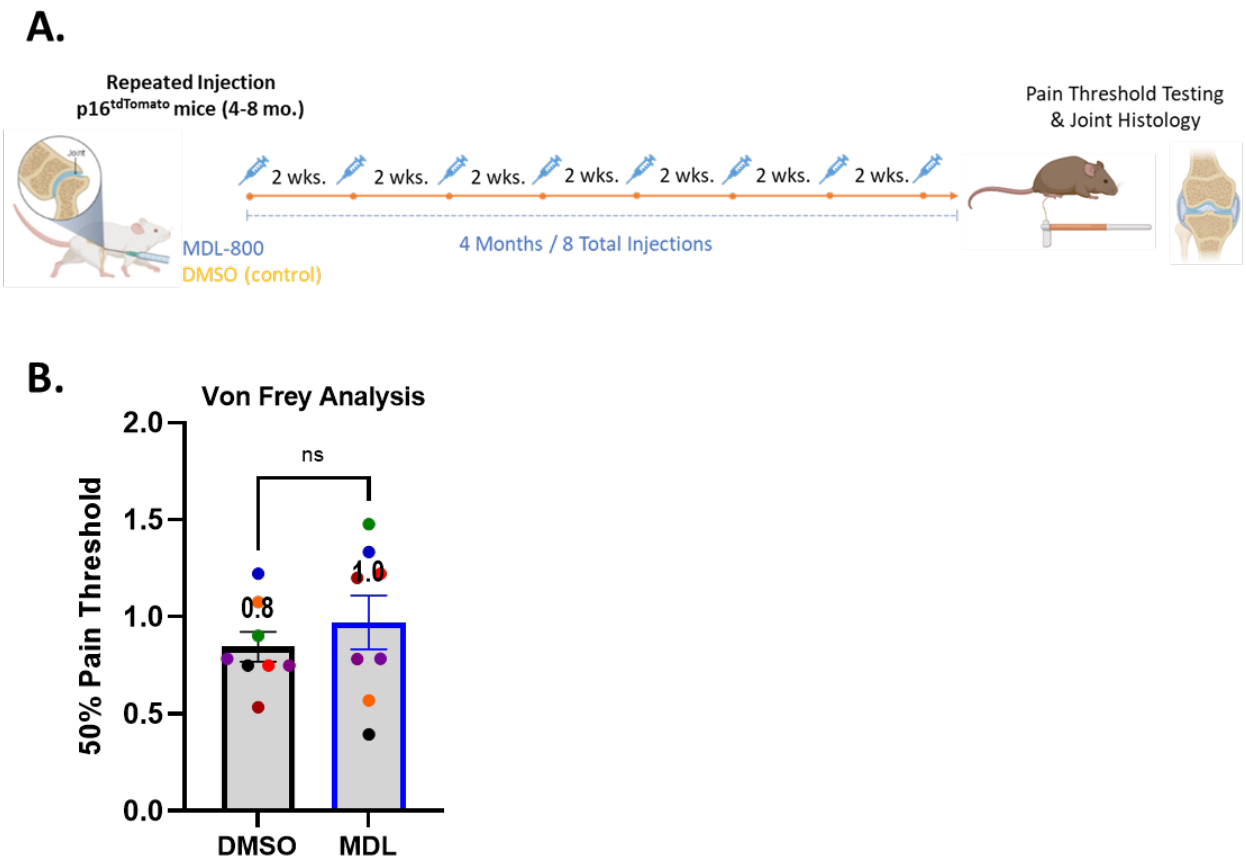

Figure 5.4: Effect of *in vivo* intra-articular MDL-800 treatment on pain threshold and OA development. (A) Experimental design of the repeated *in vivo* MDL-800 injections. One hindlimb of 4-month-old wildtype and p16^{tdTomato} mice were injected with 1ug of MDL-800 in 10uL and the other injected with matched DMSO, every 2 weeks, for a total of 8 injections. Two weeks following the last injection, the pain threshold of the mice were evaluated using the Von frey assay and cartilage degradation measured via joint histology (n=8 mice). (B) The 50% pain threshold of the MDL treated limbs were slightly higher than the DMSO limb, but not significant (n=8, paired t-test, each colored dot represents a matched mouse pair).

REFERENCES

1. Hayflick L, Moorhead PS. The serial cultivation of human diploid cell strains. *Experimental Cell Research*. 1961;25(3):585-621. doi:10.1016/0014-4827(61)90192-6

2. Ben-Porath I, Weinberg RA. When cells get stressed: an integrative view of cellular senescence. *J Clin Invest*. 2004;113(1):8-13. doi:10.1172/JCI200420663

3. Chen JH, Hales CN, Ozanne SE. DNA damage, cellular senescence and organismal ageing: causal or correlative? *Nucleic Acids Research*. 2007;35(22):7417-7428. doi:10.1093/nar/gkm681

4. Collado M, Blasco MA, Serrano M. Cellular Senescence in Cancer and Aging. *Cell*. 2007;130(2):223-233. doi:10.1016/j.cell.2007.07.003

5. Yousefzadeh MJ, Zhao J, Bukata C, et al. Tissue specificity of senescent cell accumulation during physiologic and accelerated aging of mice. *Aging Cell*. Published online January 25, 2020:e13094. doi:10.1111/acel.13094

6. Rose J, Söder S, Skhirtladze C, et al. DNA damage, discoordinated gene expression and cellular senescence in osteoarthritic chondrocytes. *Osteoarthritis Cartilage*. 2012;20(9):1020-1028. doi:10.1016/j.joca.2012.05.009

7. Swain U, Subba Rao K. Study of DNA damage via the comet assay and base excision repair activities in rat brain neurons and astrocytes during aging. *Mech Ageing Dev*. 2011;132(8-9):374-381. doi:10.1016/j.mad.2011.04.012

8. Copp ME, Chubinskaya S, Bracey DN, et al. Comet assay for quantification of the increased DNA damage burden in primary human chondrocytes with aging and osteoarthritis. *Aging Cell*. 2022;21(9):e13698. doi:10.1111/acel.13698

9. Copp ME, Flanders MC, Gagliardi R, et al. The combination of mitogenic stimulation and DNA damage induces chondrocyte senescence. *Osteoarthritis and Cartilage*. 2020;0(0). doi:10.1016/j.joca.2020.11.004

10. Sessions GA, Copp ME, Liu JY, Sinkler MA, D'Costa S, Diekman BO. Controlled induction and targeted elimination of p16INK4a-expressing chondrocytes in cartilage explant culture. *FASEB J*. 2019;33(11):12364-12373. doi:10.1096/fj.201900815RR

11. Jeon OH, David N, Campisi J, Elisseeff JH. Senescent cells and osteoarthritis: a painful connection. *J Clin Invest*. 2018;128(4):1229-1237. doi:10.1172/JCI95147

12. Xu M, Bradley EW, Weivoda MM, et al. Transplanted Senescent Cells Induce an Osteoarthritis-Like Condition in Mice. *The Journals of Gerontology: Series A*. 2017;72(6):780-785. doi:10.1093/gerona/glw154

13. McCulloch K, Litherland GJ, Rai TS. Cellular senescence in osteoarthritis pathology. *Aging Cell*. 2017;16(2):210-218. doi:10.1111/acel.12562

14. Jeon OH, Kim C, Laberge RM, et al. Local clearance of senescent cells attenuates the development of post-traumatic osteoarthritis and creates a pro-regenerative environment. *Nat Med*. 2017;23(6):775-781. doi:10.1038/nm.4324

15. Lane N, Hsu B, Visich J, Xie B, Khan A, Dananberg J. A phase 2, randomized, double-blind, placebo-controlled study of senolytic molecule UBX0101 in the treatment of painful knee osteoarthritis. *Osteoarthritis and Cartilage*. 2021;29:S52-S53. doi:10.1016/j.joca.2021.02.077

16. Grootaert MOJ, Finigan A, Figg NL, Uryga AK, Bennett MR. SIRT6 Protects Smooth Muscle Cells From Senescence and Reduces Atherosclerosis. *Circulation Research*. 2021;128(4):474-491. doi:10.1161/CIRCRESAHA.120.318353

17. Li X, Liu L, Li T, et al. SIRT6 in Senescence and Aging-Related Cardiovascular Diseases. *Frontiers in Cell and Developmental Biology*. 2021;9. Accessed January 4, 2023. https://www.frontiersin.org/articles/10.3389/fcell.2021.641315

18. Copp ME, Shine J, Brown HL, et al. SIRT6 activation rescues the age-related decline in DNA damage repair in primary human chondrocytes. Published online February 28, 2023:2023.02.27.530205. doi:10.1101/2023.02.27.530205

19. Shang J lin, Ning S bo, Chen Y yi, Chen T xiang, Zhang J. MDL-800, an allosteric activator of SIRT6, suppresses proliferation and enhances EGFR-TKIs therapy in non-small cell lung cancer. *Acta Pharmacol Sin*. 2021;42(1):120-131. doi:10.1038/s41401-020-0442-2

20. Liu JY, Souroullas GP, Diekman BO, et al. Cells exhibiting strong p16INK4a promoter activation in vivo display features of senescence. *PNAS*. 2019;116(7):2603-2611. doi:10.1073/pnas.1818313116

21. Ji M liang, Jiang H, Li Z, et al. Sirt6 attenuates chondrocyte senescence and osteoarthritis progression. *Nat Commun*. 2022;13(1):7658. doi:10.1038/s41467-022-35424-w

22. He BH, Christin M, Mouchbahani-Constance S, Davidova A, Sharif-Naeini R. Mechanosensitive ion channels in articular nociceptors drive mechanical allodynia in osteoarthritis. *Osteoarthritis and Cartilage*. 2017;25(12):2091-2099. doi:10.1016/j.joca.2017.08.012

23. Gonzalez-Cano R, Boivin B, Bullock D, Cornelissen L, Andrews N, Costigan M. Up–Down Reader: An Open Source Program for Efficiently Processing 50% von Frey Thresholds. *Frontiers in Pharmacology*. 2018;9:433. doi:10.3389/fphar.2018.00433

24. Wu Y, Chen L, Wang Y, et al. Overexpression of Sirtuin 6 suppresses cellular senescence and NF-κB mediated inflammatory responses in osteoarthritis development. *Sci Rep*. 2015;5:17602. doi:10.1038/srep17602

25. Mehta S, He T, Bajpayee AG. Recent advances in targeted drug delivery for treatment of osteoarthritis. *Curr Opin Rheumatol*. 2021;33(1):94-109. doi:10.1097/BOR.0000000000000761

26. Rohanifar M, Johnston BB, Davis AL, et al. Hydraulic permeability and compressive properties of porcine and human synovium. *Biophys J*. 2022;121(4):575-581. doi:10.1016/j.bpj.2022.01.008

27. Gambaro FM, Ummarino A, Torres Andón F, Ronzoni F, Di Matteo B, Kon E. Drug Delivery Systems for the Treatment of Knee Osteoarthritis: A Systematic Review of In Vivo Studies. *International Journal of Molecular Sciences*. 2021;22(17):9137. doi:10.3390/ijms22179137

28. Houtkooper RH, Pirinen E, Auwerx J. Sirtuins as regulators of metabolism and healthspan. *Nat Rev Mol Cell Biol*. 2012;13(4):225-238. doi:10.1038/nrm3293

29. Fiorentino F, Carafa V, Favale G, Altucci L, Mai A, Rotili D. The Two-Faced Role of SIRT6 in Cancer. *Cancers*. 2021;13(5):1156. doi:10.3390/cancers13051156

30. Huang Z, Zhao J, Deng W, et al. Identification of a cellularly active SIRT6 allosteric activator. *Nat Chem Biol*. 2018;14(12):1118-1126. doi:10.1038/s41589-018-0150-0

31. Georgiadis MM, Chen Q, Meng J, et al. Small molecule activation of apurinic/apyrimidinic endonuclease 1 reduces DNA damage induced by cisplatin in cultured sensory neurons. *DNA Repair (Amst)*. 2016;41:32-41. doi:10.1016/j.dnarep.2016.03.009

32. Jiang C, Sun ZM, Hu JN, et al. Cyanidin ameliorates the progression of osteoarthritis via the Sirt6/NF-κB axis in vitro and in vivo. *Food Funct*. 2019;10(9):5873-5885. doi:10.1039/c9fo00742c

33. Muehleman C, Bareither D, Huch K, Cole AA, Kuettner KE. Prevalence of degenerative morphological changes in the joints of the lower extremity. *Osteoarthr Cartil*. 1997;5(1):23-37. doi:10.1016/s1063-4584(97)80029-5

CHAPTER 6: CONCLUSIONS

6.1 SUMMARY & FUTURE DIRECTIONS

In the past few decades, it has become abundantly clear that the etiology of osteoarthritis (OA) is more complex than simple wear-and-tear. Prior work has begun to elucidate the role of aging and cellular senescence in the development of OA, yet the mechanisms driving these relationships remain unknown. The body of work presented in this dissertation provides valuable insight for this area of research by (1) identifying the biological cues that initiate chondrocyte senescence, (2) confirming the increase in DNA damage with aging and OA, (3) proving that SIRT6 activation can restore the decline in DNA damage repair in advanced age, and (4) showing evidence that SIRT6 activation mitigates senescence induction by lowering DNA damage. The following paragraphs summarize the findings presented in the prior chapters, addresses how these results impact the OA and aging research fields, and identifies further areas of research.

The work in *Chapter 2: The Combination of Mitogenic Stimulation and DNA Damage Induces Chondrocyte Senescence* established a physiologically relevant human cartilage explant senescence induction system. This study demonstrated that the combination of damage (10 Gy irradiation) and mitogenic stimulation (growth factor treatment) was necessary to induce a robust senescent phenotype in human chondrocytes. This finding is relevant in the context of OA as both TGF-β1[1] and bFGF[2] are released during matrix turnover, and 10 Gy of irradiation achieves a similar level of DNA damage seen in advanced age[3]. Our observations are consistent with the hypothesis that senescence arises as a response to the conflicting cues of expansion and cell-cycle arrest[4]. An important follow-up question to this research is determining the extent to which cell cycle entry during OA pathogenesis stimulates senescence induction, which can be answered using live-cell imaging.

In *Chapter 3: Comet Assay for Quantification of the Increased DNA Damage Burden in Primary Human Chondrocytes with Aging and Osteoarthritis*, the comet assay was used to quantify the increase in DNA damage that occurs with aging and OA. By assessing chondrocytes from cadaveric donors with no

macroscopic joint damage between the ages of 34 and 78 years old, we found a linear increase in damage with age. This was the first study to report on the increase in DNA damage in chondrocytes that occurs with “normal” aging. Using a modified “two-tailed” comet assay, we were able to deduce that the higher damage in older donors is due to strand breaks, rather than base damage. However, further research will be needed to identify the specific type of DNA damage that accumulates with age in chondrocytes. Based on research of other post-mitotic cell types[5], the bulk of DNA damage likely is acquired by oxidative DNA damage and reactive oxygen species. The use of hOGG1 in the modified comet assay[6] would be able to confirm whether DNA damage associated with advanced age is a result of oxidative damage.

Chapter 4: SIRT6 Activation Rescues the Age-Related Decline in DNA Damage Repair in Primary Human Chondrocytes used an irradiation challenge assay to show that chondrocyte’s capacity for efficient DNA damage repair is compromised with age but can be improved by activating SIRT6. In the context of age-related damage, MDL-800 treatment was able to significantly reduce DNA damage in older primary human and mouse chondrocytes, proving its ability to repair damage accumulated over a long period of time. The irradiation model system was valuable for this study as it generated a consistent bolus of damage across all treatment groups and ages, enabling the direct comparison of DNA damage repair over time. One limitation of this system is that irradiation is not a physiologically relevant damage in the joint space. An alternate approach could make use of tert-butyl hydroperoxide (tBHP) to initiate DNA damage, as this reagent is a known inducer of oxidative stress[7].

The experiments detailed in *Chapter 5: Effect of Continual MDL-800 Treatment on Senescence Induction in Primary Human and Murine Chondrocytes* encompass the translational components of this doctoral work. The results of the preceding chapter led to the hypothesis that maintaining low levels of DNA damage via SIRT6 activation would prevent senescence and OA development. Towards this end, we demonstrate that Sirt6 activation in mouse hip cartilage explants lowered DNA damage and reduced senescence, as measured by flow cytometry using our $p16^{tdTom}$ senescence reporter allele. Although intra-articular injection of MDL-800 proved effective at lowering DNA damage, repeated injections over the course of 4 months did not significantly lower the senescence burden in mouse knees. A probable cause of this finding is that aging-itself did not provide a large enough increase in senescence over the

treatment duration to see a noticeable drop in senescence levels. To counteract this, we can either (1) increase the treatment timeframe from 4 months to 12 months, or (2) induce senescence through surgical means (i.e., destabilization of the medial meniscus). Alternatively, the treatment protocol and dosage of MDL-800 can be optimized. As this was a pilot study, further experiments will be required to identify the optimal time between doses and concentration of MDL-800 per injection. As DNA damage repair encompasses a wide array of pathways, combinatorial therapies with other known DNA repair boosters, like nicorandil[8], may be a worthwhile avenue to pursue.

A subset of mice that received repeated MDL-800 injections underwent von Frey testing to measure their mechano-sensitivity before their hindlimbs were isolated for histological testing. While not significant, the von Frey assay suggested that MDL-800 treatment increased the 50% pain threshold of mice, compared to the DMSO control limb. Ongoing work in the lab is measuring the cartilage degradation in the mouse knees that were treated with MDL-800 (left hindlimb) or DMSO (right hindlimb). Using histological means, we will be able to assess whether MDL-800 treatment affected the development of OA in these mice. These results will provide clarity on the impact of SIRT6 activation on OA progression.

6.2 CLOSING REMARKS

The work described in this dissertation has investigated two components of aging – DNA damage and senescence – and how they play a role in the development of osteoarthritis. While significant progress still needs to be made to fully understand the biological mechanisms leading to OA, the studies included herein provide novel information linking DNA damage, senescence, and OA. By elucidating the underlying cause of senescence and DNA damage within the joint, this work establishes a foundation for the development of novel and impactful OA therapeutics. Based on the evidence, it is my hope that further research continues to be conducted in the DNA damage repair and senolytic space with the end-goal of preventing OA.

REFERENCES

1. Bush JR, Beier F. TGF-β and osteoarthritis--the good and the bad. *Nat Med*. 2013;19(6):667-669. doi:10.1038/nm.3228

2. Felka T, Rothdiener M, Bast S, et al. Loss of spatial organization and destruction of the pericellular matrix in early osteoarthritis in vivo and in a novel in vitro methodology. *Osteoarthritis Cartilage*. 2016;24(7):1200-1209. doi:10.1016/j.joca.2016.02.001

3. Copp ME, Chubinskaya S, Bracey DN, et al. Comet assay for quantification of the increased DNA damage burden in primary human chondrocytes with aging and osteoarthritis. *Aging Cell*. 2022;21(9):e13698. doi:10.1111/acel.13698

4. Ogrodnik M, Salmonowicz H, Jurk D, Passos JF. Expansion and Cell-Cycle Arrest: Common Denominators of Cellular Senescence. *Trends in Biochemical Sciences*. 2019;44(12):996-1008. doi:10.1016/j.tibs.2019.06.011

5. Fishel ML, Vasko MR, Kelley MR. DNA repair in neurons: so if they don't divide what's to repair? *Mutat Res*. 2007;614(1-2):24-36. doi:10.1016/j.mrfmmm.2006.06.007

6. Smith CC, O'Donovan MR, Martin EA. hOGG1 recognizes oxidative damage using the comet assay with greater specificity than FPG or ENDOIII. *Mutagenesis*. 2006;21(3):185-190. doi:10.1093/mutage/gel019

7. Wedel S, Martic I, Hrapovic N, et al. tBHP treatment as a model for cellular senescence and pollution-induced skin aging. *Mech Ageing Dev*. 2020;190:111318. doi:10.1016/j.mad.2020.111318

8. Georgiadis MM, Chen Q, Meng J, et al. Small molecule activation of apurinic/apyrimidinic endonuclease 1 reduces DNA damage induced by cisplatin in cultured sensory neurons. *DNA Repair (Amst)*. 2016;41:32-41. doi:10.1016/j.dnarep.2016.03.009